Clinically relevant in vitro dissolution/release testing for parenteral formulations

Diaz De Leon Ortega, Ricardo

Award date:
2019

Awarding institution:
University of Bath

Clinically relevant *in vitro* dissolution/release testing for parenteral formulations

RICARDO DIAZ DE LEON ORTEGA

A thesis submitted for the degree of Doctor of Philosophy

University of Bath

Department of Pharmacy & Pharmacology

January 2019

Declaration of any previous submission of the work

The material presented here for examination for the award of a higher degree by research has not been incorporated into a submission for another degree.

Candidate's signature 

Declaration of authorship

I am the author of this thesis, and the work described therein was carried out by myself personally.

Candidate's signature 

Table of contents

Acknowledgements

Acknowledgements

I would like to thank my lead supervisor Dr Nikoletta Fotaki for her valuable and continuous support, and especially for her patience throughout the completion of this PhD.

I would like to thank the CONACyT (CVU: 442820) and Ing. Juan Manuel Cárdenas from ICT SA de CV for the scholarship granted.

I would like to thank Dr Deirdre D'Arcy for her feedback and support.

I would like to thank Dr Albert Bolhuis and Dr Dimitrios Lamprou for their help and collaboration for this project with the microbiology and microscopy work, respectively.

I would like to thank Professor Roland Jones, Dr Giordano pula and Fernando Acosta for helping me with the osmolality measurements, obtaining blood and viscosity measurements, respectively.

I would like to thank Prof Richard Guy and Prof Clive Wilson for accepting to review this work.

I would like to thank the members of our research group for their friendship and support (Angela Effinger, Mariana Guimaraes, Joana Martir, Nota Zarmpi) but especially to Dr John Nikolettos and Dr Fotios Baxevanis for welcoming me and guiding me through the PhD life.

I would like to thank my friends from the Banda Ganso + Carmelo: Dr Bernardo Castro, Dr Uriel Martínez and Dr Andrés Sandoval for making the hard times bearable.

I would like to thank my family (brother, sister, nephew and nieces), my friends from all my life: Angel Garrido, Jesús Martínez, Guillermo Ramos and my teachers: QFB Teresa Buentello and MSc Juan Manuel Rodríguez.

Finally, I would like to thank my wife and my mother, as nothing of this would have been possible without them.

List of Figures

concentrations of SLS, CTAB or Tween with and without BSA 4.0% w/v at 12 h (Mean ± SD; n= 3). Black horizontal line represents the AmB solubility value in human plasma from healthy subjects.

Figure 3.6. Pareto charts for the standardized effects of the main factors and 2 level interactions of the analysis of AmB solubility in media with surfactants and BSA 4.0% w/v. The black horizontal line represents the significance threshold for the effects. The factors with an effect (bar) larger than the threshold are statistically significant.

Figure 3.7. Solubility study of AmB in category 3b media: AmB concentration as a function of time in the category 3b clinically relevant media with and without BSA (mean ± SD; n= 3). Solid lines represent media with BSA 4.0% w/v and dotted lines media without BSA. AmB plasma solubility was added for comparison purposes. The BSA concentration is in %w/v units.

Figure 3.8. %AmB dissolved as a function of time in the category 3a and 3b clinically relevant media and in category 3c media with the flow through cell apparatus at 37°C (mean ± SD; n= 3). High dose = 5 mg of AmB. BSA concentration is in %w/v units. Points represent observed data and the lines the first order (Eq 3.3) equation fittings.

Figure 4.1. Workflow for the PK modeling of free AmB (Fungizone® administration) and liposomal AmB (Ambisome® administration) in order to estimate k_{rel-iv} (*in vivo* release rate constant).

Figure 4.2. Compartmental PK modeling of liposomal AmB and free AmB for the estimation of k_{rel-iv}.

Figure 4.3. %AmB released as a function of time using the sample and separate method at 37°C to investigate the effects of buffer, agitation, composition including a) BSA concentration and b) type of synthetic surfactant and BSA 4.0% w/v presence) on AmB release (Mean ± SD; n = 3).

Figure 4.4. Pareto charts for the estimated effects of the main factors and 2 level interactions of the analysis of AUC_{0-12h} from a) sample and separate and b) continuous flow methods. A factor was significant when the estimated effect (horizontal bars) was larger than the standardized effect (vertical line).

Figure 4.5. %AmB released as a function of time with the continuous flow setup at 37°C in a) KRB to investigate the effects of BSA concentration and velocity, and b) in PBS SLS 1.4 mM to investigate the effect of velocity on AmB release (Mean ± SD; n = 3).

Figure 4.6. AFM images to evaluate the effect of media components on Ambisome® liposomes. a) KRB, b) KRB BSA 4.0% w/v, c) KRB SLS 1.5 mM, d) KRB SLS 1.5 mM BSA 4.0% w/v, e) KRB CTAB 0.2 mM and f) KRB Tween 80 10.0 µM. The scale bar represents 200 nm.

Figure 4.7. Observed and predicted liposomal and released AmB plasma profiles simulated with the optimized models. Healthy subjects data (Bekersky et al, n = 5, [31]), a) Liposomal AmB, b) released AmB. Blue points and line: observed data; red

solid lines: mean of the prediction, red dotted lines: standard deviation of the prediction.

Figure 5.1. Workflow for the PBPK modeling of "liposomal AmB" and "released AmB" after the administration of Ambisome® to healthy subjects

Figure 5.2. Workflow for the PBPK-PD modeling of the liposomal and released AmB after the administration of Ambisome® l to a hypoalbuminaemic population in order to simulate the pharmacological activity of the released AmB on *C. albicans*.

Figure 5.3. %AmB released with the a) sample and separate and the b) continuous flow setup at 37 °C to investigate the effect of the type of buffer, the BSA 4.0% w/v presence and the hydrodynamics in clinically relevant media with BS – PL. (Mean ± SD, n=3; solid lines: media with BSA 4.0% w/v; dotted lines: media without BSA 4.0% w/v)

Figure 5.4. Pareto charts for the estimated effects of the main factors and 2 level interactions of the analysis of a) $\%AmB_{released}max$ and k_{rel} from the sample and separate setup and b) the AUC_{0-12h} from the continuous flow method. A factor was significant when the estimated effect (horizontal bars) was larger than the standardized effect (vertical line).

Figure 5.5. AFM images to evaluate the effect of media components on Ambisome® liposomes. a) KRB BS 20.0 mM PL 4.0 mM, b) KRB BS 20.0 mM PL 4.0 mM BSA 4.0% w/v. The scale bar represents 200 nm.

Figure 5.6. Observed and simulated (PBPK model) plasma concentration profiles of "liposomal AmB" and "released AmB" after the administration of Ambisome® to healthy subjects [25, 26].

Figure 5.7. Sensitivity analysis of PBPK model parameters on the "liposomal AmB" and "released AmB" AUC_{0-24h} obtained from simulated plasma concentrations in healthy subjects. The black line is the AUC_{0-24h} obtained from the validated PBPK model for healthy subjects.

Figure 5.8. AUC_{0-24h} calculated from simulated plasma concentration profiles with with the k_{rel} from the *in vitro* release profiles against the AUC_{0-24h} obtained from the validated PBPK model for "liposomal AmB" and "released AmB". n = 5 subjects for each population.

Figure 5.9. PBPK-PD model for a hypoalbuminaemic population (plasma protein fraction 0.5; healthy subjects: plasma protein fraction 1.0) and its pharmacodynamic effect on fungal cells. a) Simulated plasma concentration profiles of "liposomal AmB" and "released AmB" from the validated PBPK model for healthy subjects and the hypoalbuminaemic population, b) simulation of a dose administered to patients receiving Ambisome®, c) simulated k_{kill} (corresponding to the simulated plasma concentration profile of Figure 5.9b), and d) effect of the administration of Ambisome® on the growth of *Candida albicans*.

List of Tables

Table 4.3. *In vivo* studies of administration of AmB formulations (Fungizone® and Ambisome®) to healthy subjects.

Table 4.4. %AmB AUC_{0-12h} calculated for all the *in vitro* release profiles: sample and separate and continuous flow investigating the effect of buffers, BSA concentration, surfactants and agitation [for sample and separate; LA: low agitation, HA: high agitation. For continuous flow; LV: low velocity, HV: high velocity] (Mean ± SD; n = 3).

Table 4.5. Parameters obtained after fitting (first order equation model) of %AmB released profiles from Ambisome® in the sample and separate setup and in continuous flow setup (Mean ± SD, n = 3).

Table 4.6. Parameters of liposomes obtained from AFM from the samples prepared with the media components investigated in the *in vitro* release studies

Table 4.7. PK parameters from the compartmental modeling and model optimization from liposomal and released AmB after administration to healthy subjects.

Table 4.8. Statistical comparison of *in vitro* release rate constants (from the sample and separate and continuous flow setups) and *in vivo* release rate constants (estimated with the PK model for healthy subjects, k_{rel-iv} = 0.025 ± 0.002 h^{-1}). * = statistically similar [for sample and separate; LA: low agitation, HA: high agitation. For continuous flow; LV: low velocity, HV: high velocity] (Mean ± SD; n = 3).

Table 4.9. Statistical analysis for the comparison of *in vitro* AUC_{0-12h} (from the sample and separate and continuous flow setups) and *in vivo* simulated AUC_{0-12h}(AUC_{0-12h} = 165.18 ± 11.49 %AmB*h) [LA: low agitation, HA: high agitation, LV: low velocity, MV: medium velocity, HV: high velocity] (Mean ± SD; n = 3).

Table 5.1. Levels and factors investigated with the sample and separate setup for the release studies of AmB from Ambisome® in clinically relevant media (category 3a media [Chapter 3])

Table 5.2. PK-Sim model set up: physicochemical properties, distribution and clearance parameters of "released AmB" and "liposomal AmB" (Ambisome®) after administration to healthy subjects.

Table 5.3. Parameters and the range in which the parameters were investigated in the sensitivity analysis of the validated PBPK model of Ambisome® administration.

Table 5.4. Parameters obtained after fitting (Equation 5.3) of %AmB released profiles from Ambisome® with the sample and separate setup and the continuous flow setup [LA: low agitation, HA: high agitation, LV: low velocity, HV: high velocity] (Mean ± SD, n = 3).

Table 5.5. Properties of liposomes obtained from atomic force microscopy from the samples prepared in media with BS PL in the presence and absence of BSA. Mean ± SD. n = 20 Random Particles.

Table 5.6. Parameters obtained after fitting (Equation 5.6) of CFU time profiles from time killing experiments in KRB BSA 2 and 4% w/v using different concentrations of AmB (0.75, 1.5 and 3.0 μg/mL) (Mean ± SD, n = 2).

Abstract

The information available on *in vitro* release testing for controlled release parenteral formulations is limited. Thus investigating the effect of different media components and hydrodynamic setups in order to develop an *in vitro* release test that could predict the *in vivo* performance of parenteral formulations is needed.

The aim of this thesis was to develop an *in vitro* release test that coupled with *in silico* modeling could predict the *in vivo* release of a parenteral drug formulation administered intravenously [using Amphotericin B liposomal formulation (Ambisome®) as formulation model)]. Amphotericin B is a poorly soluble and highly protein bound drug, therefore the effect of albumin on Amphotericin B solubility, degradation and microbiological activity was investigated. Biorelevant and clinically relevant media were developed and used with two hydrodynamics setups for the *in vitro* release testing of Ambisome®. Compartmental pharmacokinetic (PK) and physiologically-based pharmacokinetic (PBPK) modeling were performed in data from healthy subjects receiving Ambisome® in order to relate the *in vitro* release profiles to the *in vivo* release profile. The PBPK model was extrapolated to a hypoalbuminaemic population and used to evaluate the antifungal effect of Amphotericin B on *Candida albicans*. Albumin was of high importance in the test media as it increases the solubility and degradation rate of Amphotericin B, while it decreases its microbiological activity. *In vitro* release tests in biorelevant media with the sample and separate setup was successful to predict *in vivo* AmB release, assessed with the use of PK modeling. Prediction of the AmB liposomal and released plasma concentrations was achieved with the development of a PBPK model in which the *in vitro* release profiles in the developed media (clinically relevant media with biorelevant surfactants) were used. In the simulated hypoalbuminaemic population, the PBPK/PD model developed revealed that the microbiological activity of Amphotericin B was increased due to a decrease in albumin concentration (leading to more drug available to exert a pharmacological effect).

This thesis provides an overview of how relevant media components and hydrodynamics affect the release of drug from an intravenously administered parenteral formulation and linked with either PK or PBPK modeling could predict the *in vivo* behaviour of the formulation and the released drug. This could be a starting

point for the future development of clinically relevant *in vitro* release testing for more parenteral formulations.

Aims and Objectives

The general aim of this thesis is to develop clinically relevant *in vitro* release tests for parenteral formulations (using Ambisome®, a liposomal formulation of Amphotericin B, as formulation model) by investigating how medium components and hydrodynamics affect the release of the drug from the formulation and by using PK and PBPK modeling to establish the relationship with the *in vivo* data and how this modeling could be applied to predict the antifungal activity of the drug (PBPK/PD).

The specific objectives of each chapter are:

Chapter 1: A general overview of the current experimental setups for *in vitro* release testing for parenteral formulations, media proposed, physiological conditions that could be simulated in an *in vitro* test and the challenges to simulate these conditions. The limited information for the development of *in vitro* release tests for parenteral formulations are described.

Chapter 2: The aim of this chapter was to investigate the solubility, degradation rate, dissolution and antifungal activity of Amphotericin B in simulated plasma with albumin concentrations representing healthy subjects and hypoalbuminaemic patients, and to develop a mathematical model to describe and simulate all the processes involved in AmB dissolution, in order to be the basis for the development of biorelevant dissolution testing of Amphotericin B formulations.

Chapter 3: The aim of this chapter was to investigate the impact of different media components on the solubility of Amphotericin B in order to develop media where the AmB plasma solubility (clinically relevant solubility) could be matched and to evaluate the media developed for their suitability for compendial and clinically relevant *in vitro* release testing for parenterals.

Chapter 4: The aims of this chapter were to investigate how synthetic surfactants, type of buffer and protein content (albumin concentration) along with hydrodynamics, affect the release of Amphotericin B from Ambisome® liposomes and how the *in vitro* release profiles, coupled with compartmental pharmacokinetic modeling can be used to predict the release from Ambisome® *in vivo*.

Chapter 5: The aims of this chapter were: i. to investigate how the presence of albumin in clinically relevant media containing physiological surfactants (bile salts –

phospholipids), combined with biorelevant hydrodynamics, impact on the release of Amphotericin B from Ambisome®, and ii to link the *in vitro release* tests and with a novel PBPK model, in order to guide the development of a biopredictive release test for the liposomal Amphotericin B formulation Ambisome®. The extrapolation of the PBPK model to a hypoalbuminaemic population to build a PBPK/pharmacodynamics model to simulate the pharmacological effect of Amphotericin B on fungal cells was also investigated.

Chapter 1. *In vitro* release testing for parenteral formulations: current state and challenges

Abstract

In vitro release testing is commonly used for quality control purposes. Biorelevant i*n vitro* release testing in which the *in vivo* conditions are simulated could assist formulation development and prediction of *in vivo* performance. For controlled release parenterals, the information is limited. There are different types of parenteral formulations which are mainly administered intravascularly, intramuscularly and subcutaneously. Three categories of *in vitro* release testing have been reported in the literature for parenterals but there are only few compendial release methods. Biorelevant release testing coupled with mathematical modeling of *in vitro* release profiles and observed *in vivo* data could be used to establish a correlation between the *in vitro* and *in vivo* release. The aim of this chapter is to describe the current state of release testing for controlled release parenteral formulations, the characteristics to be incorporated in the *in vitro* tests in order to improve their biorelevance and the use of mathematical modeling in the development of correlations and relations between the *in vitro* and the *in vivo* release profiles.

1.1. Introduction

In vitro release testing is conducted to ensure adequate performance of controlled release parenteral formulations (parenterals) (Table 1.1). *In vitro* release tests used for quality control will not necessarily reflect the performance of parenterals *in vivo* as many of these tests do not attempt to simulate *in vivo* conditions. The *in vitro* release could be associated with the *in vivo* release in order to find a relationship between them. An *in vitro in vivo* correlation/relation (IVIVC/IVIVR) is a tool that can relate an *in vitro* parameter (e.g. percent released) to an *in vivo* parameter (e.g. area under the curve, maximum plasma concentration). Having a meaningful *in vitro* release test or an IVIVC/IVIVR could lead to faster development of new parenterals and reduce animal and human studies. This chapter will focus on describing the methods that have been used to assess the release of parenterals, the physiological characteristics of main parenteral administration routes (intravenous, intramuscular, subcutaneous and drug-eluting stents) and the use of mathematical modeling on the development of IVIVC/ IVIVR.

Table 1.1. Parenteral formulations used in therapeutics [1-3].

Formulation	Description
Microspheres	Polymeric spherical particles in the micron size range. Drug can be entrapped in these particles either in the form of microcapsules with a polymer coating surrounding a drug core or in the form of micromatrices with the drug dispersed throughout the polymer.
Nanoparticles	Submicron-sized particles (3-200 nm), devices or systems that can be made using a variety of materials including polymers, lipids and even organometallic compounds.
Liposomes	Liposomes consist of one or more phospholipid bilayers with an enclosed aqueous phase.
Emulsions	Emulsions are formed by mixing of two or more immiscible liquids with limited mutual solubility; mixing is performed

	via high energy conditions such as *via* ultra-sonication, homogenization, or micro fluidization.
Hydrogels	Aqueous gels
Dendrimers	Dendrimers are synthetic highly branched polymers with a central core with sizes in the nanometre range. i.e. VivaGel®. (astodrimer sodium)
Drug Eluting Stents	Devices designed to be implanted into the human body. Typically, a stent consists of a tubular mesh structure onto which the drug is deposited (eg. by polymer coating).

1.2. *In vitro* release testing for parenterals: current state

1.2.1. Release media

Usually, the release medium is selected according to the solubility, stability and ease of assay of the drug analysed [4]. Currently, the release medium used for *in vitro* release testing is phosphate buffered saline (PBS) [5]. This medium just simulates plasma's pH and the osmolality.

1.2.2. Release testing apparatus and operational conditions

For parenteral formulations, there are three main methods that have been extensively reviewed in the literature [3, 4, 6-8]:

- Dialysis
- Continuous flow
- Sample and separate

Dialysis method (Figure 1.1): The sample (donor) is separated from the release medium (receptor) by a permeable membrane with an adequate molecular weight cut off (MWCO) that allows the drug to move freely until the concentrations of the donor and the receptor are equilibrated. Normal, reverse or side-by-side dialysis can be used [4, 8]. The sampling does not interfere with the formulation but particles might

aggregate, the released drug can be bound to the membrane and diffusion through the membrane may be a limiting factor for drug release [4, 6, 7].

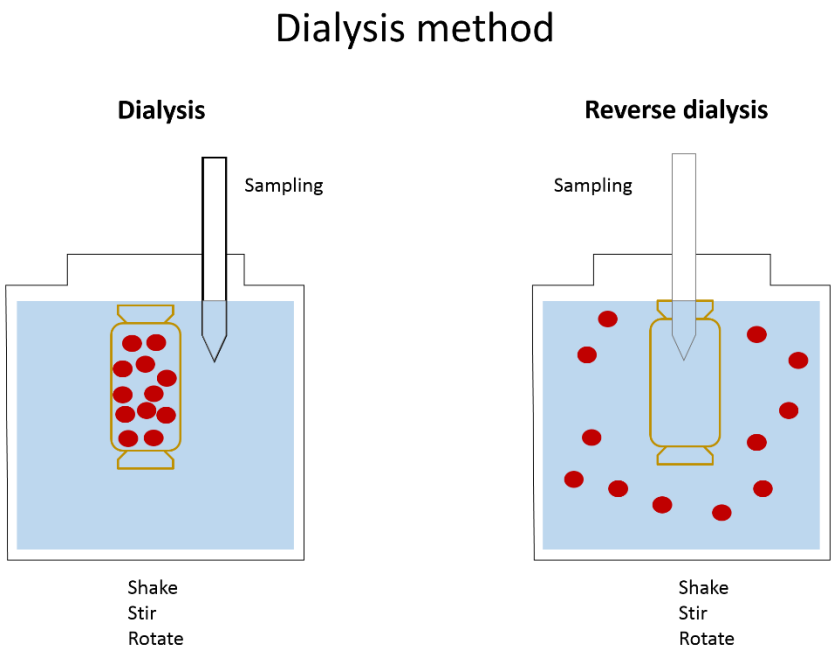

Figure 1.1. Dialysis method to assess the i*n vitro* release for parenteral formulations.

Continuous flow (CF) method (Figure 1.2): A pump is used to induce release medium flow through a cell where the formulation is placed mixed within glass beads or immobilized with a special device. An appropriate pore size filter is used to prevent the escape of the formulation but filter clogging can be problematic [4]. The flow rate can be set depending on the kind of pump (e.g. peristaltic or piston pump). Samples can be taken from the release medium without interfering with the formulation [7] and an open or closed mode can be applied.

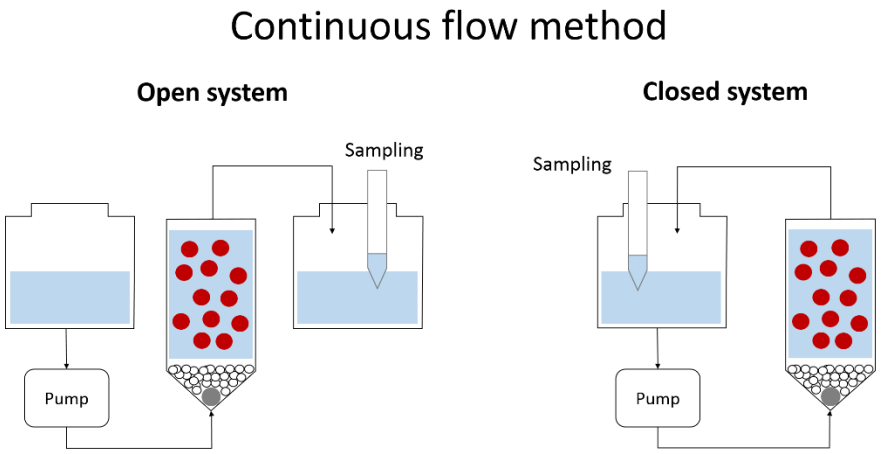

Figure 1.2. Continuous flow method to assess the i*n vitro* release for parenteral formulations.

Sample and separate (SS) method (Figure 1.3): The formulation is placed in a container with the release medium at constant temperature with stirring or shaking. Samples are taken from the release medium and volume replacement can be made (when needed). During sampling, formulation is removed and samples are either filtered or centrifuged to separate the released drug from the formulation. The separation technique of the released drug should be investigated rigorously as some formulations may not sediment even with long ultracentrifugation times, and if the separation of released drug from the formulation is not performed quickly, a representative release profile cannot be obtained [6, 8, 9]. The test can be performed in a vial or in the paddle or basket apparatus, depending on the volume of the medium and the agitation required [6, 8, 9].

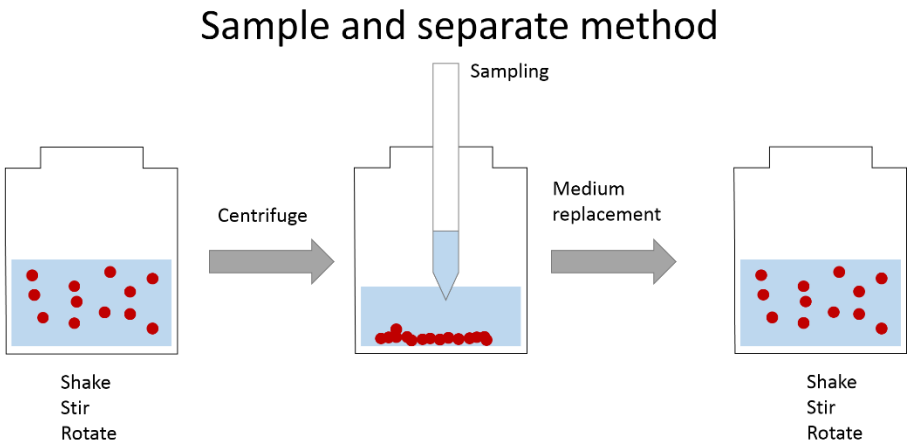

Figure 1.3. Sample and separate method to assess the i*n vitro* release for parenteral formulations.

For liposomes, the reverse dialysis has been recommended and for polymer nanoparticles the continuous flow method has been suggested due to possible aggregation with the SS method [7].

Table 1.2 shows a list with the dissolution tests for parenteral formulations presented in 2015 by Cardot et al. [10] updated with the additions made by the FDA until January 2019 [11].

Table 1.2. Dissolution methods published by the FDA for parenteral formulations

Drug	**Formulation**	**Dissolution method conditions/**
betamethasone acetate/ betamethasone sodium phosphate	Injectable suspension	USP 4 apparatus, 0.05% SLS pH 3.0, sampling times are indicated
medroxyprogesterone acetate	Injectable suspension	Test 1: USP 4 apparatus, 0.5 % SLS in water and Test 2: USP 2 apparatus, 0.35 % SLS in water, sampling times are indicated

methylprednisolone acetate	Injectable suspension	USP 4 apparatus, 0.55 % SLS, sampling times are indicated
paliperidone palmitate	Injectable suspension	USP 2 apparatus, 0.489% (w/v) Polysorbate 20 in 0.001 N HCl at 25.0°C, sampling times are indicated
triptorelin palmoate	Injectable suspension	USP 2 apparatus, water-methanol (95:5); reconstitute vial in 2 mL water for Injection, add to 500 mL medium at 37°C, sampling times are indicated
aripiprazole	Injectable suspension	UPS 2 apparatus, 0.25% SDS, sampling times are indicated
ciprofloxacin	Otic injectable suspension	USP 4 apparatus, 50 mM Acetate Buffer, pH 4.5 at 37°C [use glass beads; sample volume: 100 µL], sampling times are indicated
dantrolene sodium	intravenous suspension	USP 2 apparatus, 0.5% Benzalkonium Chloride in water, sampling times are indicated
olanzapine pamoate	intramuscular suspension	USP 4 apparatus, 1% SLS in pH 6.8 Phosphate Buffer, sampling times are indicated
triamcinolone acetonide	intra-articular suspension	USP 2 apparatus, 0.3% SLS in 10 mM phosphate buffer, pH 7.2 + 0.02% sodium azide at 35°C
leuprolide acetate	Extended release injectable	USP 2 or USP 4 apparatus are suggested

octreotride	Extended release injectable	USP 2 or USP 4 apparatus are suggested
risperidone	Extended release injectable	USP 2 or USP 4 apparatus are suggested
naltrexone	injectable suspension	USP 2 or USP 4 apparatus are suggested. Phosphate buffered saline with 0.02% Tween 20 and 0.02% Sodium azide, pH 7.4 (final osmolality should be 270 ± 20 mOsm), or any other appropriate medium, at 37°C. The development of a release test is required.
doxorubicin	liposomes	USP 2 or USP 4 apparatus are suggested. Develop a release medium starting at pH 6.00 ± 0.05 and at 47ºC ± 0.5ºC. The development of a release test is required.
azacitidine	injectable suspension	The development of a release test is required.
veteporfin	injectable suspension	The development of a release test is required.
amphotericin B	liposomes	The development of a release test is required.
granisetron	extended release injectable	The development of a release test is required.
medroxyprogesterone acetate	injectable suspension	The development of a release test is required.

In terms of regulatory aspects for the assessment of release from parenteral formulations, the FDA has published two draft guidances on a) liposomal drug products [12] and b) drug products that contain nanomaterials [13]. Regarding the *in vitro* release testing for liposomal drug products, the following statement is made: "*In vitro* release of the drug substance from the liposome drug product under the stated/described experimental conditions with supportive data and information regarding the choice of those conditions" [12]. For assessment of the *in vitro* release of drug products with nanomaterials, the draft guidance states: "Detailed descriptions of the proposed dissolution/*in vitro* release test and the developmental parameters (selection of equipment/apparatus, media, agitation/rotation speed, pH, sink conditions, surfactant type and concentration) should be included in the submission" [13]. Recently (November 2018) an article on *in vitro* release tests for parenteral formulations was published [14]. In general, the compendial paddle [United States Pharmacopea (USP) apparatus 2] or the flow through cell apparatus (USP apparatus 4) are recommended for the *in vitro* release testing of parenterals. The use of dialysis is also recommended for nanosuspensions, liposomes and microspheres. A release medium with physiological pH (7.4) and osmolality (275-300 mOsm/L) values is recommended. A surfactant or an organic solvent may be used in order to increase the solubility of the drug or to accelerate the release. For drug release from liposomal formulations the *in vitro* release tests should discriminate between different formulations and the *in vivo* conditions should be simulated to establish an IVIVC. The *in vitro* release for implants and drug eluting stents can be also assessed in the USP apparatus 7 [14].

1.3. Towards the development of biorelevant release testing for parenterals

Understanding the factors affecting release enables identification of relevant characteristics of the *in vivo* environment for drug release as one of the goals for an *in vitro* release test is to predict the *in vivo* performance. *In vivo* critical factors affecting the release of the drug from the parenteral formulation should be identified for simulation in the *in vitro* release test in order to predict the *in vivo* performance [14, 15]. Biorelevant release testing takes into consideration the hydrodynamics at the site of administration and the composition of the medium where drug will be released from the formulation [16].

1.3.1. Release media

1.3.1.1. Intravenous administration

For intravenously administered parenterals, the relevant body fluid is plasma. Plasma contains ions, biomolecules and proteins (albumin, globulins and fibrinogen) [17], with albumin being the most relevant protein in terms of drug administration as it is able to bind acidic and lipophilic drugs [18]. Plasma albumin concentration in a healthy subject is 4 g/dL [19]. α1 acid glycoprotein is another plasma protein which can bind basic and neutral lipophilic drugs and its concentration in plasma is 0.1 g/dL [20]. These plasma components should be taken into account to develop a biorelevant release medium for intravenously administered parenterals. The composition of media attempting to simulate human plasma published in the literature is presented in Table 1.2.

Table 1.3. Composition of human plasma, Krebs Ringer buffer and simulated human plasma.

Ion	Concentration (mM)		
Ion	Plasma [17]	Simulated human plasma [21]	Krebs Ringer buffer [22, 23]
HCO_3^-	24.80	27.00	14.99
K^+	4.60	5.00	4.56
Cl^-	99.00	103.00	127.32
Na^+	150.00	142.00	136.17
Ca^{2+}	4.70	2.50	1.00
Mg^{2+}	1.60	1.50	0.49
Inorganic phosphorus	1.51	1.00	2.00
D-Glucose	5.6.0	-	10.00
SO_4^{3-}	-	0.50	-

tris(hydroxymethyl) aminomethane	-	50.00	-
HCl	-	45.00	-
Osmolality (mOsm/L)	289.00	-	285.00
Viscosity	4.00 cP at 22°C, 1.40 cP at 37°C [24]	-	-
pH	7.40	7.25	7.30 – 7.40

Simulated human plasma and Krebs – Ringer buffer take into account only the ionic components of plasma but the protein content is not considered. Performing release tests with simulated human plasma or Krebs Ringer buffer for a poorly soluble highly protein-bound drug could lead to an underestimation of the drug release. It has been reported that an increasing concentration of albumin increases itraconazole solubility [25] and the same trend was found for dicumarol [26]. Presence of albumin has been suggested in some simulated body fluids (i.e. simulated vaginal fluid, simulated semen solution [21], simulated uterine fluid [27]).

1.3.1.2. Drug eluting stents

Drug eluting stents are placed into coronary arteries to prevent re-occlusion, and the released drug has to exert a pharmacological action in the region where the stent has been implanted (local action) [28]. Alginate hydrogels and long term stable hydrogels have been employed in *in vitro* release testing to provide a matrix similar to the tissue present in the implantation site [3, 28].

1.3.1.3. Intramuscular and subcutaneous administration

For these types of administration, the interstitial fluid (the liquid surrounding the tissue's cells), is the medium of interest. This fluid permeates from blood to muscle and the subctaneous enviroment and its composition has been measured indirectly from plasma, as it can be considered as a plasma ultrafiltrate (Table 1.3) [29]. A biorelevant release medium for both intramuscular and subcutaneous administration has not yet been developed. Simulated body fluid (SBF) has been employed to test the

activity of biomaterials to bind to bones [30] and its ionic composition is similar to interstitial fluid (Table 1.3), thus, it could be a good option to use for *in vitro* release tests for parenterals administered intramuscularly or subcutaneously.

Table 1.4. Composition of interstitial fluid found in the human body and simulated body fluid used for bond binding tests.

Ion	Interstitial fluid [29]	Simulated body fluid [30]
	Concentration (mM)	
Total calcium	1.6	2.7
Total magnesium	0.7	1.5
Total sodium	134.6	142.7
Total potassium	3.2	5
Total CO_2	23.9	4.2
Phosphate	0.6	1.0
Albumin	0.2 (12.5 g/L)	-
Sulphate	-	0.5
Total chloride	-	187.9
Tris(hydroxymethyl) aminomethane	-	50.5

1.3.2. Biorelevant hydrodynamics

1.3.2.1. Intravenous administration and drug eluting stents

The characteristics of the hydrodynamics in the bloodstream should be simulated to the *in vitro* release test. The cardiac output is approximately 5000 mL/min [31] and the flow rates present in the human body could seem too large and too diverse to be incorporated into a release test. The average linear velocities of blood in some blood vessels are 40 cm/s for the aorta, 15 cm/s for the vena cavae, 0.03 cm/s for capillaries

[32], 19 cm/s for arteries and 7.8 cm/s for veins [33]. The maximum flow rate that a flow through cell apparatus piston pump can achieve is 50 mL/min. If linear velocities are considered, utilizing a setup with the small cell (diameter = 12 mm) of the flow through cell apparatus and a flow rate of 50 mL/min, the linear velocity would be 0.74 cm/s, which would only be enough to match the linear velocity in the capillaries; if the same setup is used to simulate aorta's linear velocity, a flow rate of 2700 mL/min would be needed. If the flow rate of blood vessels is considered, then the flow rate for arteries would be 26 mL/min, for veins 4.8 mL/min [33] and for the coronary artery 35 mL/min [34], which could be simulated with the flow through cell apparatus' piston pump.

Simulating the *in vivo* flow rate or linear velocity of plasma in the circulatory system might be important for drug eluting stents as they are immobilized and plasma passes through them at certain flow rate/linear velocity. For *in vitro* drug release testing from stents, a flow through cell was filled with hydrogel leaving an empty space in the centre where the stent was placed and the release medium was propelled by a peristaltic pump at a flow rate of 35 mL/min to simulate the coronary artery flow rate [3].

For the administration of liposomes intravenously, the particles move with the fluid, provided adequate suspension and mixing of particles i.e. there is no static pool where particles aggregate and sediment, as this should not happen *in vivo* after intravenous administration. Hydrodynamic conditions need to facilitate dispersion of moving particles as it happens *in vivo*. The flow through cell apparatus could be adapted in order to allow free movement of particles in the whole setup of a flow through cell apparatus closed system but losing the advantages of having the particles trapped in a cell.

1.3.2.2. Intramuscular and subcutaneous administration

For intramuscular and subcutaneous administration, after the release from the formulation, the drug needs to travel to the bloodstream. There are theoretical critical steps before the absorption of drugs from intramuscular formulations and the relevant hydrodynamics are: the diffusion of water to the depot (site of injection), the diffusion away from the depot and the distance to the blood vessels and the blood flow [35].

The rate of fluid exchange between blood and the interstitium is influenced by the "Starling forces" (Equation 1.1):

$$J_v = K_f\left[(P_v - P_t) - \sigma\left(\pi_p - \pi_t\right)\right] \text{ (Eq 1.1) [36, 37]}$$

where J_v is the fluid exchange rate, P_v and P_t are the intravascular and tissue fluid hydrostatic pressures, respectively; π_p and π_t are the plasma and interstitial fluid colloid osmotic pressures, respectively; K_f is the filtration coefficient that describes the hydraulic permeability of the barrier (permeability to bulk flow of water) and σ is the reflection coefficient for plasma proteins. σ could take values from 1 (a totally impermeable barrier) and 0 (a barrier that does not offer restriction to the protein movement). The Starling force balance and the local barrier permeability to water and protein dictate fluid exchange [36, 37]. Starling force calculations provide the rate of fluid entering into the administration site and a suitable flow rate or equivalent hydrodynamics should be incorporated to the *in vitro* release test or in a mathematical model. In addition, the hydrodynamics of blood passing through the muscles and skin should be considered in the biorelevant *in vitro* release testing development.

For muscles, the blood flow rate would depend on their activity state (rest or active). The oxygen requirements in the resting state are low and thus blood flow rate ranges between 5 and 10 mL/min/100 g, while in the active state the blood flow rate reaches up to 80–100 mL/min/100 g as the demand for oxygen and substrates augments [38]. For subcutaneous formulations, the normal blood flow in skin ranges from 1.5 to 2.5 mL/ 100 g/min, with the nocturnal period and change in posture increasing blood flow up to 200% and 30-40%, respectively [39]. The release and the absorption of drugs in the subcutaneous space are similar to those observed in the intramuscular space, involving the blood flow to the zone of administration, the drainage by the lymph and the distance to blood vessels [40].

Other factors affecting the rate and the extent of absorption from intramuscular formulations, are the site that the formulation is administered (with higher absorption on the deltoids compared to the gluteus [41]), and the depth of the injection (as the needle needs to penetrate and reach the muscle, otherwise the administration would be in the adipose tissue [35]). In women, drug absorption from intramuscular formulations administered in the gluteus is slower than in men, as the adipose tissue layer in the gluteus is thicker in women, making gender a factor to take into account

for the development of *in vitro* release/dissolution tests for intramuscular administered formulations [35, 42]. All of these factors should be taken into account for the development of a biorelevant release test for a formulation intended for intramuscular administration and for the design of the *in vivo* study.

To develop a release test for subcutaneous and intramuscular formulations, the same parameters should be considered. The CF methods could be used in this case as the flow through cell apparatus pump (piston or peristaltic pump) can provide a 10 mL/min flow. Furthermore the dialysis method could be used, as the retention of the formulation in the dialysis bag could be exploited to mimic retention in muscle or subcutaneous tissue.

1.3.3. Challenges for the development of biorelevant release testing for parenterals

Some *in vivo* physiological processes might be difficult to incorporate into a biorelevant *in vitro* release test.

For subcutaneous and intramuscular administration of parenteral formulations (Figure 1.4a), there are two possible processes occurring simultaneously in the site of administration with the release of the drug. One is the degradation of the drug and the other is the clearance of the formulation by the immune system [40].

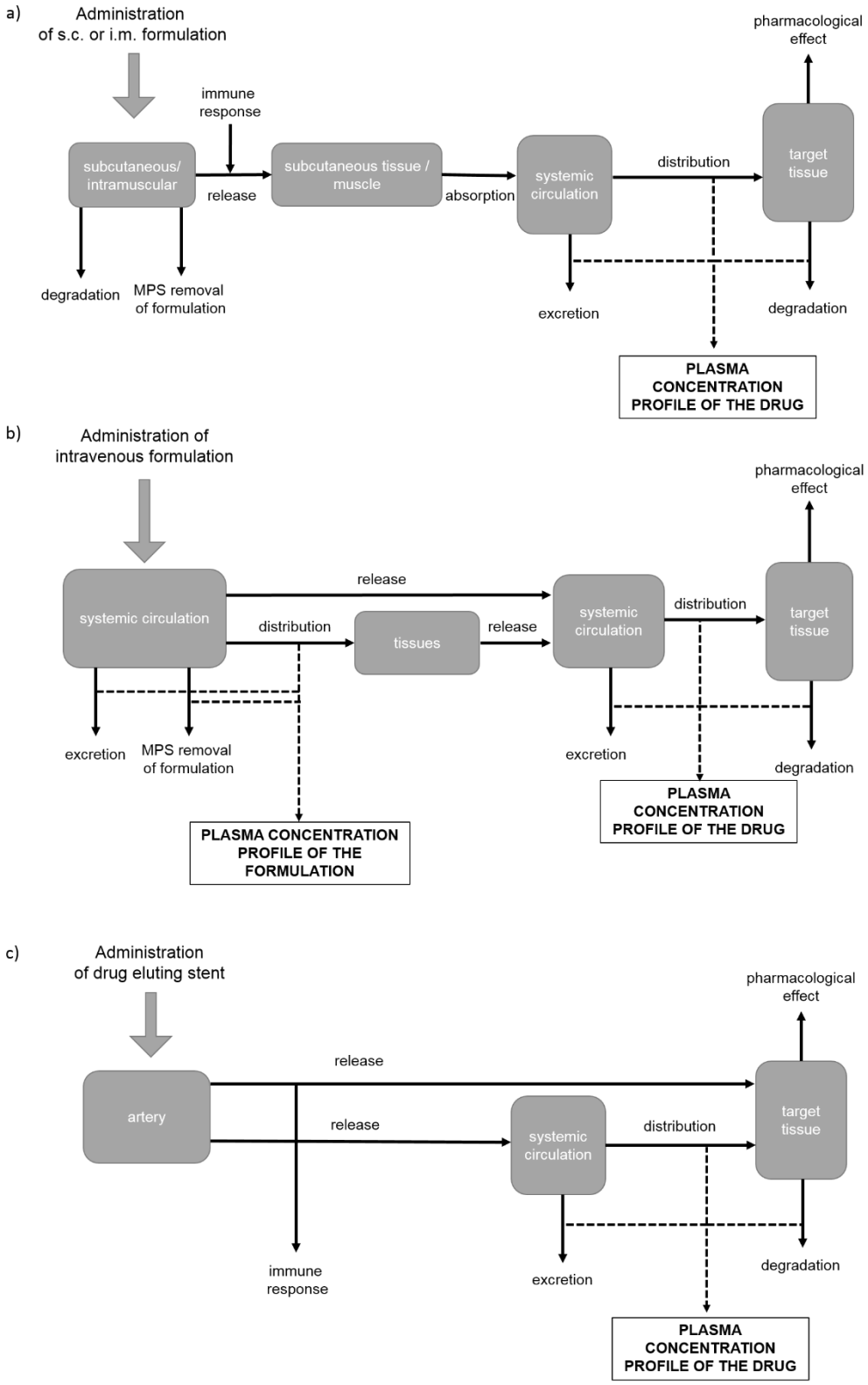

Figure 1.4. *In vivo* processes after administration of parenterals. a) Intramuscular and subcutaneous administration, b) intravenous administration, c) drug eluting stents.

For intravenous formulations (Figure 1.4b) the situation could be more complex. The formulation is administered to the bloodstream and simultaneously, the release of the drug and the distribution and elimination of the formulation (through urine or feces) are taking place. If the formulation consists of particles (liposomes), these will be removed from the circulation by the Mononuclear Phagocytic System (MPS). Cells cannot identify particles alone but they can recognize proteins bound to their surface by van der Waals, electrostatic, ionic, hydrophobic and hydrophilic forces [43]. Owens et al define opsonization as the process by which a foreign organism or particle becomes covered with opsonin proteins, thereby making it more visible to phagocytic cells [43]. Circulating opsonins include: IgG, IgM, complement fragments (C3, C5), fibronectin, laminin [44], α2-macroglobulin, apolipoprotein H (β2-glycoprotein I) and E [45], C-reactive protein, type I collagene [43] and albumin that can act either as an opsonin [46] or as a disopsonin (the opposite of an opsonin) [47, 48]. However, this needs to be addressed carefully as it was found for poly (lactic-co-glycolic acid) microparticles that the degradation of the particles was twice as fast *in vivo* than *in vitro*, due to the immune response [49].

It would be difficult to incorporate into an *in vitro* test the inflammation process at the site of administration that will affect the release from formulations. Options could include a mechanism of simultaneous release and removal of the formulation (possibly only feasible in sample and separate setup for intravenous administered formulations) in case that the immune response is relevant (stealth liposomes are less likely to be subject to removal by the immune system). In this case, the *in vivo* immune removal rate would be required but it is difficult to be estimated. It was believed that the immune response was only responsible for encapsulating the formulations and preventing drug release but new evidence has shown that cellular infiltration augments drug release [15, 29].

In the case of subcutaneous administration, the absorption of the drug is related to the molecular weight. Data from a goat model showed that small molecules are absorbed through the blood capillaries and large macromolecules through the lymph [50]. Studies performed in rats showed that molecules as large as albumin can be absorbed through blood capillaries [42].

Drug eluting stents (Figure 1.4c) are implanted in people diagnosed with arteriosclerotic disease. In the vessel wall, there will be deposition of lipids, cells of the immune system and calcification. The vessel is likely to be damaged during the implantation of the stent which may result in more inflammation and in a large modification of a normal vessel wall leading to a decrease in the absorption of drug [9]. The endothelial changes, affecting the absorption of drug from the stent would be difficult to simulate in an *in vitro* test.

1.4. Prediction of *in vivo* performance of parenterals

An IVIVC establishes the relationship between an *in vitro* parameter and an *in vivo* response after the administration of a formulation [51]. The FDA defines an IVIVC as a predictive mathematical model describing the relationship between an *in-vitro* property of a dosage form and an *in-vivo* response [52]. Generally, the *in vitro* property is the rate or the endpoint of dissolution and the *in vivo* response is the concentration or the amount of drug in plasma as a function of time [53]. According to the FDA, an IVIVC must be able to predict the *in vivo* behaviour accurately and consistently [52]. The EMA has a similar section for IVIVC in the document "Guideline on quality of oral modified release products" [54]. There are successful cases for IVIVC of oral dosage forms that utilize biorelevant media to simulate the physiological fluids of the gastrointestinal tract (GI tract) and the hydrodynamics that can be provided by the paddle apparatus [55], the flow through cell apparatus [56] or special setups that can simulate more closely the hydrodynamics of the GI tract [57]. This is translated into faster development processes and cost reductions. Although these guidelines and definitions were set for extended release oral dosage forms, they can be extrapolated to parenteral formulations. The widespread use and development of IVIVC has not been accomplished yet for parenteral formulations and examples are limited. The FDA mentions IVIVC in its draft guidance for liposomal products stating: "Although few examples exist, we encourage you to establish an IVIVC for the liposome product. Some IVIVRs may be established even if a complete IVIVC is not feasible" [12] suggesting that there is still a lot of research to be performed in this field.

1.4.1. IVIVC examples of parenteral formulations

Studies aiming to establish an IVIVC for parenteral formulations are presented in Table 1.4. It has to be noted that these studies are mainly for subcutaneous and intramuscular administrations. With respect to intravenous formulations, there are some examples of *in vitro* release tests that characterize the release of doxorubicin from liposomes (determining the residual drug remaining in the liposomes [58] or by dialysis methods [59, 60]) but these were not developed for predicting the *in vivo* behaviour and IVIVCs were not established.

Table 1.5. *In vitro in vivo* correlation (IVIVC) studies for parenteral formulations.

Drug (formulation/route of administration)	**Method**	**Medium**	***In vivo* release**	**IVIVC**	**Species**
Dialysis method					
Olanzapine microspheres/ subcutaneous [61] Risperidone Polymeric microspheres/ subcutaneous [62]	5 mL of medium in the dialysis tube and 40 mL in the receptor chamber; 37°C	phosphate buffer with sodium azide pH = 7.4	Wagner–Nelson deconvolution method fractional AUC approach	A linear relation was established between the *in vitro* and the *in vivo* drug released	Rats
Continuous flow method					
Dexamethasone PLGA microparticles/ subcutaneous [2]	Flow through cell apparatus small cell (diameter =12 mm) packed with 1 mm glass beads; microparticles	Phosphate buffer pH = 7.4 with 0.1 %w/v sodium azide.	Calculated by subtraction of the drug content in the degraded	After performing a time scaling/shifting for the *in vitro* release to match the	Rats

	dispersed in the cell; volume: 250mL (closed mode); flow rate 20mL/min; 37°C.		microspheres from the total drug loaded into the microspheres	*in vivo* release, a linear relation was achieved and an IVIVC was established.	
Risperdal®Consta® microspheres/ intramuscular [63]	Flow through cell apparatus small cell (diameter = 12 mm) packed with 1 mm glass beads; microparticles dispersed in the cell; volume: 250 mL (closed system); flow rate 8mL/min. 37, 45, 50 and 54.5°C.	Phosphate buffer pH = 7.4 with 0.1 %w/v sodium azide.	Loo–Riegelman deconvolution (from published *in vivo* data).	A linear correlation was established for the release tests performed at 50 and 54.5 °C	Human
Leuprolide osmotic implant/ subcutaneous [64]	Peristaltic pump; volume 12 mL (closed system); flow rate: 4mL/min.; 37°C.	Phosphate buffer with 2 %w/v sodium azide.	Calculated from the drug amount in the implant prior the implantation and after the	A linear relation was established between the *in vitro* and the *in vivo* drug released	Rats and male beagle dogs

	Duration of study: 3, 6, 9 and 12 months (*in vivo* study duration)		explantation in the animals at 3, 6, 9 and 12 months		
Risperidone microparticles/ intramuscular [65]	Flow through cell apparatus small cell (diameter = 12 mm) packed with 1 mm glass beads; microparticles dispersed in the cell; volume: 250 mL (closed system); flow rate 8mL/min. 37°C.	phosphate buffer	Wagner–Nelson deconvolution method	A linear relation was established between the *in vitro* and the *in vivo* drug released	Rabbits
Sample and separate methods					
Buserelin subcutaneours implants [66]	Centrifuge tubes with 12 mL of medium; 37°C	phosphate buffer pH = 7.4 with sodium azide and	Wagner–Nelson deconvolution method	A correlation between the mean *in vivo* residence time and the mean *in vitro*	Dogs

		benzalkonium chloride		dissolution time was established	
Risperidone microparticles/ intramuscular [65]	Micro particles suspended in phosphate buffer and shacked in a water bath.	phosphate buffer	Wagner–Nelson deconvolution method	Correlation not established	Rabbits
Methadone microspheres/ intraperitoneal and subcutaneous Methadone implant/ subcutaneous [67]	Microspheres or one implant were suspended in 100 mL of medium with constant stirring (50 rpm) at 37°C	Phosphate buffer pH=7.4 with 0.001% Tween 80	Numerical deconvolution	A linear relation was established between the *in vitro* and the *in vivo* drug released	Mice
Methylated lysozyme microsphere/ subcutaneous [49]	micro centrifuge tube with 1.5 mL of medium under continuous agitation at 37°C	Phosphate buffer saline	Numerical deconvolution	A linear relation was established between the *in vitro* and the *in vivo* drug released	Rats

It can be noticed that there are considerable differences among the techniques and conditions chosen for the release tests, animal models and mathematical data treatment. Furthermore there is a wide variety in the type of formulations (implants, microspheres and liposomes). The most utilized method to assess the *in vitro* release was SS followed by CF (Table 1.4). The release medium used in most examples is PBS pH = 7.4, with volumes of media used ranging from 1.5 to 250 mL.

1.4.2. PBPK modeling

Apart from the traditional approach, development of IVIVCs can be performed with the combination of *in vitro* release tests with advanced pharmacokinetic modeling approaches (i.e. physiologically based pharmacokinetic modeling (PBPK)) [68].

Physiologically based pharmacokinetic modeling (PBPK) is defined as the mathematical description of relevant physiological, physicochemical and biochemical processes in order to explain the pharmacokinetic behaviour of a compound [69]. The input parameters for the models are i) drug dependent (e.g. pka, logP, solubility, fraction unbound to proteins) and ii) drug independent (e.g. blood flows, tissue volumes) [70-73]. Commercial PBPK modeling software is available (e.g. Gastro-Plus®, simCYP® or PK-Sim® [68]) and reference to PBPK modeling is increasing from regulatory agencies [74]. The FDA have published the "Physiologically Based Pharmacokinetic Analyses — Format and Content (Guidance for Industry) [75]" and the EMA the "Guideline on the qualification and reporting of physiologically based pharmacokinetic (PBPK) modelling and simulation [76]".

PBPK models for parenteral formulations have been developed for several types of nanoparticles as reviewed by Li et. al. [77] including: carbon nanoparticles [78], polylactic-glycolic acid (PLGA) nanoparticles [78], silver nanoparticles [79], dendrimer [80] and gold/dendrimer composite nanoparticles [81].

A PBPK model for a liposomal formulation of Amphotericin B (Ambisome®) has been published. The model was based on rat and mouse data that were extrapolated to healthy humans and both the liposomal and the released drug were simulated [82, 83]. In a PBPK model for copolymer modified liposomes of docetaxel in mice, the PK of total docetaxel was described but the PK of released drug or drug in the liposomes was not taken into account [84, 85].

PBPK modeling has been used to simulate PK of long acting formulations following intramuscular administration [86].

1.4.2.2. Input of *in vitro* release data to the model

Mathematical models for *in vitro* release profiles can be divided into two main categories: empirical and mechanistic [87]. Mechanistic models include parameters related to the drug release mechanism from the dosage forms (e.g. Higuchi, Korsmeyer – Peppas [88]).

Empirical models are based on fitting data to a specific model [4]. As some parenterals are in the form of solid particles in suspension, common approaches to dissolution modeling can be used for such parenteral formulations. Examples include approaches made with the Weibull probability function for modeling the release from leuprolide polylactide and polylactide-co-glycolide microspheres [89] (Eq 1.2).

$$x = 1 - e^{-\alpha t^{\beta}} \qquad \text{Eq 1.2}$$

where x is the fraction released at time t, α is an apparent rate constant, β is the shape factor of Weibull function and t is the time.

In cases where there is an initial burst in the release, the equation can be modified to Equation 1.3:

$$x = x_{burst} + \left(1 - e^{-\alpha t^{\beta}}\right) \quad \text{Eq 1.3}$$

where x_{burst} is the fraction releasedof the initial burst, x is the fraction released at time t, α is an apparent rate constant, β is the shape factor of Weibull function and t is the time. It is important to notice that Weibull is a flexible probability function, so the release can easily fit to this equation, but it is not based in the mechanism that governs the release [89].

1.4.3. Challenges and points to consider for IVIVC for parenterals

To increase the predictability of the *in vitro* tests, understanding the fate of the formulations and the released drugs in the organism (Figure 1.2) could help to improve the development of PBPK models for parenterals. These models could be useful for IVIVC establishment and furthermore carry the potential for use in the development of a Pharmacokinetics/Pharmacodynamics (PK/PD) model [73].

A matter of the utmost importance is the fact that many of these parenteral formulations will be administered to patients whose disease may impact on the drug release; for example, the changes in protein concentration or the presence of inflammatory mediators could affect drug release [90]. The composition of the fluid at the administration site in a disease state must be considered to adapt the biorelevant release medium for simulation of this state. Currently, to the best of our knowledge, release media to simulate the disease state for parenterals are not available. Development of these types of release media would be important to predict the best clinical performance of the formulation in the target patients.

1.5. Conclusions

In vitro release testing can be a valuable tool during formulation development and assist prediction of *in vivo* behaviour. The tests might be modified in order to be biorelevant to obtain meaningful data that can be used in an IVIVC model. There are some promising results of IVIVC for parenteral formulations performed in animals but studies with humans are lacking. These limitations could be addressed through understanding of relevant *in vivo* factors at the site of administration and their application to *in vitro* testing through adjustment of test conditions, or alternatively judicious application of modeling techniques to reflect *in vivo* processes which are impossible to be replicated *in vitro*.

There is still a lot of research to be performed in the field of parenteral release/dissolution testing for establishment of compendial and biorelevant *in vitro* release tests.

Acknowledgments

The authors would like to thank the Mexican Council of Science and Technology (CONACyT) for the PhD scholarship of Mr R Diaz de Leon-Ortega.

1.6. References

[1]. Cho K, Wang X, Nie S, Chen Z, Shin DM. Therapeutic Nanoparticles for Drug Delivery in Cancer. Clinical Cancer Research. 2008;14(5):1310-6.

[2]. Zolnik BS, Burgess DJ. Evaluation of in vivo-in vitro release of dexamethasone from PLGA microspheres. Journal of controlled release : official journal of the Controlled Release Society. 2008;127(2):137-45.

[3]. Seidlitz A, Nagel S, Semmling B, Grabow N, Sternberg K, Weitschies W. Biorelevant Dissolution Testing of Drug-Eluting Stents: Experiences with a Modified Flow-Through Cell Setup. Dissolution Technologies. 2011;18(1):26-34.

[4]. D'Souza S. A Review of In Vitro Drug Release Test Methods for Nano-Sized Dosage Forms. Advances in Pharmaceutics. 2014;2014.

[5]. Phosphate-buffered saline (PBS). Cold Spring Harbor Protocols. 2006;2006(1):pdb.rec8247.

[6]. Shen J, Burgess DJ. In vitro dissolution testing strategies for nanoparticulate drug delivery systems: recent developments and challenges. Drug delivery and translational research. 2013;3(5):409-15.

[7]. D'Souza SS, DeLuca PP. Methods to assess in vitro drug release from injectable polymeric particulate systems. Pharm Res. 2006;23(3):460-74.

[8]. Shen J, Burgess DJ. Accelerated in-vitro release testing methods for extended-release parenteral dosage forms. J Pharm Pharmacol. 2012;64(7):986-96.

[9]. Seidlitz A, Weitschies W. In-vitro dissolution methods for controlled release parenterals and their applicability to drug-eluting stent testing. Journal of Pharmacy and Pharmacology. 2012;64(7):969-85.

[10]. Cardot J-M, Tomic I. In vitro in vivo correlation basis and application to slow release injectable formulation, a review. Farmacia. 2015;63(6):781 - 91.

[11]. FDA. Dissolution Methods database 2019 [09/01/2019]. Available from: https://www.accessdata.fda.gov/scripts/cder/dissolution/dsp_getallData.cfm.

[12]. FDA. Liposome Drug Products: Chemistry, Manufacturing, and Controls; Human Pharmacokinetics and Bioavailability; and Labeling Documentation. https://wwwfdagov/downloads/drugs/guidances/ucm070570pdf. 2005.

[13]. FDA. Draft guidance for industry: Drug products, including biological products, that contain nanomaterials. 2017.

[14]. Gray V, Cady S, Curran D, DeMuth J, Eradiri O, Hussain M, et al. In Vitro Release Test Methods for Drug Formulations for Parenteral Applications. Dissolution technologies. 2018;25(4):8-13.

[15]. Martinez M, Rathbone M, Burgess D, Huynh M. In vitro and in vivo considerations associated with parenteral sustained release products: a review based upon information presented and points expressed at the 2007 Controlled Release Society Annual Meeting. Journal of controlled release : official journal of the Controlled Release Society. 2008;129(2):79-87.

[16]. Wang Q, Fotaki N, Mao Y. Biorelevant dissolution: methodology and application in drug development. Dissolution Technologies. 2009;16(3):6-12.

[17]. Shepherd JT. The human cardiovascular system : facts and concepts. Vanhoutte PM, editor. New York: New York : Raven Press; 1979.

[18]. Ghuman J, Zunszain PA, Petitpas I, Bhattacharya AA, Otagiri M, Curry S. Structural Basis of the Drug-binding Specificity of Human Serum Albumin. Journal of Molecular Biology. 2005;353(1):38-52.

[19]. Ulldemolins M, Roberts JA, Rello J, Paterson DL, Lipman J. The effects of hypoalbuminaemia on optimizing antibacterial dosing in critically ill patients. Clinical Pharmacokinetics. 2011;50(2):99-110.

[20]. Fournier T, Medjoubi NN, Porquet D. Alpha-1-acid glycoprotein. Biochimica et biophysica acta. 2000;1482(1-2):157-71.

[21]. Marques MR, Loebenberg R, Almukainzi M. Simulated biological fluids with possible application in dissolution testing. Dissolution Technologies. 2011;18(3):15-28.

[22]. Krebs-Ringer Modified Buffer (KRB). Cold Spring Harbor Protocols. 2014;2014(1).

[23]. HiMedi-Labs. Krebs Ringer Buffer composition. http://himedialabscom/TD/TL1097pdf. 2013.

[24]. Rand PW, Lacombe E, Hunt HE, Austin WH. Viscosity of normal human blood under normothermic and hypothermic conditions. Journal of Applied Physiology. 1964;19(1):117-22.

[25]. Ghazal HS, Dyas AM, Ford JL, Hutcheon GA. In vitro evaluation of the dissolution behaviour of itraconazole in bio-relevant media. Int J Pharm. 2009;366(1):117-23.

[26]. Macheras P, Reppas C. Dissolution and in vitro permeation behaviours of dicumarol nitrofurantoin and sulfamethizole in the presence of protein. Int J Pharm. 1987;37(1):103-12.

[27]. Bastidas DM, Cano E, Mora E. Influence of oxygen, albumin and pH on copper dissolution in a simulated uterine fluid. Eur J Contracept Reprod Health Care. 2005;10(2):123-30.

[28]. Semmling B, Nagel S, Sternberg K, Weitschies W, Seidlitz A. Long-term stable hydrogels for biorelevant dissolution testing of drug-eluting stents. Journal of Pharmaceutical Technology and Drug Research. 2013;2(1):19.

[29]. Fogh-Andersen N, Altura BM, Altura BT, Siggaard-Andersen O. Composition of interstitial fluid. Clinical Chemistry. 1995;41(10):1522-5.

[30]. Kokubo T, Takadama H. How useful is SBF in predicting in vivo bone bioactivity? Biomaterials. 2006;27(15):2907-15.

[31]. Ganong WF. Review of medical physiology. 20th international ed. New York London. Lange Medical/McGraw-Hill; 2001.

[32]. Tortora GJ. Principles of anatomy and physiology. 11th ed. ed. Derrickson B, Tortora GJ, editors. Hoboken, N.J.: Hoboken, N.J. : Wiley; 2006.

[33]. Klarhofer M, Csapo B, Balassy C, Szeles JC, Moser E. High-resolution blood flow velocity measurements in the human finger. Magnetic resonance in medicine. 2001;45(4):716-9.

[34]. Di Mario C, Meneveau N, Gil R, de Jaegere P, de Feyter PJ, Slager CJ, et al. Maximal blood flow velocity in severe coronary stenoses measured with a Doppler guidewire: Limitations for the application of the continuity equation in the assessment of stenosis severity. The American Journal of Cardiology. 1993;71(14):D54-D61.

[35]. Zuidema J, Pieters FAJM, Duchateau GSMJE. Release and absorption rate aspects of intramuscularly injected pharmaceuticals. Int J Pharm. 1988;47(1):1-12.

[36]. Townsley MI, Stevens T. Lung Endothelium: Biota Publishing; 2015.

[37]. Levick JR. Revision of the Starling principle: new views of tissue fluid balance. The Journal of Physiology. 2004;557(Pt 3):704-.

[38]. Korthuis RJ, editor Skeletal muscle circulation. Colloquium Series on Integrated Systems Physiology: From Molecule to Function; 2011: Morgan & Claypool Life Sciences.

[39]. Iyer SS, Barr WH, Karnes HT. Profiling in vitro drug release from subcutaneous implants: a review of current status and potential implications on drug product development. Biopharmaceutics & drug disposition. 2006;27(4):157-70.

[40]. Howard JR, Hadgraft J. The clearance of oily vehicles following intramuscular and subcutaneous injections in rabbits. Int J Pharm. 1983;16(1):31-9.

[41]. Evans EF, Proctor JD, Fratkin MJ, Velandia J, Wasserman AJ. Blood flow in muscle groups and drug absorption. Clin Pharmacol Ther. 1975;17(1):44-7.

[42]. Kagan L, Gershkovich P, Mendelman A, Amsili S, Ezov N, Hoffman A. The role of the lymphatic system in subcutaneous absorption of macromolecules in the rat model. Eur J Pharm Biopharm. 2007;67(3):759-65.

[43]. Owens DE, Peppas NA. Opsonization, biodistribution, and pharmacokinetics of polymeric nanoparticles. Int J Pharm. 2006;307(1):93-102.

[44]. Kettiger H, Schipanski A, Wick P, Huwyler J. Engineered nanomaterial uptake and tissue distribution: from cell to organism. Int J Nanomed. 2013;8:3255-69.

[45]. Yan X, Scherphof GL, Kamps JA. Liposome opsonization. Journal of liposome research. 2005;15(1-2):109-39.

[46]. Savay S, Szebeni J, Baranyi L, Alving CR. Potentiation of liposome-induced complement activation by surface-bound albumin. Biochimica et biophysica acta. 2002;1559(1):79-86.

[47]. Thiele L, Diederichs JE, Reszka R, Merkle HP, Walter E. Competitive adsorption of serum proteins at microparticles affects phagocytosis by dendritic cells. Biomaterials. 2003;24(8):1409-18.

[48]. Ogawara K, Furumoto K, Nagayama S, Minato K, Higaki K, Kai T, et al. Pre-coating with serum albumin reduces receptor-mediated hepatic disposition of polystyrene nanosphere: implications for rational design of nanoparticles. Journal of controlled release : official journal of the Controlled Release Society. 2004;100(3):451-5.

[49]. van Dijkhuizen-Radersma R, Wright SJ, Taylor LM, John BA, de Groot K, Bezemer JM. In Vitro/in Vivo Correlation for 14C-Methylated Lysozyme Release from Poly(Ether-Ester) Microspheres. Pharmaceutical Research. 2004;21(3):484-91.

[50]. McLennan DN, Porter CJH, Charman SA. Subcutaneous drug delivery and the role of the lymphatics. Drug Discovery Today: Technologies. 2005;2(1):89-96.

[51]. Shargel L. Applied biopharmaceutics and pharmacokinetics. 6th ed. ed. Yu ABC, Wu-Pong S, editors. New York London: New York London : McGraw-Hill; 2012.

[52]. FDA. Extended Release Oral Dosage Forms: Development, Evaluation, and Application of In Vitro/In Vivo Correlations.

http://wwwfdagov/downloads/drugs/guidancecomplianceregulatoryinformation/guidances/ucm070239pdf. 1997.

[53]. Sakore S, Chakraborty B. In vitro–in vivo correlation (IVIVC): a strategic tool in drug development. J Bioequiv Availab S. 2011;3:2.

[54]. EMA. Guideline on quality of oral modified release products (Drafts). 2012.

[55]. Kovačević I, Parojčić J, Homšek I, Tubić-Grozdanis M, Langguth P. Justification of Biowaiver for Carbamazepine, a Low Soluble High Permeable Compound, in Solid Dosage Forms Based on IVIVC and Gastrointestinal Simulation. Molecular Pharmaceutics. 2009;6(1):40-7.

[56]. Sunesen VH, Pedersen BL, Kristensen HG, Müllertz A. In vivo in vitro correlations for a poorly soluble drug, danazol, using the flow-through dissolution method with biorelevant dissolution media. Eur J Pharm Sci 2005;24(4):305-13.

[57]. Souliman S, Blanquet S, Beyssac E, Cardot J-M. A level A in vitro/in vivo correlation in fasted and fed states using different methods: Applied to solid immediate release oral dosage form. Eur J Pharm Sci 2006;27(1):72-9.

[58]. Silverman L, Barenholz Y. In vitro experiments showing enhanced release of doxorubicin from Doxil(R) in the presence of ammonia may explain drug release at tumor site. Nanomedicine : nanotechnology, biology, and medicine. 2015;11(7):1841-50.

[59]. Mussi SV, Parekh G, Pattekari P, Levchenko T, Lvov Y, Ferreira LA, et al. Improved pharmacokinetics and enhanced tumor growth inhibition using a nanostructured lipid carrier loaded with doxorubicin and modified with a layer-by-layer polyelectrolyte coating. Int J Pharm. 2015;495(1):186-93.

[60]. Ohnishi N, Tomida H, Ito Y, Tahara K, Takeuchi H. Characterization of a doxorubicin liposome formulation by a novel in vitro release test methodology using column-switching high-performance liquid chromatography. Chemical & pharmaceutical bulletin. 2014;62(6):538-44.

[61]. D'Souza S, Faraj JA, Giovagnoli S. IVIVC from Long Acting Olanzapine Microspheres. International journal of biomaterials. 2014;2014:407065.

[62]. D'Souza S, Faraj JA, Giovagnoli S, DeLuca PP. In vitro–in vivo correlation from lactide-co-glycolide polymeric dosage forms. Progress in Biomaterials. 2014;3(2-4):131-42.

[63]. Rawat A, Bhardwaj U, Burgess DJ. Comparison of in vitro-in vivo release of Risperdal((R)) Consta((R)) microspheres. Int J Pharm. 2012;434(1-2):115-21.

[64]. Wright JC, Tao Leonard S, Stevenson CL, Beck JC, Chen G, Jao RM, et al. An in vivo/in vitro comparison with a leuprolide osmotic implant for the treatment of prostate cancer. Journal of controlled release : official journal of the Controlled Release Society. 2001;75(1-2):1-10.

[65]. Shen J, Choi S, Qu W, Wang Y, Burgess DJ. In vitro-in vivo correlation of parenteral risperidone polymeric microspheres. Journal of controlled release : official journal of the Controlled Release Society. 2015;218:2-12.

[66]. Schliecker G, Schmidt C, Fuchs S, Ehinger A, Sandow J, Kissel T. In vitro and in vivo correlation of buserelin release from biodegradable implants using statistical moment analysis. Journal of controlled release : official journal of the Controlled Release Society. 2004;94(1):25-37.

[67]. Negrin CM, Delgado A, Llabres M, Evora C. In vivo-in vitro study of biodegradable methadone delivery systems. Biomaterials. 2001;22(6):563-70.

[68]. Kesisoglou F, Chung J, van Asperen J, Heimbach T. Physiologically Based Absorption Modeling to Impact Biopharmaceutics and Formulation Strategies in Drug Development-Industry Case Studies. Journal of pharmaceutical sciences. 2016;105(9):2723-34.

[69]. Khalil F, Laer S. Physiologically based pharmacokinetic modeling: methodology, applications, and limitations with a focus on its role in pediatric drug development. Journal of biomedicine & biotechnology. 2011;2011:907461.

[70]. Batchelor HK, Fotaki N, Klein S. Paediatric oral biopharmaceutics: key considerations and current challenges. Advanced drug delivery reviews. 2014;73:102-26.

[71]. Espie P, Tytgat D, Sargentini-Maier ML, Poggesi I, Watelet JB. Physiologically based pharmacokinetics (PBPK). Drug metabolism reviews. 2009;41(3):391-407.

[72]. Jones HM, Gardner IB, Watson KJ. Modelling and PBPK simulation in drug discovery. The AAPS journal. 2009;11(1):155-66.

[73]. Morita T, Sakamura Y, Horikiri Y, Suzuki T, Yoshino H. Evaluation of in vivo release characteristics of protein-loaded biodegradable microspheres in rats and severe combined immunodeficiency disease mice. J Control Release. 2001;73(2–3):213-21.

[74]. Zhuang X, Lu C. PBPK modeling and simulation in drug research and development. Acta Pharmaceutica Sinica B. 2016;6(5):430-40.

[75]. FDA. Physiologically Based Pharmacokinetic Analyses — Format and Content 2018 [cited 2018 15/11/2018]. Available from: https://www.fda.gov/downloads/Drugs/GuidanceComplianceRegulatoryInformation/Guidances/UCM531207.pdf.

[76]. EMA. Guideline on the qualification and reporting of physiologically based pharmacokinetic (PBPK) modelling and simulation: EMA; 2016 [cited 2018 15/11/2018]. Available from: https://www.ema.europa.eu/documents/scientific-guideline/guideline-qualification-reporting-physiologically-based-pharmacokinetic-pbpk-modelling-simulation_en.pdf.

[77]. Li M, Zou P, Tyner K, Lee S. Physiologically Based Pharmacokinetic (PBPK) Modeling of Pharmaceutical Nanoparticles. The AAPS Journal. 2017;19(1):26-42.

[78]. Péry ARR, Brochot C, Hoet PHM, Nemmar A, Bois FY. Development of a physiologically based kinetic model for 99m-Technetium-labelled carbon nanoparticles inhaled by humans. Inhalation Toxicology. 2009;21(13):1099-107.

[79]. Bachler G, von Goetz N, Hungerbühler K. A physiologically based pharmacokinetic model for ionic silver and silver nanoparticles. International journal of nanomedicine. 2013;8:3365-82.

[80]. Opitz AW, Wickstrom E, Thakur ML, Wagner NJ. Physiologically based pharmacokinetics of molecular imaging nanoparticles for mRNA detection determined in tumor-bearing mice. Oligonucleotides. 2010;20(3):117-25.

[81]. Mager DE, Mody V, Xu C, Forrest A, Lesniak WG, Nigavekar SS, et al. Physiologically Based Pharmacokinetic Model for Composite Nanodevices: Effect of Charge and Size on In Vivo Disposition. Pharmaceutical Research. 2012;29(9):2534-42.

[82]. Kagan L, Gershkovich P, Wasan KM, Mager DE. Physiologically Based Pharmacokinetic Model of Amphotericin B Disposition in Rats Following Administration of Deoxycholate Formulation (Fungizone®): Pooled Analysis of Published Data. The AAPS Journal. 2011;13(2):255.

[83]. Kagan L, Gershkovich P, Wasan KM, Mager DE. Dual Physiologically Based Pharmacokinetic Model of Liposomal and Nonliposomal Amphotericin B Disposition. Pharmaceutical Research. 2014;31(1):35-45.

[84]. Lu X-F, Bi K, Chen X. Physiologically based pharmacokinetic model of docetaxel and interspecies scaling: comparison of simple injection with folate receptor-targeting amphiphilic copolymer-modified liposomes. Xenobiotica. 2016;46(12):1093-104.

[85]. Bradshaw-Pierce EL, Eckhardt SG, Gustafson DL. A Physiologically Based Pharmacokinetic Model of Docetaxel Disposition: from Mouse to Man. Clinical Cancer Research. 2007;13(9):2768.

[86]. Rajoli RKR, Back DJ, Rannard S, Freel Meyers CL, Flexner C, Owen A, et al. Physiologically Based Pharmacokinetic Modelling to Inform Development of Intramuscular Long-Acting Nanoformulations for HIV. Clinical Pharmacokinetics. 2015;54(6):639-50.

[87]. Siepmann J, Göpferich A. Mathematical modeling of bioerodible, polymeric drug delivery systems. Advanced Drug Delivery Reviews. 2001;48(2):229-47.

[88]. Costa P, Sousa Lobo JM. Modeling and comparison of dissolution profiles. European Journal of Pharmaceutical Sciences. 2001;13(2):123-33.

[89]. D'Souza SS, Faraj JA, DeLuca PP. A model-dependent approach to correlate accelerated with real-time release from biodegradable microspheres. Aaps PharmSciTech. 2005;6(4):E553-E64.

[90]. Blot SI, Pea F, Lipman J. The effect of pathophysiology on pharmacokinetics in the critically ill patient — Concepts appraised by the example of antimicrobial agents. Advanced Drug Delivery Reviews. 2014;77(0):3-11.

Chapter 2. Investigation and simulation of dissolution with concurrent degradation under healthy and hypoalbuminaemic simulated parenteral conditions- case example Amphotericin B

Abstract

Guidance on dissolution testing for parenteral formulations is limited and not often related to *in vivo* performance. Critically ill patients represent a target cohort, frequently hypoalbuminaemic, to whom certain parenteral formulations are administered. Amphotericin B (AmB) is a poorly soluble, highly protein-bound drug, available as lipid-based formulations and used in critical illness. The aim of this study was to develop media representing hypoalbuminaemic and healthy plasma, and to understand and simulate the dissolution profile of AmB in biorelevant media. Dissolution media were prepared with bovine serum albumin (BSA) in Krebs-Ringer buffer, and tested in a flow through cell apparatus and a bottle/stirrer setup. Drug activity was tested against *Candida albicans*. BSA concentration was positively associated with solubility, degradation rate and maximum amount dissolved, and negatively associated with dissolution rate constant and antifungal activity. In the bottle/stirrer setup, a biexponential model successfully described simultaneous dissolution and degradation, and increased in agitation reduced the discriminatory ability of the test. The hydrodynamics provided by the flow-through cell apparatus were not adequate to dissolve the drug. Establishing discriminating test methods with albumin present in the dissolution media, representing the target population, supports future development of biorelevant and clinically relevant tests for parenteral formulations.

Keywords:

biorelevant; dissolution; albumin; hypoalbuminaemia; solubility; degradation; amphotericin B

2.1. Introduction

The parenteral administration route is utilized when a quick or a depot effect is needed, when the patient cannot take oral formulations for systemic therapy or when the physicochemical properties of the drug make it impossible to be delivered by any other route [1]. Formulations such as microspheres, liposomes, nanoparticles and emulsions (among others) have been developed to be able to meet the requirements of a long or a sustained exposure. The dissolution test is an *in vitro* test designed to characterize the dissolution/release of the drug from a formulation and hopefully, predict the behaviour of the drug *in vivo*. There are 3 main methods to assess dissolution/release from controlled release parenterals that have been described extensively in the literature: Sample and separate, Continuous flow and Dialysis methods [2-6].

Several factors may influence the dissolution of a formulation *in vivo*. As the ultimate goal of the dissolution test is to ensure clinical performance, these factors should be reflected in the dissolution test [7]. Biorelevant dissolution testing takes into consideration the characteristics of the site of administration *in vivo* that may impact on the dissolution and release of a drug from a formulation. This involves the composition and the physicochemical properties of the medium and the hydrodynamics where the drug will be released [8].

For parenterals administered intravenously the release medium is blood, consisting of 2 fractions, the cellular fraction and plasma. Plasma is a fluid that contains ions and biomolecules. Albumin is the major circulating protein in human plasma (up to the 60% of plasma proteins). The normal reference value of plasma albumin for a healthy subject is 40 g/L ± 10% [9]. Albumin is the most relevant protein in terms of drug administration as it is a carrier for metals, ions, fatty acids, amino acids, bilirubin, enzymes and drugs [9].

Several parenteral formulations, that are not simple aqueous solutions, can be administered in the clinical setting to patients that have significant morbidities such as cancer or critically illness. Hypoalbuminaemia is common in the critical ill patients (affecting approximately 50% of patients), and while there is no reference value for hypoalbuminaemia, it can be considered when the plasma albumin levels are lower than < 25 g/L [9]. Low levels of serum albumin may affect pharmacokinetics and pharmacodynamics of highly protein bound drugs. With a decrease in the protein

levels in plasma there is more unbound drug in circulation which would lead to an increased pharmacological effect. On the other hand, the free drug can penetrate into tissues with a corresponding increase in the volume of distribution and a subsequent decrease in the maximum plasma concentration [9, 10]. Release/dissolution of poorly soluble, highly protein bound drugs from parenteral formulations, and associated local drug concentrations are likely to be influenced by protein concentration at the site of release. Therefore, *in vitro* dissolution tests that simulate the *in vivo* environment are needed for parenteral formulations that are not aqueous solutions, which take into account the likely changes that arise in target patient groups, with particular reference to albumin concentration.

One drug that is administered to critically ill patients is Amphotericin B (AmB), which is still one of the most effective therapies for systemic fungal infections. In clinical practice, AmB is administered as an infusion using a multidose scheme usually lasting for several days [11]. AmB is highly bound (>95%) to plasma proteins (Low Density Lipoproteins, albumin and α1 glycoproteins [12, 13]). The major drawback of AmB is its poor water solubility (reported values: 0.09 µg/mL [14], 1.38 µg/mL [15] and 6 µg/mL [16] at pH = 7). To tackle this problem, several formulations have been developed, including Liposomal AmB (Ambisome®) and AmB in a lipid complex (Abelcet®), where AmB is within the lipid structures. Furthermore, a correlation has been observed between volume of distribution at steady state of total AmB following administration of Abelcet® and albumin concentration, in critically ill patients [17], illustrating the relevance of albumin concentration to AmB pharmacokinetics in the target patient cohort.

The aim of this study was to investigate the solubility and the dissolution of AmB in simulated plasma with albumin concentrations representing healthy subjects and hypoalbuminaemic patients, and to develop a mathematical model to describe and simulate all the processes involved in its dissolution, in order to be the basis for the development of biorelevant dissolution testing of AmB formulations.

2.2. Materials and Methods

2.2.1 Materials

AmB analytical standard (87.8%), Methanol (MeOH) High Performance Liquid Chromatography (HPLC) grade, formic acid, Sabouraud Dextrose (SBD) Broth, NaOH, $MgCl_2$, $CaCl_2$, $NHCO_3$ and NH_4HCO_2 were obtained from Sigma Aldrich (Germany); AmB active pharmaceutical ingredient (API) powder (85%) from Cayman Chemical (USA); BSA Protease Free Powder Fraction V, dimethyl sulfoxide (DMSO), dextrose, Na_2HPO_4, NaH_2PO_4, NaCl and KCl were obtained from Fisher Scientific (USA); Sabouraud dextrose (SBD) agar was obtained from Oxoid (UK), 25 mL sterile universal culture tubes were obtained from Sterilin Thermo Scientific (UK); 10 µL plastic loops from Microspec (UK); GF/D (pore size 2.7 µm, 25 mm diameter) and GF/F (pore size 0.7 µm, 25 mm diameter) filters were obtained from Whatman (UK) and regenerated cellulose (RC) filters 0.45 µm 13 mm diameter from Cronus (UK). The yeast strain used in the microbiology experiments was *Candida albicans* SC5314 [18].

2.2.2. Dissolution biorelevant media composition and characterization

The dissolution media employed were Krebs-Ringer Buffer (KRB), supplemented with BSA at different concentrations according to the experiment: 1.5, 2.0, 3.0 or 4.0% w/v. The pH was adjusted to 7.2 – 7.3 with 0.1 M HCl using a Seven Compact pH meter (Mettler Toledo, China). The osmolality of the media with 2.0 and 4.0% w/v BSA was measured via the freezing-point depression method with a Micro-Osmometer 3300 (Advanced Instruments, Massachusetts USA). Viscosity of all media was measured with a Bohlin Rheometer (Germany) with a shear rate 0.1 - 1.5 Pa (logarithmic scale), 20 integrations per measurement and with a delay time of 5 seconds and an integration time of 20 seconds. The geometry was a 4° and 40 mm diameter (CP 4/40) cone parallel to a plate and the experiments were conducted at 25°C in triplicate. The measurement at the closest value to the steady state was recorded as the viscosity value.

2.2.3. Chromatographic conditions for the analysis of AmB from biorelevant dissolution media samples

The chromatographic method to quantify AmB was a modification of the method reported by Nilsson-Ehle et al [19]. Briefly, AmB was quantified by HPLC analysis using a Hewlett Packard Series 1100 equipped with an auto sampler, temperature regulated column compartment, quaternary pump and diode array detector (DAD detector) (Agilent Technologies). The column was a C18 Waters Sunfire Column (Ireland) 150 x 46 mm 5μm. The temperature of the column compartment was set at 25°C. The mobile phase consisted of formate buffer (50 mM; pH = 3.2): MeOH (25:75, v/v); the flow rate was 1 mL/min and analysis was performed with the DAD detector at λ = 406 nm. The UV spectrum was recorded from 300 to 450 nm (where necessary for detection of the degradant). Quantification of AmB in samples was made based on calibration curves. Freshly prepared standard solutions (0.5 – 10 μg/mL) in the corresponding medium were prepared by appropriate dilution of a 500 μg/mL stock solution of AmB analytical standard in 1:1 MeOH: DMSO v/v. The 5 μg/mL standard solution in KRB – BSA 4% w/v was incubated at 37°C and was monitored every hour to check the stability of the samples for up to 24 h. The limit of detection and the limit of quantification were 0.12 and 0.37 μg/mL, respectively.

2.2.4. Sample treatment of AmB in the biorelevant dissolution media

Proteins were precipitated by adding 2 volumes of methanol to 1 volume of the sample followed by mixing in a vortex (Scientific Industry Inc., USA) for 30 seconds and then centrifuged for 10 minutes at 12000 rpm and 5°C (Eppendorf Heraeus Fresco 17 centrifuge, Thermo Electron LED GmbH., Germany). The supernatant was filtered through a 0.45 μm RC filter before injected to the HPLC.

2.2.5. Liquid chromatography – Mass Spectrometry (LCMS) studies

The identification of the mass of the molecular structures detected as peaks in the HPLC chromatograms was performed by LCMS. An excess of AmB was added to the medium (KBR-BSA 4.0% w/v) and after stirring for 8 h at 130 rpm [Variomag multipoint stirring plate (Thermo Electron Corporation, Germany); 15 x 6 mm magnetic stirrers (Fisherbrand, UK)] at 37°C, the undissolved drug was removed by centrifugation [3000 rpm 5 min 5°C]. The supernatant was treated for protein precipitation (section 2.2.4) and analysed by LCMS [Ultimate 3000 UHPLC (Dionex,

USA); autosampler; quaternary pump; DAD detector; maXisHD Time-of-Flight Mass Spectrometer coupled with an electrospray source (ESI-TOF) (Bruker Daltonics, Germany)]. The conditions of the chromatography analysis were the same as previously described (section 2.2.3), with the exception of the injection volume being 30 µL and a split flow post column before the mass spectrometry detector to a flow rate of 0.3 mL/min. In this case, the formate buffer (50 mM) was prepared with formic acid and ammonium formate, in order to make it suitable for Mass Spectrometry (absence of sodium ions). The samples were analysed in negative mode. Data was processed using external calibration with the Bruker Daltonics software (DataAnalysisTM) as part of the overall hardware control software (CompassTM).

2.2.6. Degradation studies of AmB in the biorelevant dissolution media

In order to characterise the degradation of AmB in the dissolution media, approximately 10 mg of AmB API powder was added to 50 mL of the dissolution media (KRB-BSA 1.5, 2.0, 3.0, or 4.0% w/v) and then stirred for 1 h at 130 rpm (in Variomag multipoint stirring plate) at 37°C. The samples were centrifuged for 5 minutes at 3000 rpm and 4°C (Heraeus Biofuge Primo R Centrifuge, Thermo Electron LED GmbH. Germany), to remove the undissolved AmB and the supernatant was incubated at 37°C. Samples were taken at 0.5, 1.0, 1.5, 2.0, 3.0, 4.0, 5.0, 6.0 and 8.0 h, injected to the HPLC after sample treatment (protein precipitation; section 2.2.4) and the concentration of AmB in the samples was calculated. All experiments were performed in triplicate. A linear fit was applied to the degradation data from 4 h to the last time point, after a natural logarithm transformation of the measured concentration (Excel 2013, Microsoft. USA) and the degradation rate constant (k_{deg}) was calculated from the slope of the line.

2.2.7. Solubility studies of AmB in the biorelevant dissolution media

Approximately 2.5 mg of AmB API powder were placed in a 100 mL glass bottle (56 mm diameter/ 105 mm height; Duran, Germany) with 30 mL of KRB supplemented with BSA 1.5, 2.0, 3.0 or 4.0% w/v, stirred at 130 rpm (in Variomag multipoint stirring plate) and incubated at 37°C. The sampling times were 0.5, 1.0, 1.5, 2.0, 3.0, 4.0, 5.0, 6.0, 8.0, 10.0, 12.0 and 24.0 hours. The undissolved AmB was removed by centrifugation (Eppendorf centrifuge 3000 rpm, 5 min, 5°C; following validation (data not shown) centrifugation was selected as a cost-effective alternative to filtration) and

after sample treatment (protein precipitation; section 2.2.4), the samples were injected to the HPLC and the concentration of AmB in the samples was calculated. All experiments were performed in triplicate.

2.2.8 Mass balance studies of AmB in the biorelevant dissolution media

The total undissolved, dissolved and degraded percentages of AmB in KRB-BSA 2.0% and 4.0% w/v media were calculated. Approximately 0.3 mg of the AmB API powder were weighed on a micro balance (Sartorius SE 2-F connected to an Eliex E550 antistatic device). The AmB was placed in a 100 mL glass bottle containing 15 mL of dissolution medium (KRB with 2.0 or 4.0% w/v BSA), and then stirred at 130 rpm and incubated at 37°C. A 1 mL sample withdrawn at 24 h was centrifuged (3000 rpm, 5 min, 5°C; removal of the undissolved AmB), and after addition of methanol for the protein precipitation (section 2.2.4), was injected to the HPLC and the AmB concentration ($AmB\ dissolved\ at\ 24\ h$) was calculated. The remaining AmB in the bottle was dissolved with methanol (protein precipitation procedure; section 2.2.4), analysed and the final concentration of AmB ($AmB\ final$) was calculated. All experiments were performed in triplicate. The total undissolved ($AmB\ T_{undissolved}$: AmB undissolved powder in the bottle), the total dissolved ($AmB\ T_{dissolved}$: AmB in solution at 24 h and AmB degraded up to 24 h) and the total degraded ($AmB\ T_{degraded}$: AmB degraded up to 24 h) percentages of AmB were calculated based on Eq (2.1 – 2.3):

$$AmB\ T_{undissolved} = AmB\ final - AmB\ dissolved\ at\ 24\ h \quad \text{Eq 2.1}$$

$$AmB\ T_{dissolved} = AmB\ initial - AmB\ T_{undissolved} \quad \text{Eq 2.2}$$

where $AmB\ initial$ is the mass (0.3 mg) placed into the reservoir initially (100%)

$$AmB\ T_{degraded} = AmB\ T_{dissolved} - AmB\ dissolved\ at\ 24\ h \quad \text{Eq 2.3}$$

2.2.9. Antimicrobial activity assay of AmB in the biorelevant media: MIC and MFC determination

2.2.9.1. Quantification of C. albicans.

The strain was maintained on SBD agar plates. A new culture was started from a single colony in a culture tube with 5 mL of SBD broth and was incubated at 37°C overnight in a shaking incubator (Innova 44, New Brunswick Scientific, USA), after which the

optical density (OD) was measured at 600 nm (OD_{600}). The Colony Forming Units (CFU) of the culture was determined by preparing serial dilutions from 10^{-1} to 10^{-6}. 100 μL of the suspensions were plated on SBD agar plates, incubated overnight at 37°C, the number of colonies was counted and the relationship with the OD_{600} of the culture was established.

2.2.9.2. MIC and MFC studies.

The OD_{600} of an overnight culture of *C. albicans* was measured, and diluted to a final concentration of 10^5 CFU/mL. Minimum Inhibitory Concentration (MIC) studies were performed with the following concentrations of AmB: 0, 1.5, 3.0, 4.5, 6.0, 7.5, 9.0 and 10.5 μg/mL for the experiments with BSA 2.0% w/v, and 0, 3.0, 4.5, 6.0, 7.5, 9.0, 10.5 and 12.0 μg/mL for the experiments with BSA 4.0% w/v. Culture medium without BSA was set as the control for these experiments. The MIC was defined as the lowest concentration of AmB at which there was no visual turbidity in the liquid broth. The Minimum Fungicidal Concentration (MFC) experiments were performed by plating 10 μL of the yeast cultures from the MIC assays on SBD agar plates and incubated for 24 h at 37°C. The MFC was defined as the lowest concentration of AmB where there was no visible growth on the agar plates. The results are expressed as the intervals where the MIC and MFC were found. The experiments were performed in duplicate.

2.2.10. Dissolution studies of AmB in biorelevant media

2.2.10.1. Sample and separation method (bottle/stirrer)

Dissolution studies were carried in a glass bottle with a similar setup as the solubility experiments (section 2.2.7). 0.5 mg of AmB API powder was weighed and placed into a 100 mL glass bottle with 30 mL of the dissolution medium. Two hydrodynamic conditions were tested: low agitation (130 rpm) for KRB – BSA 0, 1.5, 2.0, 3.0 and 4.0% w/v and high agitation (380 rpm) for experiments with KRB – BSA 2.0% w/v and BSA 4.0% w/v. Samples were withdrawn up to 24 h were treated and analysed as previously described (sections 2.2.7 and 2.2.4) and the % AmB dissolved over time was calculated. All experiments were performed in triplicate.

2.2.10.2. Continuous Flow method (flow through cell apparatus)

The dissolution studies were carried out in a flow-through cell dissolution apparatus (Sotax CE7 smart connected to a Sotax piston pump CP7, Sotax, Switzerland) operated in the closed mode [20]. A 5mm ruby glass bead was positioned at the bottom of the cell (small cell:12 mm diameter; large cell: 22.6 mm diameter), the conical part of the cell was filled with 1 mm glass beads and 5 mg of AmB API powder were weighed and placed on top of the glass beads. Glass fibre filters (GF/D, GF/F) were positioned at the top of the cell. Two different hydrodynamic conditions were tested: i. small cell with a flow rate of 35 mL/min (high velocity) and ii. large cell with a flow rate of 16 mL/min (low velocity). 50 mL of the dissolution medium (KRB with BSA 2.0% w/v or 4.0% w/v) were put in the reservoir under constant stirring. 0.5 mL samples were collected at specific time points up to 8 h and volume replacement with fresh medium was made. Dissolution experiments were also performed with 0.5 mg of AmB in the two media (KRB with BSA 2.0% w/v or 4.0% w/v) under both velocity conditions and with 5 mg of AmB API in water (HPLC grade) under high velocity conditions. The samples after treatment (protein precipitation; section 2.2.4) were injected to the HPLC and the % AmB dissolved over time was calculated. All experiments were performed in triplicate at 37°C.

2.2.11. Treatment of dissolution data

The AmB dissolution profiles were corrected for degradation using the corresponding degradation rate constants (section 2.2.6). The concentration over time accounting for degradation ($C_{corrected}$) was calculated using Eq 2.4.

$$C_{corrected} = C_t + k_{deg} * AUC_{0-t} \quad \text{Eq 2.4.}$$

Where C_t is the observed concentration at time t, $AUC_{0\text{-}t}$ is the Area Under the Observed Concentration – Time Curve from time 0 to time t and k_{deg} is the degradation rate constant obtained from the degradation experiments. The corrected dissolution profiles were calculated based on $C_{corrected}$ and a first order curve fitting (Eq 2.5) was performed in order to obtain the dissolution rate constant (GraphPad Prism 6, GraphPad Software, Inc, USA).

$$X_{corrected} = X_{max} * (1 - e^{-k_{diss}t}) \quad \text{Eq 2.5.}$$

where $k_{diss}$is the dissolution rate constant, $X_{corrected}$ is the corrected percent dissolved at time t and X_{max} is the maximum corrected percent dissolved. The goodness of fit was assessed based on the correlation coefficient (R^2) and the Akaike Information Criterion (AIC). Equation 2.6 was utilized to simulate the dissolution profiles ($X_{simulated}$) in the bottle/stirrer accounting for degradation. The simulations were performed using GraphPad Prism 6.

$$X_{simulated} = \frac{X_{max} * k_{diss}}{k_{diss} - k_{deg}} \left(e^{-k_{deg}t} - e^{-k_{diss}t}\right) \qquad \text{Eq 2.6.}$$

Where X_{max} is the maximum corrected percent dissolved, k_{diss} is the dissolution rate constant and k_{deg} is the degradation rate constant.

2.2.12. Statistical analysis

Data were analysed with one-way ANOVA and the Tukey test was selected in order to perform pair wise multiple comparison of all groups (significance p<0.05). A t- test was used to compare two experimental means (significance p < 0.05). The analyses were performed with Statgraphics Centurion XVII (Statpoint Technologies Inc, USA).

2.3. Results and Discussion

2.3.1. Biorelevant dissolution media simulating healthy and hypoalbuminaemic parenteral conditions

The composition of KRB and its physicochemical properties are similar to human plasma (Table 2.1). The biorelevance of KRB supplemented with BSA is described in terms of composition, pH, osmolality and viscosity as compared with the corresponding properties of human plasma from healthy subjects (Table 2.1) [21-24]. A small variation in pH is observed due to the pH adjustment before the addition of the proteins. The addition of BSA marginally increases the viscosity of the medium (p<0.01) whereas the increase of the osmolality is not statistically significant (p > 0.05). The BSA concentration in the medium (1.5 – 4.0 % w/v) reflects the albumin levels in the plasma of a critically ill patient and of a healthy subject [9]. A 76% sequence identity between Human Serum Albumin (HSA) and BSA has been measured [25], justifying the use of BSA as a substitute for HSA. In addition, an *in silico* analysis utilizing molecular modeling, predicted only one favourable binding

site in both HSA and BSA for AmB B [26], further supporting the biorelevance of KRB supplemented with BSA.

Table 2.1. Composition and physicochemical properties of healthy human plasma and KRB; Mean ± SD of measured physicochemical properties with different concentrations of BSA (n = 3).

Ion	**Healthy Human Plasma**	**KRB**
	Composition (Concentration (mM); [21-23])	
HCO_3^-	24.80	14.99
K^+	4.60	4.56
Cl^-	99.00	127.32
Na^+	150.00	136.17
Ca^{2+}	4.70	1.00
Mg^{2+}	1.60	0.49
Inorganic phosphorus	1.51	2.00
D-Glucose	5.60	10.00
	Physicochemical properties	
pH	7.40 [21]	7.34 ± 0.03 (+BSA 1.5% w/v) 7.35 ± 0.03 (+BSA 2.0% w/v) 7.34± 0.03 (+BSA 3.0% w/v) 7.36 ± 0.01 (+BSA 4.0% w/v)
Osmolality (mOsm/L)	289.0 [21]	298.0 ± 10.4 (+BSA 2.0% w/v) 308.7 ± 2.5 (+BSA 4.0% w/v)
Viscosity (cps)	3.8 – 4.7 cP at 22°C [24]	Measurement at 25°C 3.70 ± 0.03 (+BSA 1.5% w/v) 3.79 ± 0.03 (+BSA 2.0% w/v) 3.88 ± 0.02 (+BSA 3.0% w/v) 3.98 ± 0.02 (+BSA 4.0% w/v)

2.3.2. Identification of the AmB degradation product

During the development of the AmB quantification method, an extra peak in AmB chromatograms with a shorter retention time was noted. When the sample was incubated at 37°C, the area of this unknown peak increased with time and the AmB peak area decreased. The UV spectra of the two peaks are broadly similar with a main difference in the λ_{max} [λ_{max} for AmB: 406 nm; λ_{max} for unknown compound: 380 nm (Figure 2.1)], suggesting that the unknown compound is related to AmB.

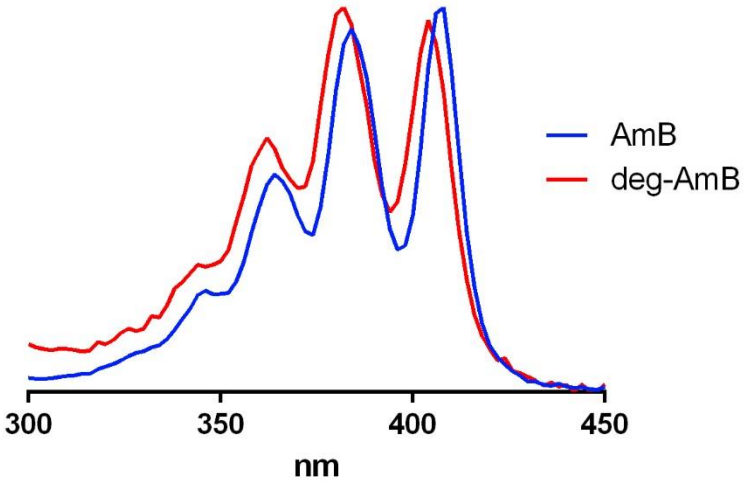

Figure 2.1. Representative UV spectra of AmB and deg-AmB.

LCMS experiments revealed that the mass spectrum of the unknown compound has a difference in mass (corresponding to a chlorine adduct) compared to the mass of AmB (Figure 2.2).

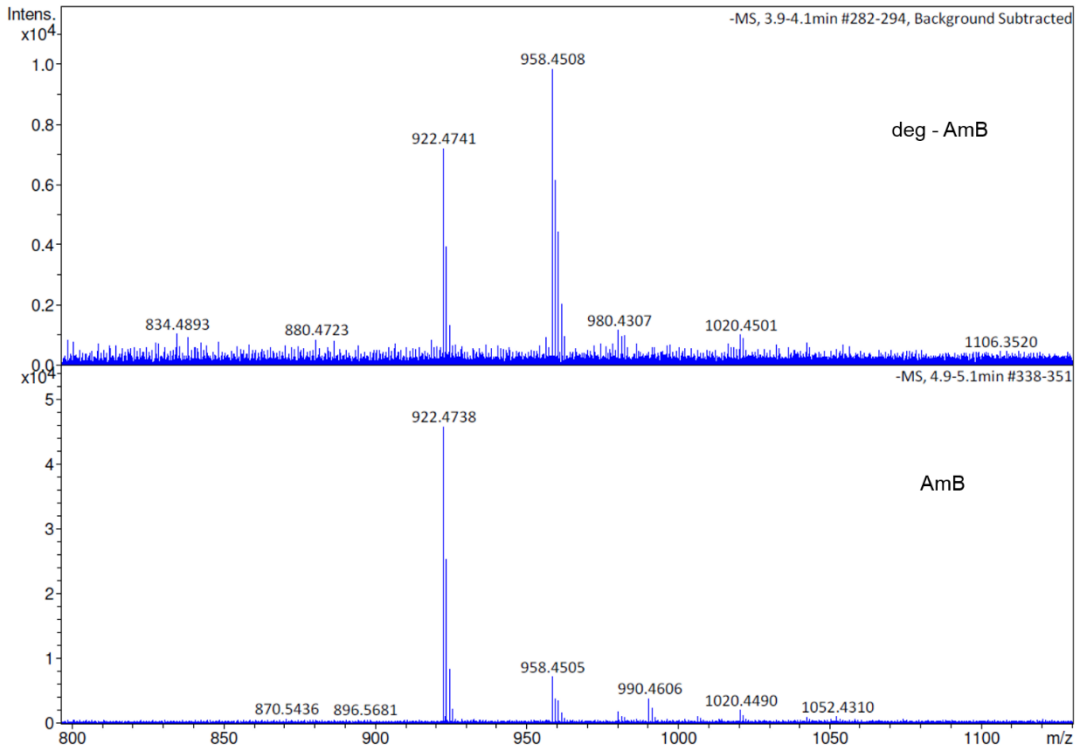

Figure 2.2. Mass spectra of AmB and deg-AmB in KRB-BSA 4% w/v obtained by LCMS in negative mode.

Based on these studies, this unknown compound is more polar than AmB (due to its shorter retention time) and it can be suggested that it is AmB's degradation product (deg-AmB). It has been reported that AmB auto–oxidates in the presence of oxygen with formation of free radicals and epoxidation is the most probable route of degradation (but the epoxidation products have not yet been characterized) [27-29]. A degradation product has not been reported previously in studies where AmB was quantified. This could be due to the specific ion transition followed by the multiple reaction monitoring [30-33] and the elution of the more polar AmB degradation product in the washing step of the solid phase extraction used for the purification of the sample [31, 34-36] in these methods. Furthermore, plasma components could potentially prevent/alter the rate of AmB degradation.

2.3.3. Degradation studies of AmB in the biorelevant media

The degradation of AmB in dissolution media with different concentrations of BSA was assessed in order to enable the quantification of the actual AmB dissolved in the

dissolution studies. Degradation data and degradation rate constants of AmB in the studied media are presented in Figure 2.3 and Table 2.2, respectively.

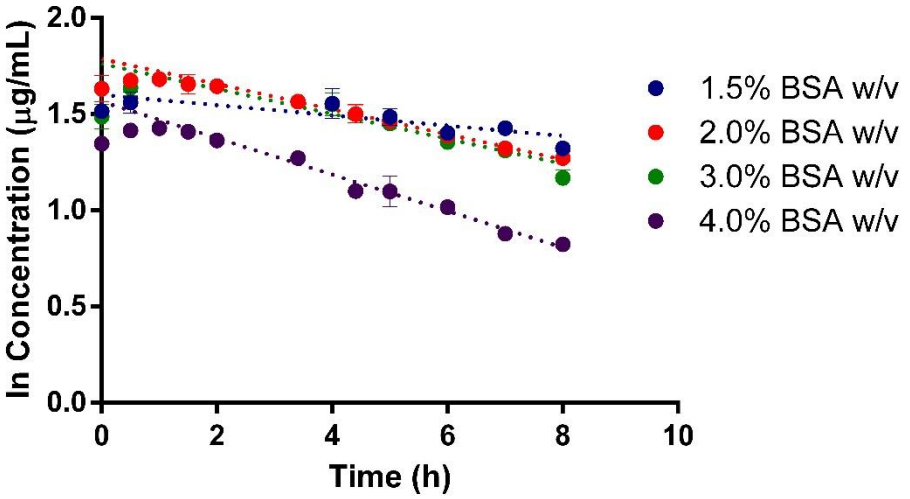

Figure 2.3. ln AmB concentration as a function of time in KRB with BSA 1.5 – 4.0 %w/v with the bottle/stirrer set up (130 rpm) at 37°C (degradation study; Mean ± SD; n = 3).

The concentration of BSA in the medium has a statistically significant effect on the degradation rate constants of AmB ($p<0.01$). The increasing concentration of BSA results in an increase in the degradation rate constant of AmB, with the degradation rate constant being 3 times higher in the media with 4.0% w/v BSA compared to the one in media with BSA 1.5% w/v.

Table 2.2. AmB degradation rate constants (k_{deg}) and solubility values in KRB with different BSA concentrations (Mean ± SD; n = 3).

KRB-BSA (%w/v)	k_{deg} (h^{-1})	Solubility (µg/mL)
1.5	0.03 ± 0.01	13.03 ± 1.09
2.0	0.07 ± 0.00	13.80 ± 1.40
3.0	0.07 ± 0.00	15.28 ± 0.78
4.0	0.10 ± 0.02	17.56 ± 0.82

2.3.4. Solubility studies of AmB in the biorelevant media

The AmB solubility data for 24 h in KRB with different concentrations of BSA are presented in Figure 2.4.

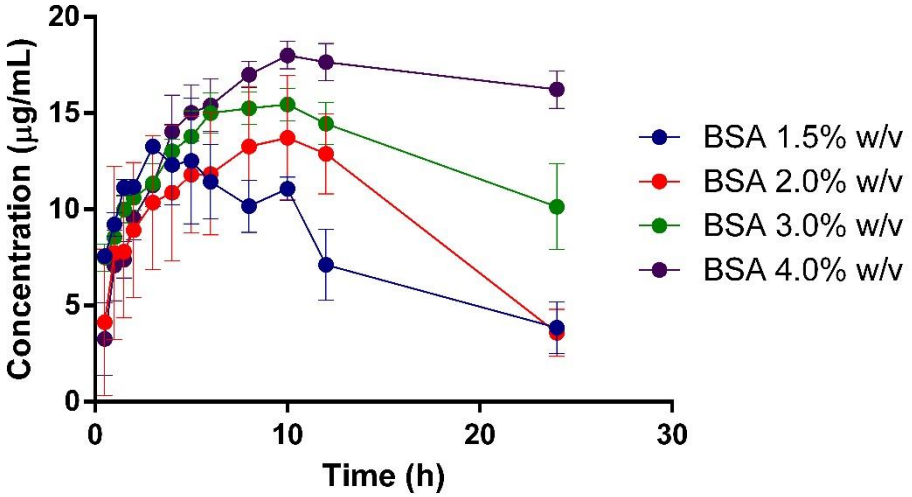

Figure 2.4. AmB concentration as a function of time in KRB with BSA 1.5 – 4.0 %w/v with the bottle/stirrer set up (130 rpm) at 37°C (solubility study; Mean ± SD; n = 3).

The solubility of AmB in the biorelevant media increases with an increase in BSA concentration in the medium. While drug loss through degradation facilitates further solubilisation, as the dissolution rate is faster than the degradation rate, the AmB solubility saturation value is considered to be the point at which the concentration reaches a plateau, generally at around 10 h – 12 h (3 – 5 h for KRB BSA 1.5% w/v) (Table 2.2) and after this point, the AmB concentration is decreased due to degradation being the dominant process at this time when there is no longer the same excess of the drug. The deg-AmB peak was present in all samples' chromatograms and its area increased with increased mass dissolved. The increase in drug solubility mediated by albumin has been reported for another anti-fungal drug, Itraconazole, illustrating the importance of BSA concentration in the medium for poorly soluble, highly protein bound drugs [37]. These solubility values should be taken into account when developing biorelevant test conditions for an AmB formulation, with a view to developing an *in vivo / in vitro* correlation. As the patients who are going to receive AmB therapy may present with hypoalbuminaemia, albumin concentration could

impact on the observed mass dissolved/released from the formulation, which will be reflected in the pharmacokinetics of the drug.

2.3.5. Mass Balance studies of AmB in the biorelevant media

The results of the mass balance studies of AmB in KRB with BSA 2.0% w/v and KRB with BSA 4.0% w/v are presented in Table 2.3. The $AmB\ dissolved\ at\ 24\ h$ is similar for both concentrations of BSA (2.0% w/v and 4.0% w/v) in the medium, but the $AmB\ T_{dissolved}$ in which the degradation of AmB is taken into account is higher in the medium with BSA 4.0% w/v, as the AmB degradation is higher in this BSA concentration. This supports the results in sections 2.3.3 and 2.3.4, implying that BSA has a critical effect on the degradation and solubility of AmB in the medium, confirming the faster degradation and increased mass dissolved in medium with higher BSA concentration.

Table 2.3. Percentage of AmB in mass balance studies in KRB – BSA media after 24 h at 37°C (Mean ± SD; n = 3).

	KRB BSA 2.0% w/v	KRB BSA 4.0% w/v
$AmB\ dissolved\ at\ 24\ h$	39.43 ± 11.09	34.46 ± 4.29
$AmB\ final$	76.61 ± 7.98	59.21 ± 2.15
$AmB\ T_{undissolved}$	37.18 ± 3.11	24.75 ± 6.20
$AmB\ T_{dissolved}$	62.82 ± 3.11	75.25 ± 6.20
$AmB\ T_{degraded}$	23.39 ± 7.98	40.79 ± 2.15

2.3.6. Antimicrobial activity of AmB in the biorelevant media

In order to assess the effect of BSA in the activity of AmB against *Candida albicans*, MIC and MFC values were determined (Table 2.4). A marked effect of BSA on the activity of AmB is shown. The results for the control experiments are in agreement with what is reported in the literature for the MIC of AmB against *C. albicans* (0.06 – 1 mg/L) [36-39]. When BSA was added to the culture media, the MIC increased 10-fold in the medium with BSA 2.0% w/v and approximately 20-fold in the medium with BSA 4% w/v. In the absence of BSA, the MFC was fairly close to the MIC values,

indicating that AmB is fungicidal. However, in the presence of BSA, the MFC was higher than the highest concentration of AmB that was tested, suggesting a fungistatic activity instead. The increase in the concentration of AmB to exert its antifungal activity has been reported before in studies where the source of albumin was HSA (human serum albumin) [40]. This could be explained by the fact that AmB is highly bound to proteins, and only the free fraction can exert a pharmacological effect. If there is more albumin in the medium, more drug will be bound to it and the concentration required to have the same efficacy will be higher. *In vivo*, AmB can also be bound to α1-acid glycoprotein [12, 13], but as this protein's blood concentration is only 0.1% w/v (24 μM) compared to the 2.0 – 4.0% w/v BSA (300 – 600 μM) (that is used to substitute HSA) its effect can be considered negligible for the purposes of this study.

Table 2.4. MIC and MFC (μg/mL) of AmB against *Candida albicans* in SBD broth and KRB supplemented with BSA (n = 2).

Condition	MIC (μg/mL)			
	SBD-BSA 2.0%w/v	SBD-BSA 4.0%w/v	KRB-BSA 2.0%w/v	KRB-BSA 4.0%w/v
Control	0.2 – 0.4			
AmB	3 – 4.5	6.4	4.5	7.5
Condition	**MFC (μg/mL)**			
	SBD-BSA 2.0%w/v	SBD-BSA 4.0%w/v	KRB BSA 2.0%w/v	KRB BSA 4.0%w/v
Control	0.8			
AmB	> 10.5	> 12.0	> 10.5	> 12.0

MIC: minimal inhibitory concentration, MFC: minimal fungicidal concentration

2.3.7. Dissolution studies of AmB in biorelevant media

2.3.7.1. Sample and separation method (bottle/stirrer)

The AmB dissolution profiles in biorelevant media (KRB with the addition of BSA 1.5 – 4.0 %w/v) obtained with the bottle/stirrer setup are presented in Figure 2.5.

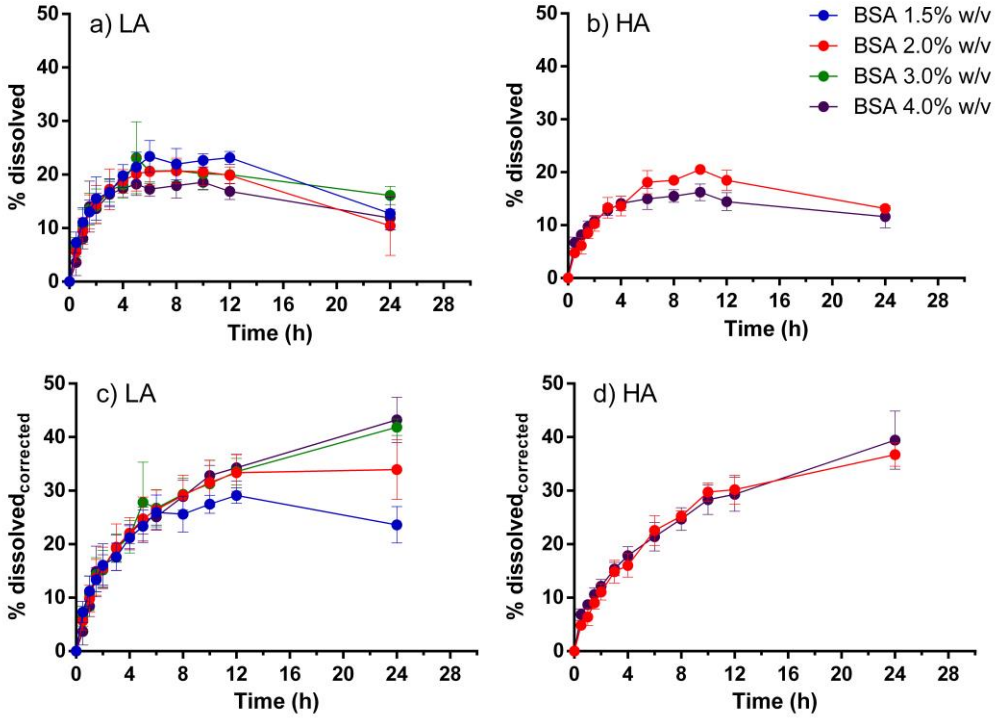

Figure 2.5. % AmB dissolved in KRB with different concentrations of BSA (%w/v) with the bottle/stirrer set up at 37°C a) and b) dissolution profiles before correction for degradation; c) and d) dissolution profiles after correction for degradation. (Mean ± SD; n = 3) [LA: low agitation; HA: high agitation].

Dissolution studies were performed in KRB without BSA, however neither the AmB dissolution nor the AmB degradation could be quantified due to the very low solubility, and hence minimal dissolution, of the drug in this medium. The AmB dissolution with its degradation occurring simultaneously is similar at both agitation levels with a plateau value ranging from 18.55% – 23.14% (low agitation) and 16.21% – 20.50% (high velocity). A drop in the % dissolved is observed at 24 h due to the degradation, with this being higher for the low agitation conditions and the low levels of BSA (1.5% w/v and 2% w/v) (Figure 2.5a and 2.5b). When the dissolution profiles are corrected for the degradation (Figure 2.5c and 2.5d) the continuous dissolution of

AmB in the media with high levels of BSA (3.0% w/v and 4.0% w/v) in both agitation conditions can be observed. At low agitation conditions and at low levels of BSA in the medium the % dissolved from 12 h to 24 h is decreased (5.49% in the medium with 1.5% w/v BSA) or remains unchanged (in the medium with 2.0% w/v BSA). The dissolution of AmB corrected for degradation is described by a first order process and the calculated dissolution rate constants are presented in Table 2.5. There is a statistically significant decrease in dissolution rate constant (k_{diss}) between the same levels of BSA (2.0% w/v) in high agitation conditions compared to low agitation conditions ($p = 0.033$). While there is a trend towards a decrease in k_{diss} with increase in BSA concentration in the medium in low agitation conditions, the differences in k_{diss} between each medium in the same agitation conditions were not statistically significant ($p > 0.05$). The maximum % AmB dissolved (X_{max}) is statistically similar between the same levels of BSA in the two agitation conditions ($p > 0.05$). X_{max} increases with a higher concentration of BSA in the medium, with this increase being statistically significant only for the low level of BSA (1.5% w/v) when compared to the other three levels of BSA under low agitation ($p < 0.05$) (in agreement with the mass balance studies). For the different levels of BSA under high agitation statistically significant differences in X_{max} were not observed ($p > 0.05$). These results suggest that agitation rate is of greater relevance when using media with lower albumin concentrations probably due to the better powder dispersal and its exposure to the albumin that is present. When the high agitation is applied, the discriminatory ability of the test is reduced. The simulated dissolution profiles of AmB in media with different levels of BSA and under both agitation conditions in the bottle/stirrer setup are presented in Figure 2.6.

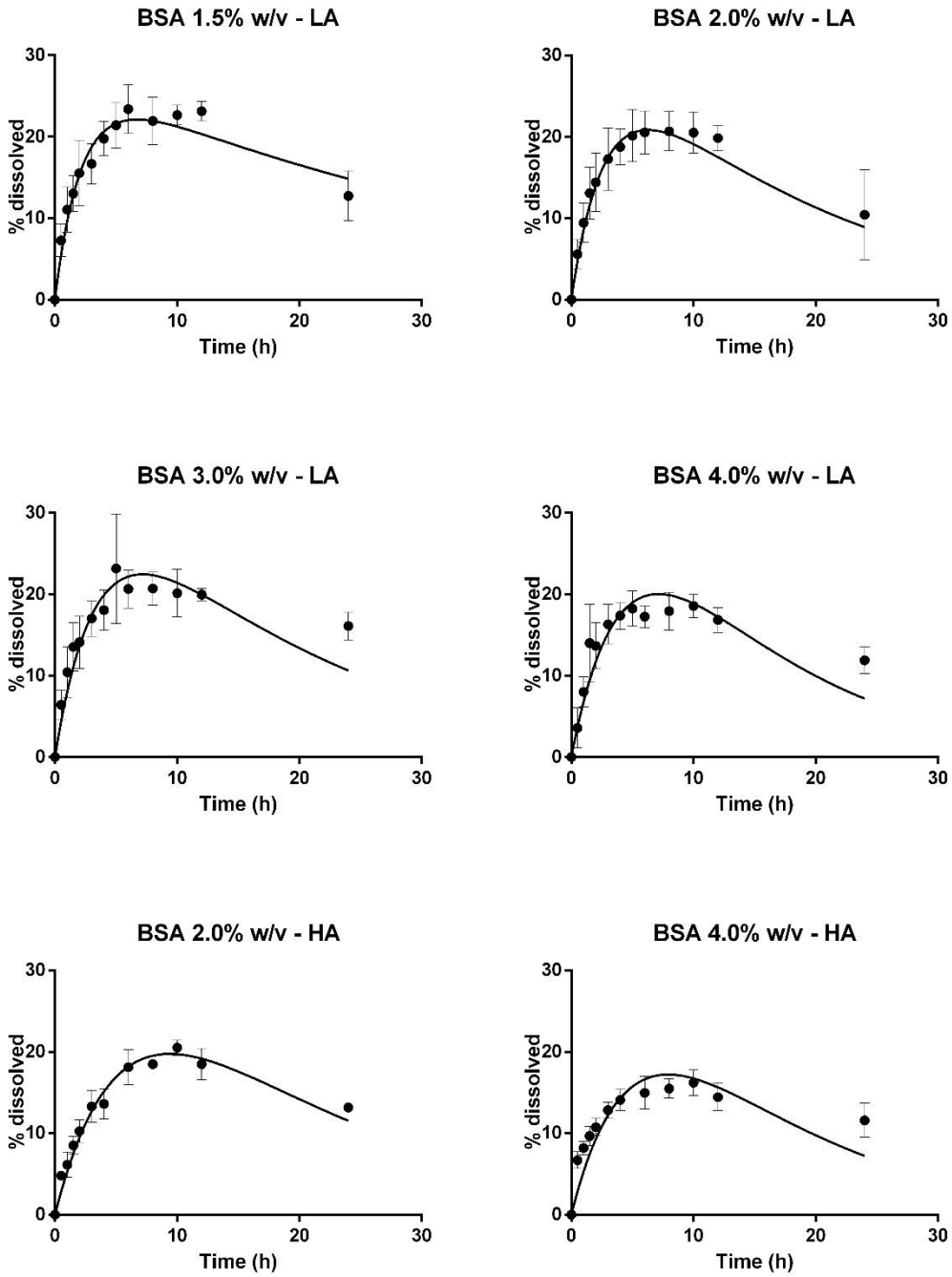

Figure 2.6. Simulated and observed % AmB dissolved as a function of time [lines: simulated profiles (obtained with Eq 6); points observed values (Mean ± SD; n=3)]

The use of a biexponential function in which the dissolution (k_{diss}) and degradation rate (k_{deg}) constants were incorporated results in successful prediction of AmB dissolution. Dissolution modeling could be a valuable tool to provide a mechanistic

understanding of drug dissolution in cases where other processes, such as degradation, occur simultaneously with dissolution.

Table 2.5. Dissolution rate constants (k_{diss}), maximum corrected AmB % dissolved (X_{max}) and goodness of fit parameters (first order curve fitting; R^2, AIC) for the dissolution studies with the bottle/stirrer setup (Mean ± SD; n = 3).

KRB BSA (% w/v)	**Agitation /velocity**	k_{diss} **(h^{-1})**	X_{max} **(%)**	R^2	**AIC**
1.5	Low	0.46 ± 0.10	26.73 ± 1.52	0.93 ± 0.01	28.93 ± 1.56
2.0	Low	0.30 ± 0.13	34.85 ± 3.29	0.98 ± 0.01	20.20 ± 3.62
3.0	Low	0.25 ± 0.10	38.33 ± 2.81	0.95 ± 0.02	32.16 ± 4.28
4.0	Low	0.20 ± 0.03	40.05 ± 3.98	0.95 ± 0.02	33.53 ± 8.04
2.0	High	0.16 ± 0.02	36.54 ± 1.25	0.99 ± 0.00	13.71 ± 2.20
4.0	High	0.16 ± 0.02	37.20 ± 5.43	0.95 ± 0.01	28.71 ± 4.57

R^2: correlation coefficient, AIC: Akaike Information Criterion.

2.3.7.2. Continuous Flow method (flow through cell apparatus)

AmB dissolution profiles in KRB with BSA 2.0% w/v and BSA 4.0% w/v under low and high velocity conditions with the flow through cell apparatus are presented in Figure 2.7.

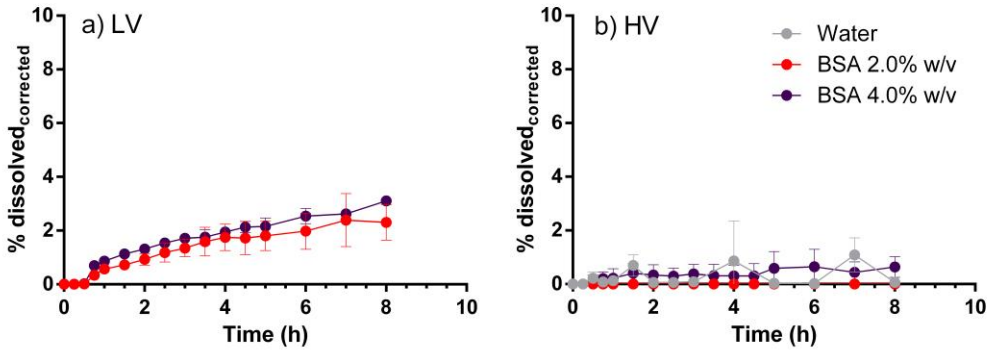

Figure 2.7. % AmB dissolved in KRB with different concentrations of BSA (%w/v) with the flow through cell apparatus at 37°C (Mean ± SD; n = 3) [LV: low velocity; HV: high velocity].

The dissolution of AmB was very low in all cases, with the maximum % dissolved being 3.10 ± 0.08 % dissolved in the medium with BSA 4% w/v under low velocity after 8h and the samples' concentrations did not reach the corresponding AmB solubility in the medium (Figure 2.4). A low % AmB dissolved was also observed in the case where a lower amount of AmB was used (0.5mg; data not shown) revealing that the low dissolution does not relate to the AmB amount in the cell. The AmB dissolution with the flow through set up was lower than the AmB dissolution with the bottle/stirrer set up (Figure 2.5). The theoretical average linear velocities, based on flow rate and cell diameter, employed in the flow through cell apparatus were 0.07 cm/s (low velocity) and 0.52 cm/s (high velocity) while the outer edge of the stirrer in the bottle had a rotational linear velocity of 10.2 cm/s (low agitation) and 29.5 cm/s (high agitation). With the lowest velocity in the bottle/stirrer setup being at least 20 times greater than the highest velocity of the flow-through cell apparatus, the reduced AmB power dispersal leading to aggregation in the flow through cell compared to the bottle/stirrer set up is evident. As the AmB binding to BSA is a dynamic process, selection of appropriate hydrodynamics which facilitate interaction between BSA and solute, which in this case is a poor soluble compound with wetting issues [41], is essential.

2.4. Conclusions

AmB is used for the treatment of systemic fungal infections and it is highly bound to plasma proteins, including albumin. In clinical practice, AmB is used in patient

cohorts that frequently exhibit hypoalbuminaemia. As hypoalbuminaemia is known to affect pharmacokinetics of highly protein bound drugs, AmB is a useful model compound to explore the development of dissolution tests that closely simulate *in vivo* conditions for parenteral therapies. In this work, we have developed biorelevant dissolution media with BSA concentrations representing hypoalbuminaemic patients and healthy subjects. BSA was shown to be a critical component in the media as the solubility and the degradation rate constant of AmB were dependent on the concentration of BSA. Accounting for concurrent degradation, dissolution over time could be modeled and simulated with the proposed approach (Equation 2.4 – 2.6), facilitating calculation of the total amount of AmB dissolved. The results of the two different setups for dissolution showed that the AmB powder needed a strong agitation (in terms of average linear velocity) for dissolution. Following correction of AmB dissolution to account for degraded AmB, a difference can be observed between the dissolution profiles (dependent on the BSA concentration), which is reflected in the values of the dissolution rate and maximum amount dissolved. Conversely, in the high agitation conditions, there was reduced discrimination between dissolution profiles following correction of dissolution for degraded AmB. Furthermore, the microbiological studies support the observation that the AmB is solubilised by binding to BSA, reducing the free fraction for activity and increasing the observed MIC. Establishing discriminating test methods with BSA present in the dissolution media supports future development of both biorelevant and clinically relevant tests for parenteral formulations. For biorelevant dissolution testing for poorly soluble, highly protein bound drugs such as AmB, protein concentration should be considered as a medium component and the concentration used is critical, particularly given the relevance of the concentrations to target patient populations. Going forward it is important to include this element in biorelevant dissolution test development for release of AmB from lipid based formulations.

Acknowledgments

Part of this work has been previously presented at the 10th PBP world meeting April 2016 (oral presentation) and accepted for presentation at the AAPS annual meeting in San Diego November 2017 (poster presentation). The authors would like to thank the Mexican Council of Science and Technology (CONACyT) for the PhD scholarship of Mr R Diaz de Leon-Ortega and Mr Fernando Acosta (Department of Chemical Engineering, University of Bath) for his help with the operation of the rheometer.

2.5. References

[1]. Ansel's pharmaceutical dosage forms and drug delivery systems. 10th edition. ed. Ansel HC, Allen LV, Lippincott W, Wilkins, Wolters Kluwer H, editors: Philadelphia : Wolters Kluwer/Lippincott Williams & Wilkins Health; 2014.

[2]. Seidlitz A, Nagel S, Semmling B, Grabow N, Sternberg K, Weitschies W. Biorelevant Dissolution Testing of Drug-Eluting Stents: Experiences with a Modified Flow-Through Cell Setup. Dissolution Technologies. 2011;18(1):26-34.

[3]. Shen J, Burgess DJ. In vitro dissolution testing strategies for nanoparticulate drug delivery systems: recent developments and challenges. Drug delivery and translational research. 2013;3(5):409-15.

[4]. D'Souza SS, DeLuca PP. Methods to assess in vitro drug release from injectable polymeric particulate systems. Pharm Res. 2006;23(3):460-74.

[5]. Shen J, Burgess DJ. Accelerated in-vitro release testing methods for extended-release parenteral dosage forms. J Pharm Pharmacol. 2012;64(7):986-96.

[6]. D'Souza S. A Review of In Vitro Drug Release Test Methods for Nano-Sized Dosage Forms. Advances in Pharmaceutics. 2014;2014.

[7]. Fotaki N, Vertzoni M. Biorelevant dissolution methods and their applications in in vitro-in vivo correlations for oral formulations. Open Drug Deliv J. 2010;4(2):2-13.

[8]. Wang Q, Fotaki N, Mao Y. Biorelevant dissolution: methodology and application in drug development. Dissolution Technologies. 2009;16(3):6-12.

[9]. Ulldemolins M, Roberts JA, Rello J, Paterson DL, Lipman J. The effects of hypoalbuminaemia on optimizing antibacterial dosing in critically ill patients. Clinical Pharmacokinetics. 2011;50(2):99-110.

[10]. Nicholson JP, Wolmarans MR, Park GR. The role of albumin in critical illness. British journal of anaesthesia. 2000;85(4):599-610.

[11]. Adedoyin A, Swenson CE, Bolcsak LE, Hellmann A, Radowska D, Horwith G, et al. A pharmacokinetic study of amphotericin B lipid complex injection (Abelcet)

in patients with definite or probable systemic fungal infections. Antimicrob Agents Chemother. 2000;44(10):2900-2.

[12]. Bellmann R. Clinical pharmacokinetics of systemically administered antimycotics. Current Clinical Pharmacology. 2007;2(1):37-58.

[13]. Bekersky I, Fielding RM, Dressler DE, Lee JW, Buell DN, Walsh TJ. Plasma protein binding of amphotericin B and pharmacokinetics of bound versus unbound amphotericin B after administration of intravenous liposomal amphotericin B (Ambisome®) and amphotericin B deoxycholate. Antimicrob Agents Chemother. 2002;46(3):834-40.

[14]. Lamy-Freund MT, Ferreira VF, Schreier S. Polydispersity of aggregates formed by the polyene antibiotic amphotericin B and deoxycholate. A spin label study. Biochim Biophys Acta, Biomembr. 1989;981(2):207-12.

[15]. Mazerski J, Grzybowska J, Borowski E. Influence of net charge on the aggregation and solubility behaviour of amphotericin B and its derivatives in aqueous media. European biophysics journal. 1990;18(3):159-64.

[16]. Barwicz J, Christian S, Gruda I. Effects of the aggregation state of amphotericin B on its toxicity to mice. Antimicrob Agents Chemother. 1992;36(10):2310-5.

[17]. Malone ME, Gowing C, Barry M, Deasy E, Kavanagh P, Corrigan OI, et al. ESICM 2012 Monday Sessions 15 October, 2012. Intensive Care Medicine. 2012;38(Suplement 1):P S154 (number 548).

[18]. Gillum AM, Tsay EY, Kirsch DR. Isolation of the Candida albicans gene for orotidine-5'-phosphate decarboxylase by complementation of S. cerevisiae ura3 and E. coli pyrF mutations. Mol Gen Genet. 1984;198(2):179-82.

[19]. Nilsson-Ehle I, Yoshikawa TT, Edwards JE, Schotz MC, Guze LB. Quantitation of amphotericin B with use of high-pressure liquid chromatography. Journal of infectious diseases. 1977;135(3):414-22.

[20]. Fotaki N. Flow-through cell apparatus (USP apparatus 4): Operation and features. Dissolution Technologies. 2011;18(4):46-9.

[21]. Shepherd JT. The human cardiovascular system : facts and concepts. Vanhoutte PM, editor. New York: New York : Raven Press; 1979.

[22]. Krebs-Ringer Modified Buffer (KRB). Cold Spring Harbor Protocols. 2014;2014(1):pdb.rec076406.

[23]. Labs H. Krebs Ringer Buffer composition. http://himedialabscom/TD/TL1097pdf. 2013.

[24]. Rand PW, Lacombe E, Hunt HE, Austin WH. Viscosity of normal human blood under normothermic and hypothermic conditions. Journal of Applied Physiology. 1964;19(1):117-22.

[25]. Michnik A, Michalik K, Kluczewska A, Drzazga Z. Comparative DSC study of human and bovine serum albumin. J Therm Anal Calorim. 2006;84(1):113-7.

[26]. Kudva AK, Manoj M, Swamy BM, et al. Complexation of amphotericin B and curcumin with serum albumins: solubility and effect on erythrocyte membrane damage. Journal of Experimental Pharmacology. 2011.

[27]. Connors KA, Amidon GL, Stella VJ. Chemical stability of pharmaceuticals: a handbook for pharmacists: John Wiley & Sons; 1986.

[28]. Schreier S, Lamy-Freund MT. Spectroscopic studies of aggregation and autoxidation properties of the polyene antibiotic amphotericin B. Quim Nova. 1993;16(4):343-9.

[29]. Gagoś M, Czernel G. Oxidized forms of polyene antibiotic amphotericin B. Chem Phys Lett. 2014;598:5-9.

[30]. Xiong X, Zhai S, Liu F. Determination of Amphotericin B in Human Cerebrospinal Fluid by LC–MS–MS. Chromatographia. 2009;70(1-2):329-32.

[31]. Deshpande NM, Gangrade MG, Kekare MB, Vaidya VV. Determination of free and liposomal amphotericin B in human plasma by liquid chromatography-mass spectroscopy with solid phase extraction and protein precipitation techniques. J Chromatogr B: Anal Technol Biomed Life Sci. 2010;878(3-4):315-26.

[32]. Qin W, Tao H, Chen Y, Chen Z, Wu N. Sensitive, accurate and simple liquid chromatography-tandem mass spectrometric method for the quantitation of amphotericin B in human or minipig plasma. J Chromatogr Sci. 2012;50(7):636-43.

[33]. Lee JW, Petersen ME, Lin P, Dressler D, Bekersky I. Quantitation of free and total amphotericin B in human biologic matrices by a liquid chromatography tandem mass spectrometric method. Therapeutic drug monitoring. 2001;23(3):268-76.

[34]. Eldem T, Arican-Cellat N. Determination of amphotericin B in human plasma using solid-phase extraction and high-performance liquid chromatography. J Pharm Biomed Anal. 2001;25(1):53-64.

[35]. Egger P, Bellmann R, Wiedermann CJ. Determination of amphotericin B, liposomal amphotericin B, and amphotericin B colloidal dispersion in plasma by high-performance liquid chromatography. J Chromatogr B: Anal Technol Biomed Life Sci. 2001;760(2):307-13.

[36]. Yamamoto E, Hyodo K, Ohnishi N, Suzuki T, Ishihara H, Kikuchi H, et al. Direct, simultaneous measurement of liposome-encapsulated and released drugs in plasma by on-line SPE-SPE-HPLC. J Chromatogr B: Anal Technol Biomed Life Sci. 2011;879(30):3620-5.

[37]. Ghazal HS, Dyas AM, Ford JL, Hutcheon GA. In vitro evaluation of the dissolution behaviour of itraconazole in bio-relevant media. Int J Pharm. 2009;366(1):117-23.

[38]. Johnson EM, Ojwang JO, Szekely A, Wallace TL, Warnock DW. Comparison of In Vitro Antifungal Activities of Free and Liposome-Encapsulated Nystatin with Those of Four Amphotericin B Formulations. Antimicrob Agents Chemother. 1998;42(6):1412-6.

[39]. Ellis D. Amphotericin B: spectrum and resistance. The Journal of antimicrobial chemotherapy. 2002;49 Suppl 1:7-10.

[40]. Lewis RE, Wiederhold NP, Prince RA, Kontoyiannis DP. In vitro pharmacodynamics of rapid versus continuous infusion of amphotericin B deoxycholate against Candida species in the presence of human serum albumin. J Antimicrob Chemother. 2006;57(2):288-93.

[41]. Yu B, Okano T, Kataoka K, Kwon G. Polymeric micelles for drug delivery: solubilization and haemolytic activity of amphotericin B. J Controlled Release. 1998;53(1):131-6.

Letter of Copyright Permission and Statement of Authorship

Title: Investigation and simulation of dissolution with concurrent degradation under healthy and hypoalbuminaemic simulated parenteral conditions- case example Amphotericin B

Author: Ricardo Díaz de León-Ortega,Deirdre M. D'Arcy,A. Bolhuis,N. Fotaki

Publication: European Journal of Pharmaceutics and Biopharmaceutics

Publisher: Elsevier

Date: June 2018

Logged in as:
Ricardo Diaz de Leon
Account #:
3001387305
LOGOUT

Please note that, as the author of this Elsevier article, you retain the right to include it in a thesis or dissertation, provided it is not published commercially. Permission is not required, but please ensure that you reference the journal as the original source. For more information on this and on your other retained rights, please visit: https://www.elsevier.com/about/our-business/policies/copyright#Author-rights

BACK CLOSE WINDOW

This declaration concerns the article entitled:										
Investigation and simulation of dissolution with concurrent degradation under healthy and hypoalbuminaemic simulated parenteral conditions- case example Amphotericin B.										
Publication status (tick one)										
draft manuscript		**Submitted**		**In review**		**Accepted**		**Published**	✓	
Publication details (reference)	Diaz de Leon-Ortega, R., D'Arcy, D.M., Bolhuis, A., Fotaki N. Investigation and simulation of dissolution with concurrent degradation under healthy and hypoalbuminaemic simulated parenteral conditions- case example Amphotericin B, European Journal of Pharmaceutics and Biopharmaceutics, Volume 127, June 2018, Pages 423 - 431, ISSN 0939-6411, https://doi.org/10.1016/j.ejpb.2018.03.009 (https://www.sciencedirect.com/science/article/abs/pii/S0939641117311487?via%3Dihub)									
Candidate's contribution to the paper (detailed, and also given as a percentage).	The candidate contributed considerably in: **Formulation of ideas**: The ideas were developed by Dr Fotaki (the academic supervisor) (60%), Dr D'Arcy (20%) and the candidate (30%). The idea belonged to Dr Fotaki and the candidate presented his suggestions and were reviewed and modify by Dr Fotaki and Dr D'Arcy in order to give structure to the paper. **Design of methodology**: The methodology was developed by Dr Fotaki (45%), Dr D'Arcy (15%), Dr Bolhuis (5%) and the candidate (35%). **Experimental work**: The experimental work was carried out by the candidate. **Presentation of data in journal format**: The data was formatted and reviewed by Dr Fotaki (45%), Dr D'Arcy (20%), Dr Bolhuis (5%) and the candidate (30%)									
Statement from Candidate	This paper reports on original research I conducted during the period of my Higher Degree by Research candidature.									
Signed					**Date**					

Chapter 3: *In vitro* conditions for performance evaluation of products for intravascular administration: Developing appropriate test media using Amphotericin B as a model drug

Abstract

Currently, there are no compendial *in vitro* release tests specifically indicated for parenteral formulations. Consideration of biorelevant and clinically relevant test media represents a valuable approach for the development of *in vitro* tests that ideally can provide information on the formulation performance *in vivo*. The aim of this study was to investigate the effect of different media components on the solubility of Amphotericin B (a poorly soluble highly protein-bound drug) in order to develop biorelevant and clinically relevant media for future *in vitro* release testing from its liposomal formulation. Three categories of media were considered in the development approach: Category 1 media: effect of albumin concentration; category 2 media: effect of biorelevant concentrations of plasma components (bile salts, phospholipids, cholesterol, albumin); category 3 media: attaining clinically relevant solubility with biorelevant and synthetic surfactants with and without albumin and setting the basis for the development of a simulated hypoalbuminaemic's plasma medium. All the surfactants tested increased Amphotericin B solubility while the simultaneous presence of albumin had a negative effect on solubility. Clinically relevant media with the use of biorelevant, synthetic surfactants and albumin were developed. One medium in which the solubility of Amphotericin B was reduced was identified as potential candidate medium to simulate hypoalbuminaemic patients' plasma. The development of biorelevant and clinically relevant media and understanding the effect of media components and their interactions, supports future development of meaningful *in vivo* predictive release tests for parenteral formulations.

Keywords:

Amphotericin B; dissolution; solubility; clinically; relevant; biorelevant; degradation

3.1. Introduction.

Recently, the development of parenteral formulations (for low water soluble and toxic drugs) has grown as they are a suitable alternative to tackle drug related issues or to increase the duration of the pharmacological effect.

Currently, there is not an *in vitro* compendial method specifically assessing how changes to formulations might result in a change in *in vivo* performance of a parenteral drug product [1-5]. The *in vitro* dissolution/release testing used in quality control does not provide information about the dissolution/release of the drug in the environment where the formulations will be administered (such as the intravenous, intramuscular and subcutaneous routes [1]).

Biorelevant dissolution testing refers to an attempt to mimic the conditions of the *in vivo* environment in terms of the composition and physicochemical characteristics of the *in vivo* fluids and the hydrodynamics at the site of administration [6]. Recently, clinically relevant dissolution testing has been defined: the term "clinically relevant" implies the establishment of a link between a drug product quality attribute (e.g. solubility) and *in vivo* performance (e.g. *in vivo* solubility) [7, 8]. This terminology has been agreed in a workshop organised by US FDA and the International Consortium for Innovation and Quality in Pharmaceutical Development (IQ) [8]. This approach enables dissolution testing to establish safe boundaries and reject drug product batches falling outside of the established safe range enabling the method to become clinically relevant [8].

Another aspect that is not usually covered in compendial *in vitro* release testing in terms of the media composition is the variation in *in vivo* physiological conditions induced by illness. In addition to simulating the fluid where the formulation will be administered, these physiological changes should, when appropriate, be reflected in the test medium.

From previous studies, our group has developed a biorelevant test medium that simulates plasma (using Krebs Ringer Buffer (KRB) for the ionic content and bovine serum albumin (BSA) to represent the human serum albumin) which was used to evaluate the impact of albumin concentration on the solubility and degradation of Amphotericin B (AmB) [9]. AmB, a highly protein-bound (including to albumin and lipoproteins [10-12]) and poorly soluble drug [13], was selected as a model drug as it

is commerically available as parenteral lipid-based formulations (including Ambisome® and Abelcet®) for intravenous administration. AmB formulations can be used in patients suffering from severe systemic fungal infections. The presentation of sepsis in critically ill patients can include hypoalbuminaemia, possibly caused by reduced albumin synthesis but also by increased vascular permeability during the inflammatory response to sepsis. Thus, hypoalbuminaemia is a common feature of the vascular fluid into which AmB is administered *in vivo.*

The aim of this chapter was to investigate the impact of different media components on the solubility of AmB to develop media able to target AmB plasma solubility (clinically relevant solubility) and to evaluate if the composition of a medium is suitable for future compendial *in vitro* release testing. Media were developed based on three categories (Figure 3.1). Category 1 media: biorelevant media, investigating the impact of concentration of albumin. Category 2 media: Biorelevant media, investigating the impact of biorelevant concentrations of plasma components to which AmB binds *in vivo* [cholesterol, bile salts, phospholipids with and without BSA]. Category 3 media: Clinical relevant media; category 3a media, attaining clinically relevant solubility with surfactants found in plasma (bile salts and phospholipids); Category 3b media, attaining clinically relevant solubility with synthetic surfactants (SLS, CTAB or Tween 80); Category 3c media, potential for category 3b media to be used as a basis to develop media for solubility and release studies simulating hypoalbuminaemic patients. The development of biorelevant and clinically relevant test media (based on the active pharmaceutical ingredient (API)) is a primary step towards the development of biorelevant and clinically relevant release testing of parenteral formulations.

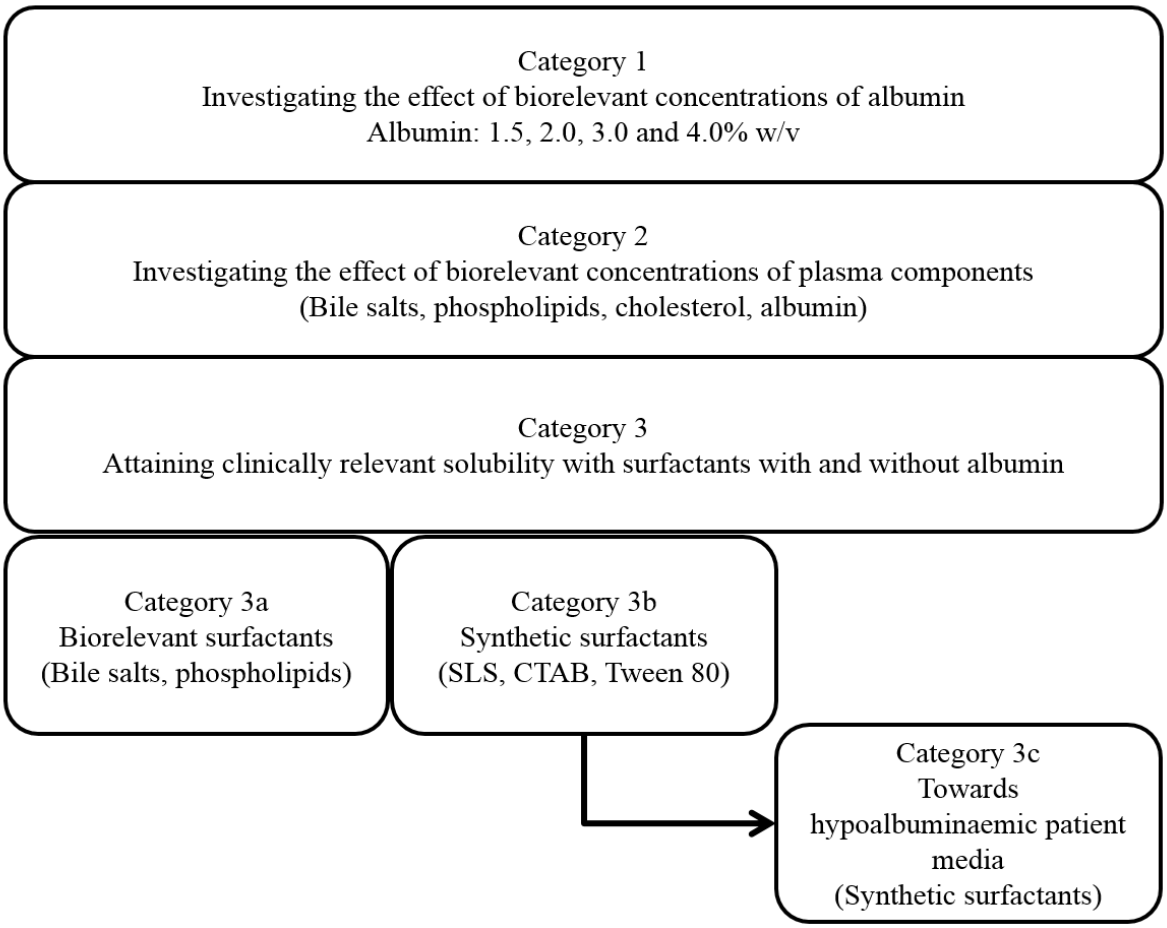

Figure 3.1. Categories of media development.

3.2. Materials and Methods

3.2.1. Materials

AmB analytical standard (87.8%), methanol (MeOH) high performance liquid chromatography (HPLC) grade, formic acid mass spectrometry grade, NaOH, $MgCl_2$, $CaCl_2$, hexadecyltrimethylammonium bromide (CTAB), $NHCO_3$ and NH_4HCO_2 were obtained from Sigma Aldrich (Germany); ethylenediaminetetracetic acid anhydrous (EDTA) from Sigma Aldrich (USA); AmB API powder (85%) from Cayman Chemical (USA); BSA protease free powder fraction V, dimethyl sulfoxide (DMSO), dextrose, sodium dodecyl sulphate (SLS), Na_2HPO_4, NaH_2PO_4, KH_2PO_4, NaCl and KCl from Fisher Scientific (USA); Tween 80 from Amresco (USA); phosphatidylcholine from egg from Lipoid GmbH (Germany); sodium taurocholate from Prodotti Chimici e Alimentaria (Italy); GF/D (pore size 2.7 μm, 25 mm diameter)

and GF/F (pore size 0.7 μm, 25 mm diameter) filters from Whatman (UK) and regenerated cellulose (RC) filters 0.45 μm 13 mm diameter from Cronus (UK).

3.2.1.1. Human plasma collection

Blood was drawn from healthy volunteers (having given informed consent) by median cubital vein venipuncture by a trained phlebotomist following local ethics committee approval (EIRA1, Issue 3, 11/5/2010). To act as anticoagulant, 2 mL of an EDTA 50 mg/mL solution were added to a final volume of 50 mL of blood, for a final concentration of 2 mg/mL. Plasma was separated from blood cells by centrifugation for 10 min at 2000 x g (Heraeus Biofuge Primo R Centrifuge, Thermo Electron LED GmbH. Osterode, Germany) and the supernatant was separated into aliquots and kept at -80°C.

3.2.2. Sample treatment of AmB in plasma and test media

The sample treatment method was described previously [9]. Briefly, proteins were precipitated by adding 2 volumes of methanol to 1 volume of the sample followed by mixing in a vortex mixer and centrifuged for 10 minutes at 12000 rpm at 5°C. The supernatant was filtered through a 0.45 μm RC filter before injection to the HPLC.

3.2.3. Chromatographic conditions for the analysis of AmB from plasma samples and test media

The chromatographic method to quantify AmB was described previously [9]. Briefly, AmB was quantified by HPLC with a C18 Waters Sunfire column (Ireland) 150 x 46 mm 5 μm at 25°C. The mobile phase was formate buffer (50 mM; pH = 3.2): MeOH (25:75, v/v); the flow rate was 1 mL/min and AmB was detected at λ = 406 nm. The UV spectrum was recorded from 300 to 450 nm. Quantification of AmB in samples was based on standard curves. Freshly prepared standard solutions (0.5 – 15 μg/mL) in the corresponding medium were prepared by appropriate dilution of a 500 μg/mL stock solution of AmB analytical standard in 1:1 MeOH: DMSO v/v. The limit of detection and the limit of quantification were 0.12 and 0.37 μg/mL, respectively.

3.2.4. Test media for evaluation of performance of parenteral drug products

Media were developed following the scheme of the 3 categories of development (Figure 3.1).

3.2.4.1. Category 1 media: investigating the impact of albumin concentration

Category 1 media consisted of KRB with varying biorelevant albumin concentrations and were developed and characterized as previously described [9].

3.2.4.2. Category 2 media: investigating the effect of biorelevant concentrations of plasma components on AmB solubility

Plasma components with the potential to affect the solubility of AmB *in vivo*, were added to KRB in biorelevant concentrations: bile salts 12.0 μM (mean value of highest concentrations reported in literature [14-16]); phosphoslipids 2.5 mM [17, 18] and CH 4.5 mM [19]. For media preparation bile salts [sodium taurocholate was used as source of bile salts (BS)] were weighed and dissolved in KRB and then phospholipids [phosphatidylcholine from egg was used as source of phospholipids (PL)] from a stock solution of 100 mg/mL (dissolved in dichloromethane) were added; afterwards, where relevant, CH dissolved in chloroform (3.5 mg/mL) was added to the medium. Organic solvents were evaporated with a rotary evaporator consisting of a Büchi Waterbath B-480 set at 40°C and a Büchi Rotovapor R-114 (Büchi Labotechnik. Flawil, Switzerland) attached to a vacuum pump unit PC 2001 Vario (Vacuubrand GMBH. Wertheim, Germany). The pressure was decreased from 650 mbar in steps of 70 mbar every two minutes to 100 mbar, where the pressure was maintained for 10 minutes. When included in the medium, BSA was added after the evaporation of the organic solvents. The composition of the media is listed in Table 3.2 (Category 2 media). Osmolality, viscosity, pH and buffer capacity of these media were measured (section 3.2.5) and AmB solubility studies (section 3.2.7) were also performed in these media.

3.2.4.3. Category 3 media: investigating the impact of biorelevant and synthetic surfactants to achieve clinically relevant AmB solubility

Media were developed to achieve clinically relevant solubility values of AmB by using surfactants found in plasma (BS and PL) and synthetic surfactants (SLS, CTAB, Tween 80), the effect of BSA was also evaluated (media with and without BSA 4.0%

w/v). Media with synthetic surfactants was investigated for potential use for the simulation of hypoalbuminaemic patients' plasma.

3.2.4.3.1. Category 3a: Biorelevant surfactants

Attaining clinically relevant solubility with surfactants found in plasma (BS and PL), with and without BSA. In order to evaluate the impact of concentration of BSA and biorelevant surfactants on AmB solubility; media with BS, PL and BSA were prepared. The use of PBS as a simpler buffer solution than KRB was also investigated as a basis for media development. A 2 level factorial design of experiments (DoE) was used to identify which factors had a significant effect on AmB solubility. Factors investigated were type of buffer: PBS or KRB; BS concentration: 3.0 or 10.0 mM; and PL concentration: 0.2 or 3.0 mM. The BS concentration was selected in order to have a higher concentration than the biorelevant concentration and be studied in a wide range. The PL concentration was set in order that the PL (BS+PL) molar fraction was below than 0.6, which is the necessary for mixed micelles formation [20]. 8 experimental setups resulted from the combination of these factors, and BSA 4.0% w/v was added to all media. Solubility studies were performed in the 8 media and AmB solubility values were used as the response for the DoE in order to predict the composition of a dissolution medium in each buffer able to produce a clinically relevant AmB solubility value. After the identification of the statistical significant factors affecting AmB solubility, the composition of clinically relevant media were predicted with the DoE (section 3.2.10), targeting the AmB solubility in plasma, and AmB solubility studies were conducted in these media for comparison with AmB plasma solubility values to validate the prediction. To investigate how BSA affects AmB solubility in the presence of the biorelevant surfactants, the predicted media were also prepared without BSA. Media characterization, AmB degradation and solubility studies were performed in the developed media with and without BSA (section 3.2.5, 3.2.6 and 3.2.7).

3.2.4.3.2. Category 3b: Synthetic surfactants

Attaining clinically relevant solubility with synthetic surfactants (SLS, CTAB or Tween 80) with and without BSA, KRB and PBS were tested with 3 different types of surfactants: SLS (anionic surfactant), CTAB (cationic surfactant) and Tween 80 (non-ionic surfactant). The critical micelle concentration (CMC) of charged surfactants was

determined in PBS and KRB by conductimetry (Conductivity Meter, WPA CMD 500, Scientific Laboratory Supplies Ltd, UK) to assure that the concentrations selected were above the CMC. 1 mL of a 10.0 mM solution of the surfactant in the corresponding buffer was added to either 20 mL (for SLS) or 50 mL (for CTAB) of the same buffer and the conductivity recorded. Conductivity was plotted against the surfactant concentration and the CMC was established when there was a change in the slope. Measurements were performed in triplicate.

To study the effect of the surfactants on AmB solubility, the surfactant concentrations investigated were 5.0, 50.0 and 100.0 mM with and without BSA 4.0 %w/v. Single point AmB solubility experiments were conducted in all the media following the procedure described in section 2.7, with 1 mg of AmB API powder added in 10 mL of medium and sampling at 12 h (solubility plateau value was reached around 12 h in previous solubility determinations [9]). The media with the surfactant resulting in an AmB solubility value closer to the AmB plasma solubility, with and without BSA, were selected to develop the clinically relevant media. Surfactant concentrations, in the range where media comprised the clinically relevant AmB solubility value, were investigated in order to obtain the surfactant concentration to produce clinically relevant AmB solubility [5.0 - 50.0 mM with BSA and 0.1 - 4.0 mM without BSA]. Media characterization, degradation and solubility studies (section 3.2.5, 3.2.6 and 3.2.7) were performed in the developed media.

3.2.4.3.3. Category 3c: Potential media to simulate hypoalbuminaemic patients.

Potential for media with synthetic surfactants and BSA, to be used as a basis to develop media simulating hypoalbuminaemic patients.

In order to identify conditions that could direct future hypoalbuminaemic medium development, clinically relevant medium in PBS from category 3b was used as a base. For these studies there was no target solubility value as a reference AmB solubility in hypoalbuminaemic plasma is not available. In order to mimic hypoalbuminaemic plasma, the use of PBS was explored with a) 2.0 % w/v BSA and the corresponding concentration of surfactant developed as clinically relevant medium in category 3b, b) 2.0% w/v BSA with half of the concentration of surfactant from category 3b media and c) 4.0% w/v BSA with half of the concentration of surfactant from category 3b

media. Media characterization, degradation studies (section 3.2.5 and 3.2.6) and single point solubility studies as described in section 3.2.4.3.2 were performed in the media.

3.2.5. Test media characterization

Media characterization methodology was described previously [9]. Briefly, pH was measured in all the media following addition of all components. Osmolality was measured via the freezing-point depression method with a Micro-Osmometer 3300 (Advanced Instruments, Massachusetts USA). Viscosity of all media was measured with a Bohlin Rheometer (Germany) at 25°C in triplicate. The measurement at the value closest to steady state was recorded as the viscosity value. Buffer capacity was determined by adding HCl 0.1 M until there was a change of 1 unit in the pH (Equation 1).

$$\frac{dB}{dpH} = \frac{(HCl\ volume\ (L))([HCl])}{\binom{average\ volume\ of\ sample}{over\ range\ involved}(\Delta pH)} \qquad \text{Equation 3.1}$$

where $\frac{dB}{dpH}$ is the buffer capacity, $[HCl]$ is the concentration of hydrochloric acid and ΔpH is the pH increment. The measurement was performed in triplicate.

3.2.6. Degradation studies of AmB in plasma and in test media

The degradation study methodology was described previously [9]. Briefly, 3 mg of AmB API powder was added to 20 mL of plasma and then stirred for 1 hour at 130 rpm at 37°C. Samples were centrifuged for 5 minutes at 3000 rpm at 4°C and the supernatant incubated at 37°C. Samples were taken at 0.5, 1.0, 1.5, 2.0, 3.0, 4.0, 5.0, 6.0, 8.0 and 24.0 hours, injected to the HPLC after sample treatment and the concentration of AmB in the samples was determined. For dissolution media, the same procedure was followed with 10 mg of AmB API powder added to 50 mL of dissolution media and monitored for 8 hours. All experiments were performed in triplicate. A linear fit was applied to the degradation data from 4 h to the last time point, after a natural logarithm transformation of the measured concentration (Excel 2013, Microsoft. USA) and the degradation rate constant (k_{deg}) was calculated from the slope of the line.

3.2.7. Solubility studies of AmB in plasma and in test media

Solubility study methodology was described previously [9]. Briefly, approximately 2.5 mg of AmB API powder were placed in a 100 mL glass bottle with 30 mL of the corresponding dissolution media, stirred at 130 rpm and incubated at 37°C. The sampling times were 0.5, 1.0, 1.5, 2.0, 3.0, 4.0, 5.0, 6.0, 8.0, 10.0, 12.0 and 24.0 hours. The undissolved AmB was removed by centrifugation and after protein precipitation, samples were injected to the HPLC and the concentration of AmB in the samples was calculated. Solubility studies in plasma were performed with 1.5 mg of AmB in 10 mL of plasma. The AmB solubility saturation value was considered when the concentration reached a plateau value. An AmB solubility value in the dissolution media similar to the AmB plasma solubility was considered "clinically relevant". All experiments were performed in triplicate.

3.2.8. Dissolution studies of AmB in clinically relevant media from category 3a and 3b, and category 3c media, with the flow through-cell dissolution apparatus

Dissolution studies were carried out in a flow-through cell dissolution apparatus (Sotax CE7 smart connected to a Sotax piston pump CP7, Sotax, Switzerland) operated in the closed mode [21]. Tests were carried in category 3 clinically relevant media (3a and 3b) and in media from category 3c. A 5mm ruby glass bead was positioned at the bottom of the cell (small cell: 12 mm diameter; large cell: 22.6 mm diameter). 0.5 mg of AmB API powder was weighed and mixed with 6.0 g or 0.75 g of 1 mm glass beads, for the large or small cell, respectively, and were placed into the cell filling the conical part. Glass fibre filters (GF/D, GF/F) were positioned at the top of the cell. Two different hydrodynamic conditions were tested: i. small cell with a flow rate of 35 mL/min (high velocity: 0.52 cm/s) and ii. large cell with a flow rate of 16 mL/min (low velocity: 0.07 cm/s). 50 mL of test medium were placed into the reservoir under constant stirring at 37°C. 0.5 mL samples were collected at specific time points up to 8 hours and volume was replaced with fresh medium. Dissolution studies were also performed with 5 mg (high dose) of AmB in category 3b PBS medium without BSA under both velocity conditions. Samples were injected to the HPLC after sample treatment and AmB concentration was quantified in order to calculate the %AmB dissolved over time. All experiments were performed in triplicate.

3.2.9. Treatment of dissolution data

Treatment of dissolution data was described previously [9]. Briefly, AmB dissolution profiles were corrected for degradation using the corresponding degradation rate constants with Equation 3.2.

$$C_{corrected} = C_t + k_{deg} * AUC_{0-t} \quad \text{Eq 3.2}$$

where C_t is the observed concentration at time t, AUC_{0-t} is the Area Under the Observed Concentration – Time Curve from time 0 to time t and k_{deg} is the degradation rate constant obtained from the degradation experiments.

The corrected dissolution profiles were calculated based on $C_{corrected}$ and a first order curve fitting (Eq 3.3) was performed in order to obtain the dissolution rate constant (GraphPad Prism 7, GraphPad Software, Inc, USA).

$$X_{corrected} = X_{max} * (1 - e^{-k_{diss}t}) \quad \text{Eq 3.3}$$

where $k_{diss}$is the dissolution rate constant, $X_{corrected}$ is the corrected percent dissolved at time t and X_{max} is the maximum corrected percent dissolved.

3.2.10. Statistical analysis

Equation 3.4 was used to analyse the DoE of the category 3a clinical relevant media development.

$$y = \mu + A + B + C + A * B + A * C + B * C \quad \text{Equation 3.4}$$

where y is the response (AmB solubility), μ is the total mean; A, B and C are the main factors (buffer, BS concentration and PL concentration, respectively); $A * B$, $A * C$ and $B * C$ are the 2 level interactions. Buffer type was represented by a value of -1 for PBS and +1 for KRB. The coefficient of each term was determined by analysing the DoE and the substituted equation was used to calculate the composition of clinically relevant media (targeting AmB solubility plasma values).

To evaluate the effect of surfactants and BSA on AmB solubility, the in category 3a and 3b clinically relevant media, estimated and the standardized effects for surfactants (BS-PL, SLS, CTAB and Tween 80), BSA presence and its interaction, were calculated and used to construct a Pareto chart. A factor was significant when the standardized effect (bars) was larger than the line for statistical significance level (α =

0.05) (vertical line). To compare degradation rate constants, a t-test was used to compare two experimental independent means and a paired t-test to compare two experimental related means (significance $p < 0.05$). Data analysis and the DoE (design and analysis) were performed with the statistical software Statgraphics Centurion XVII (USA).

3.3. Results and discussion

3.3.1. Determination of solubility and degradation rate constant of AmB in human plasma from healthy volunteers

AmB solubility in plasma reached a plateau between 3 – 12 h at a concentration of 32.52 ± 0.98 µg/mL (Figure 3.2) and the AmB degradation rate constant in plasma was 0.033 ± 0.002 h^{-1} (Table 3.1).

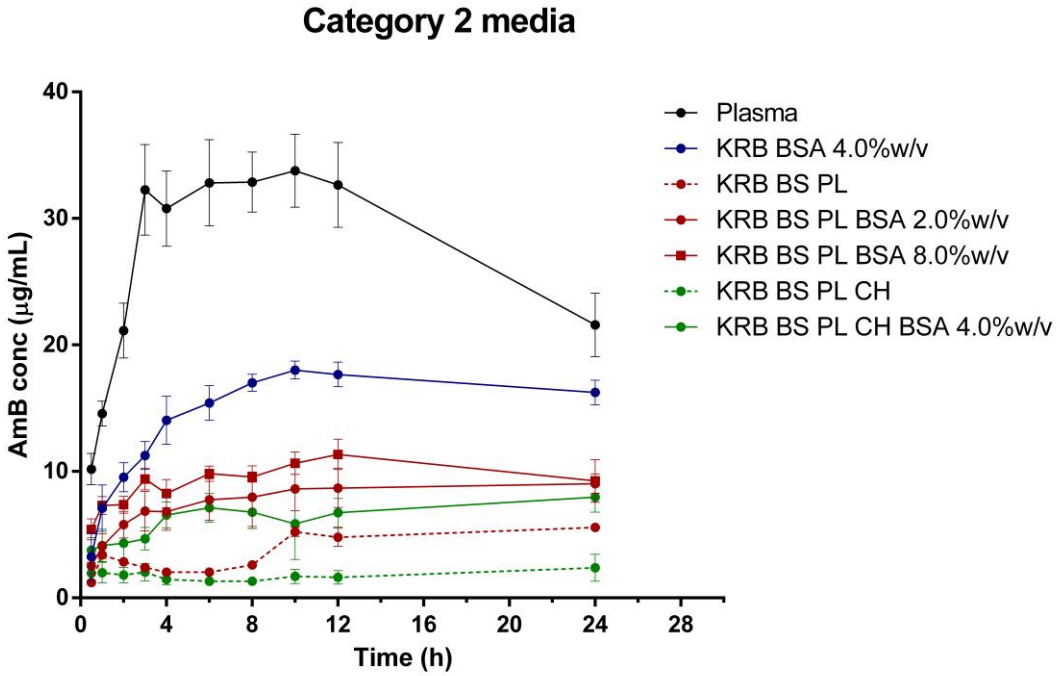

Figure 3.2. Solubility study of AmB in category 2 media: AmB concentration as a function of time in plasma and category 2 media (Mean ± SD; n= 3). KRB BSA 4.0 %w/v solubility (category 1 medium) was added for comparison purposes [9].

Table 3.1. Degradation rate constants of AmB in plasma, category 1 and 3 media. (Mean ± SD; n = 3).

Type of medium		**Medium**	k_{deg} **(h^{-1})**
Plasma		Plasma	0.033 ± 0.002
Category 1		KRB BSA 1.5% w/v	0.026 ± 0.000 [9]
		KRB BSA 2.0% w/v	0.065 ± 0.005 [9]
		KRB BSA 3.0% w/v	0.065 ± 0.021 [9]
		KRB BSA 4.0% w/v	0.095 ± 0.003 [9]
Category 3	3a	KRB BS 20.0 mM PL 4.0mM	0.023 ± 0.010
		KRB BS 20.0 mM PL 4.0 mM BSA 4.0% w/v	0.060 ± 0.008
		PBS BS 19.8 mM PL 7.9 mM	0.048 ± 0.006
		PBS BS 19.8 mM PL 7.9 mM BSA 4.0% w/v	0.097 ± 0.021
	3b	KRB SLS 1.5mM	0.009 ± 0.007
		KRB SLS 30.0mM BSA 4.0% w/v	0.038 ± 0.001
		PBS SLS 1.4 mM	0.005 ± 0.003
		PBS SLS 60.0 mM BSA 4.0% w/v	0.052 ± 0.015
	3c	PBS SLS 30.0 mM BSA 2.0% w/v	0.062 ± 0.014
		PBS SLS 30.0 mM BSA 4.0% w/v	0.082 ± 0.015
		PBS SLS 60.0 mM BSA 2.0% w/v	0.041 ± 0.013

3.3.2. Test media development for evaluation of performance of parenteral drug products

3.3.2.1. Category 1 media

AmB solubility values in category 1 media, obtained in our previous study, were lower (13.03 - 17.56 µg/mL) than the one observed in plasma and the degradation rate constants were not statistically similar to the one observed in plasma (Figure 3.2, Table 3.1) [9].

3.3.2.2. Category 2 media

The osmolality and viscosity values of these media are similar to those of plasma (Table 3.2).

Table 3.2. Media composition and media characterization. Plasma characterization is included (Mean ± SD; n = 3 for Vis and BC HCl).

Category		Medium	Osm (mOsm/L)	Vis (cPs)	pH	BC HCl (mEq/L/pH)
Plasma		Plasma	275 - 300 [22]	3.5 [23]	7.34 ± 0.04 [24]	16.1 ± 0.9 [25]
Category 1		KBR BSA 4.0% w/v	308 [9]	4.0 ± 0.0 [9]	7.36 [9]	12.0 ± 1.2
Category 2		KRB BS 12.0 μM PL 2.5 mM	278	5.0 ± 0.1	8.64	1.5 ± 0.0
		KRB BS 12.0 μM PL 2.5 mM CH 4.5 mM	273	5.0 ± 0.1	8.79	1.5 ± 0.1
		KRB BS 12.0 μM PL 2.5 mM BSA 2.0% w/v	314	5.2 ± 0.1	7.79	7.8 ± 0.0
		KRB BS 12.0 μM PL 2.5 mM CH 4.5 mM BSA 4.0% w/v	306	5.0 ± 0.1	7.80	7.5 ± 0.2
		KRB BS 12.0 μM PL 2.5 mM BSA 8.0% w/v	351	5.2 ± 0.0	7.65	7.7 ± 0.0
Category 3	3a	KRB BS 20.0 mM PL 4.0 mM	310	4.8 ± 0.1	8.25	1.7 ± 0.0

		PBS BS 19.8 mM PL 7.9 mM	330	4.7 ± 0.1	7.36	6.1 ± 0.1
		KRB BS 20.0 mM PL 4.0 mM BSA 4.0% w/v	415	5.0 ± 0.1	8.50	5.2 ± 0.1
		PBS BS 19.8 mM PL 7.9 mM BSA 4.0% w/v	425	4.9 ± 0.1	7.18	14.2 ± 0.8
	3b	KRB SLS 1.5 mM	289	4.6 ± 0.1	8.54	1.2 ± 0.0
		PBS SLS 1.4 mM	280	4.4 ± 0.1	7.43	5.6 ± 0.1
		KRB SLS 30.0 mM BSA 4.0% w/v	350	5.0 ± 0.1	7.84	7.9 ± 0.1
		PBS SLS 60.0 mM BSA 4.0% w/v	325	5.2 ± 0.1	7.56	10.3 ± 0.2
	3c	PBS SLS 30.0 mM BSA 2.0% w/v	300	4.8 ± 0.0	7.10	9.3 ± 0.2
		PBS SLS 30.0 mM BSA 4.0% w/v	297	4.6 ± 0.0	7.18	9.6 ± 0.6
		PBS SLS 60.0 mM BSA 2.0% w/v	302	4.9 ± 0.1	7.04	11.6 ± 0.3

Osm: Osmolality, Vis: Viscosity, BC HCl: buffer capacity determined with HCl.

On the other hand pH is only similar to plasma in the media with BSA but the buffer capacity was not as high as in plasma. BSA increased the osmolality and the buffer capacity, and kept the pH at ~7.5. However, when any other component apart from BSA was added, an increase in the pH and a decrease in the buffer capacity were observed (Table 3.2).

Addition of BSA, in a concentration range from 1.5 to 4.0 % w/v in KRB buffer (category 1 biorelevant media), was reported to increase AmB solubility [9]. The addition of biorelevant plasma components, to which AmB is bound *in vivo*, to the medium would be expected to increase AmB solubility bringing it closer to its plasma solubility. AmB concentration profiles in category 2 media show a decrease in AmB solubility compared to its solubility in KRB BSA 4.0% w/v (category 1 media) and plasma (Figure 3.2). In the concentrations utilized for media development, PL and CH are not soluble [26, 27]; this might be counterproductive to AmB solubilisation, as the components are needed to be in solution in order to dissolve AmB. When CH or BS-PL are present in the media without BSA (Table 3.2), the AmB solubility values are the lowest of all the values measured in all the tested media (Figure 3.2). In the media where BSA is present along with BS-PL or BS-PL CH, regardless of its concentration, AmB solubility is slightly higher than in these media without BSA, but lower than the solubility values measured in media with only BSA (Figure 3.2). It has been reported that BSA is capable of binding bile salts [28-30], cholesterol [31, 32] and phospholipids [33]. The results suggest that, rather than CH or BS-PL having an additive effect to BSA on the solubility of AmB, BSA is hindering solubilisation by biorelevant components added to the medium leading in their inability to bind/dissolve AmB while at the same time the biorelevant components are reducing the solubilising effect of BSA on AmB. Only in the category 2 medium with the highest BSA concentration, (KRB BS PL BSA 8.0% w/v) AmB solubility was increased, but still it was lower than in the medium with only BSA 4.0% w/v (category 1 biorelevant medium). As category 2 media failed to produce better solubility values than category 1 media, no further studies were performed with these media.

3.3.2.3.1. Category 3a media

The concentration of BS and PL in the medium were the only significant factors on the analysis of AmB solubility for the development of category 3a media (Figure 3.3).

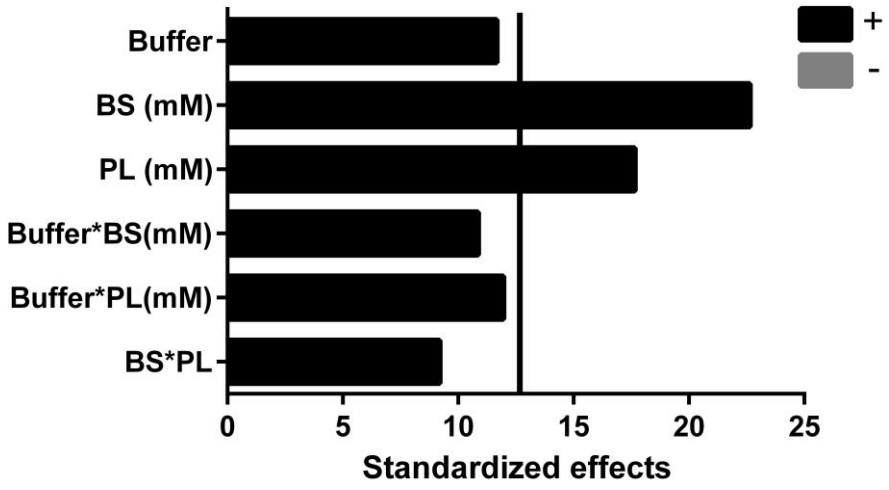

Figure 3.3. Pareto chart for the standardized effects of the main factors and 2 level interactions of the analysis of AmB solubility in media with BS, PL and different types of buffer. The black horizontal line represents the significance threshold for the effects. The factors with an effect (bar) larger than the threshold are statistically significant.

Equation 3.5 was obtained from the DoE analysis and was used to predict the concentrations of BS and PL in both KRB and PBS to produce AmB solubility values similar to the ones observed in plasma (clinically relevant).

$$Solubility\ (\mu g/mL) = 5.56 - 2.09 * Buffer + 0.33 * BS(mM) + 0.04 * PL(mM) + 0.29 * Buffer * BS(mM) + 0.81 * Buffer * PL(mM) + 0.18 * BS(mM) * PL(mM)$$ (Eq 3.5).

The predicted concentrations of BS and PL were BS 20.0 mM PL 4.0 mM for KRB BSA 4.0% w/v and BS 19.7 mM PL 7.9 mM for PBS BSA 4.0%w/v. The media characterization showed that the presence of BSA increases the buffer capacity, the osmolality and the pH (in KRB); similar to the effects noted in category 2 media (Table 3.2). Osmolality was similar to the one of plasma only for the media prepared without BSA (the concentration of BS-PL had a high impact on the osmolality and when BSA

was added, the osmolality increased up to 425 mOsm/L). The pH value was only similar to the one of plasma for the medium prepared in PBS. The buffer capacity statistically similar to the plasma value only in PBS BS 19.8 mM PL 7.9 mM BSA 4.0% w/v. Degradation rate constants were not statistically similar to the one observed in plasma except in the KRB BS 20.0 mM PL 4.0 mM medium (Table 3.1). In KRB, the presence of BSA resulted in faster degradation of AmB than in the medium without BSA; in PBS this effect is not observed. The higher AmB degradation rate constant values in these media could be due to the absence of certain plasma components which could reduce the AmB degradation.

AmB solubility in these media was lower than the one observed in plasma, but in these media without BSA, AmB solubility values were similar to the ones observed in plasma (clinically relevant) (Figure 3.4).

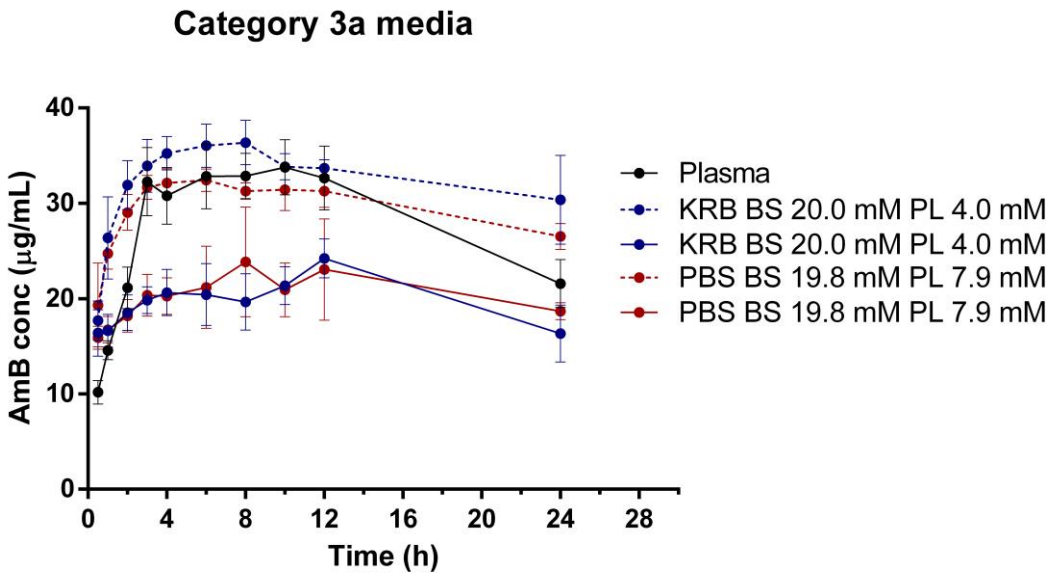

Figure 3.4. Solubility study of AmB in category 3a media: AmB concentration as a function of time in category 3a media with and without BSA (Mean ± SD; n= 3). Solid lines represent media with BSA 4.0% w/v and dotted lines media without BSA. AmB plasma solubility was added for comparison purposes.

The predicted BS and PL concentrations were much higher than the initial exploration ranges, and the effects of BS - PL on solubilising potential of BSA and vice versa, were not captured in the media as the equation was not suitable for extrapolation.

However, the effect of BSA in the first place seems to have been immaterial in equation 3.5, as clinical relevant solubility was achieved without any BSA.

3.3.2.3.2. Category 3b: clinically relevant media

The CMC of SLS and CTAB in water is 8.1 mM and 1.0 mM, respectively [34]. The CMC of surfactants tends to decrease in a medium where the ionic strength is high, such as in saline buffers like PBS and KRB [35]. The CMC of SLS in PBS and KRB was 1.3 ± 0.0 mM and 1.4 ± 0.2 mM, respectively and the CMC of CTAB in PBS and KRB was 0.9 ± 0.0 mM and 0.2 ± 0.0 mM, respectively. The surfactant concentrations selected for the solubility studies were above of their CMC. CTAB was not soluble at 100.0 mM and KRB CTAB 50.0 mM BSA 4.0%w/v medium gelatinized, thus, AmB solubility could not be measured in these media. Figure 3.5 shows the AmB solubility in the different media with and without BSA.

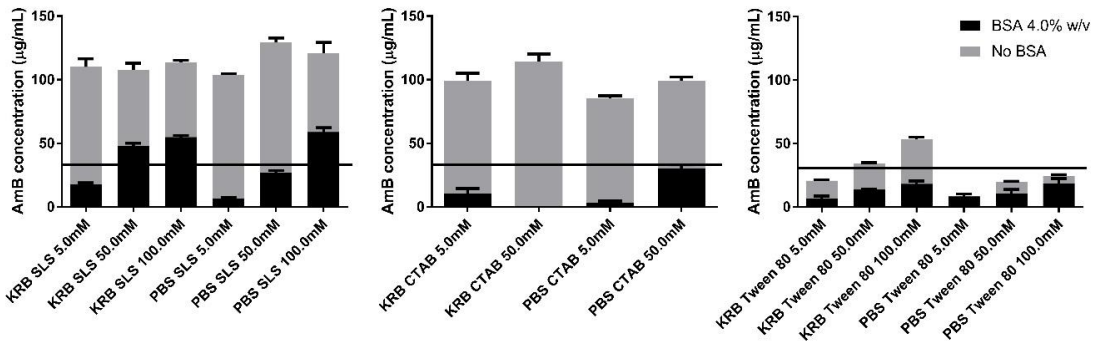

Figure 3.5. Solubility study of AmB in media with surfactants for the development of category 3b media: AmB concentration in PBS or KRB with 5.0, 50.0 and 100.0 mM concentrations of SLS, CTAB or Tween with and without BSA 4.0% w/v at 12 h (Mean ± SD; n= 3). Black horizontal line represents the AmB solubility value in human plasma from healthy subjects.

The apparent limit on AmB concentration, even with the highest surfactant concentration, was due to the AmB amount added ~ 1.0 mg, hence, concentration could not be higher than ~100.0 µg/mL and this value cannot be considered as the AmB solubility value. The charged surfactants (anionic and cationic) solubilised more AmB than the non-ionic surfactant despite the fact that AmB is a hydrophobicmolecule (log P 0.8 [36]). AmB, as an amphoteric molecule with two pKa values (pKa_1 = 5.5, pKa_2 = 10.0) will be charged at pH 7, thus, the interaction between

its charges and those of the surfactant would promote contact of the molecules leading to solubilisation of the drug. Similar to category 2 and 3a media observations, BSA presence in the media decreased AmB solubility. It has been reported that BSA binds to SLS, CTAB and Triton X-100 (non-ionic surfactant) with with the weakest binding observed for Triton X-100 [37-39]. Figure 3.6 shows the effect of surfactants (in both category 3a and 3b media) and BSA on AmB solubility.

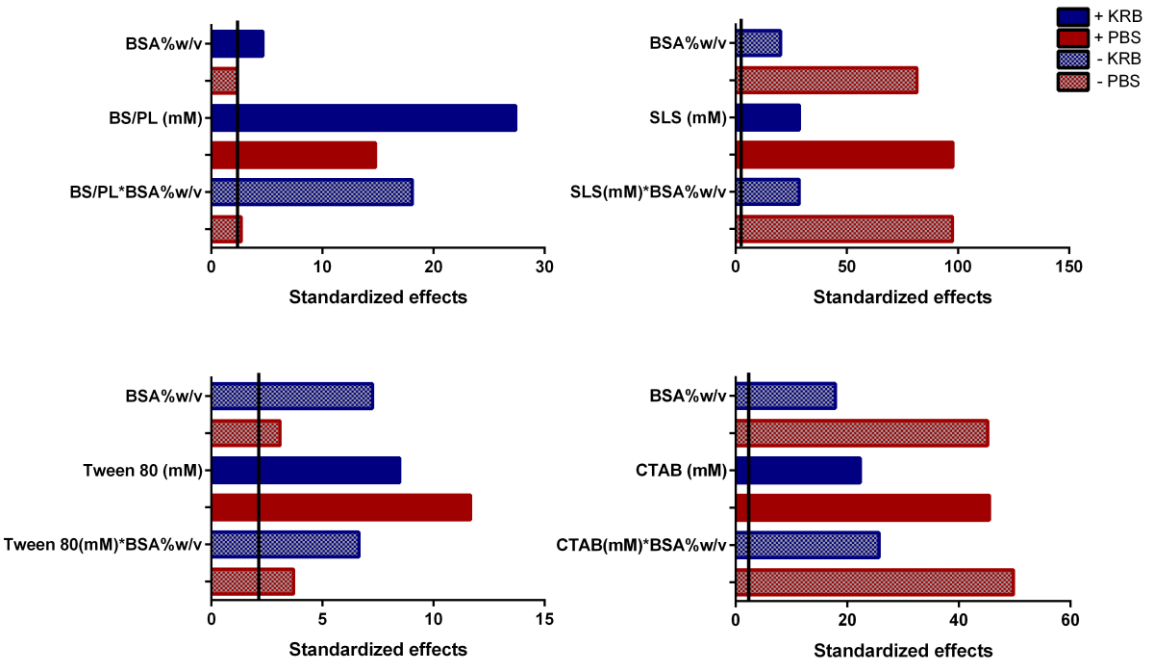

Figure 3.6. Pareto charts for the standardized effects of the main factors and 2 level interactions of the analysis of AmB solubility in media with surfactants and BSA 4.0% w/v. The black horizontal line represents the significance threshold for the effects. The factors with an effect (bar) larger than the threshold are statistically significant.

The surfactant presence has a statistically significant positive effect on AmB solubility, whereas BSA and the interaction between BSA and surfactant have a negative effect. The results suggest that the presence of BSA and the surfactant alone in the medium, solubilise AmB [9], but when both are in the medium, they interfere with each other preventing AmB solubilisation and leading to a decrease in the solubility compared to the solubility reached in the medium with the surfactant alone. The ability of BSA to interfere with several types of molecules (BS, PL, CH, SLS, CTAB, Tween 80, as found in this study) has to be taken into account when a biorelevant or clinically relevant medium, incorporating BSA, is developed. The

required concentration of other components with surfactant/solublising activity could be under-estimated due to protein-surfactant interactions, leading to an unintended reduction in API solubility. Among the media with the different surfactants tested, the presence of SLS in the medium was the only one to produce clinically relevant solubility values of AmB in KRB and PBS, with and without BSA.

The composition of media based on either KRB or PBS with BSA were calculated to target an AmB clinically relevant solubility value. The calculated compositions of the media to reach AmB solubility values similar to the observed in plasma were KRB SLS 30.0 mM BSA 4.0%w/v and PBS 60.0 mM BSA 4.0%w/v. The media composition without BSA could not be obtained directly by just removing BSA from the media as AmB solubility would be extremely high (Figure 3.5). Therefore, lower concentrations of SLS (0.1 – 4.0 mM) were tested in PBS and KRB to find the appropriate concentration for clinically relevant AmB solubility values without BSA. The SLS concentrations where the AmB solubility was similar to the one observed in plasma were 1.5 mM for KRB and 1.4 mM for PBS. In the clinically relevant media developed with SLS, the presence of BSA did not affect the viscosity but increased the buffer capacity and the osmolality as in category 3a media (Table 3.2). AmB degradation rate constants were not statistically similar to the one observed in plasma. AmB degradation rate constants were the lowest in media composed of SLS alone in buffer solution, which can be considered minimal (Table 3.1), and the AmB degradation rate constant in media with BSA were significantly higher than in the medium with SLS only. This effect could be related to observations found in category 1 media (Table 3.1) where an increasing BSA concentration had a positive effect on the degradation rate constant. The results of the solubility studies in the developed category 3b media with and without BSA are presented in Figure 3.7. It can be observed that the AmB concentration profiles are similar to the one observed in plasma.

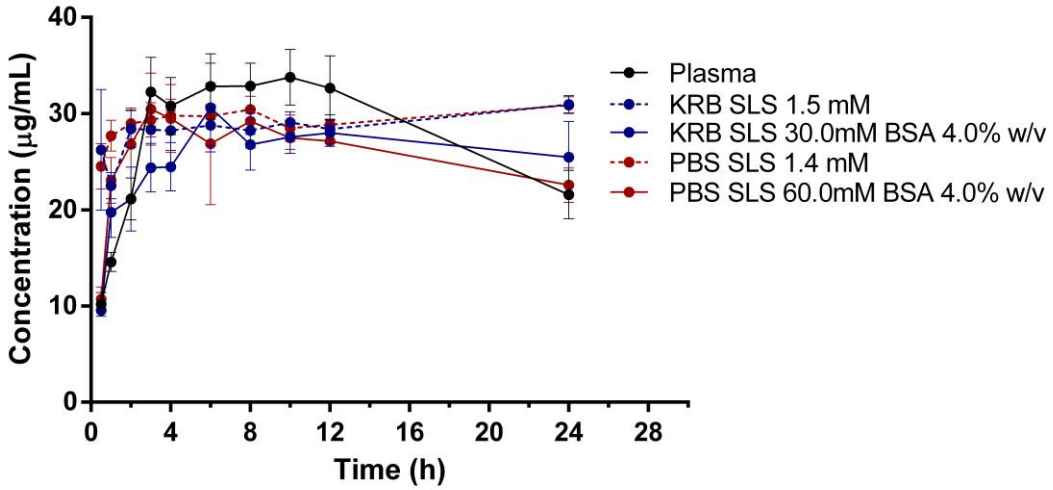

Figure 3.7. Solubility study of AmB in category 3b media: AmB concentration as a function of time in the category 3b clinically relevant media with and without BSA (mean ± SD; n= 3). AmB plasma solubility was added for comparison purposes. The BSA concentration is in %w/v units.

3.3.2.3.3. Category 3c: clinically relevant media

As solubility data in plasma was only available from plasma obtained from healthy subjects, a target solubility value for hypoalbuminaemic patients was not available. This section therefore represents characterisation of media evolved from category 3b as potential candidates for further patient-centric media development. The composition of the media was the following: a) PBS SLS 60.0 mM BSA 2.0 % w/v, b) PBS SLS 30.0 mM BSA 2.0% w/v to reflect the reduced inhibition of BSA on SLS (observed during category 2 and 3a and 3b media development) when the lower BSA concentration was used and c) PBS SLS 30.0 mM BSA 4.0% w/v to explore the reduced potential for SLS solubilisation which might better reflect a potentially lower solubility in hypoalbuminaemia. These 3 media had characteristics similar to healthy plasma (Table 3.2) apart from a reduced buffer capacity and slightly lower pH. The AmB degradation rate constants in media with BSA 4.0% w/v are apparently higher than the ones obtained in media with BSA 2.0% w/v but the difference was not statistically significant. All the degradation rate constants were statistically different to the one observed in plasma. The results of the single point AmB solubility studies in these media were: a) PBS SLS 60.0 mM BSA 2.0 % w/v = 65.57 ± 4.98 µg/mL, b) PBS SLS 30.0 mM BSA 2.0% w/v = 25.84 ± 0.97 µg/mL, c) PBS SLS 30.0 mM BSA 4.0% w/v = 19.77 ± 0.29 µg/mL. This supports the hypothesis that BSA interferes with

the action of the surfactants, in this case SLS, as in the medium with SLS 60.0 mM and BSA 2.0% w/v concentrations, the AmB concentration at 12 h was the highest and in the medium with SLS 30.0 mM and BSA 4.0% w/v, was the lowest.

3.3.2.4. Summary and evaluation of the test media

Table 3.3 presents a summary and an evaluation of the media in terms of biorelevance/clinically relevance of the media developed in comparison with the parameters obtained from plasma. Although category 1 media [9] was not clinically relevant for solubility or degradation, this media could be useful to investigate the impact of the albumin concentration on poorly soluble and highly – bound to proteins drugs as it was shown for AmB on its solubility, degradation and pharmacological activity [9]. Clinically relevant AmB solubility values are achieved by using biorelevant surfactants in category 3a media without BSA. These media could be used for *in vitro* release tests of AmB lipid-based formulations and also, these media with BSA could be used in order to identify an effect of BSA on the formulation even if it is not clinically relevant. Clinically relevant AmB solubility values were achieved in all the category 3b media developed. Category 3b media without BSA, as it is easier to prepare and the degradation of the drug is minimal (Table 3.1) it could be the base towards the development of appropriate media for compendial release tests. For category 3c media the AmB there was no reference values for solubility, degradation and media characterization due to the unavailability of hypoalbuminaemic plasma. PBS SLS 30.0 mM BSA 4.0% w/v it is a good candidate towards the development of simulated hypoalbuminaemic plasma as the AmB solubility at 12 h in this medium was lower than the clinically relevant value.

Neither the solubility nor the degradation rate constant could be related to any of the properties of media characterization (Table 3.2). Solubility was found to be highly related to the concentration of BSA and of the surfactants in the medium (Figure 3.6), while the degradation rate constant was generally higher in the media with BSA (Table 3.1).

Table 3.3. Overall evaluation of biorelevance, clinically relevance and easiness of preparation of the media developed. The values of media characterization were compared against the values reported in the literature for plasma and the AmB solubility found in plasma. NA = not determined due to data unavailable for comparison, ✖ = not biorelevant, ✓ = biorelevant. Easiness of preparation (EoP) received values from 1 to 4, being 1 to the easiest and 4 the most difficult to prepare.

Category	Medium	CRS	CRD	Osm	Vis	pH	BC HCl	EoP
Category 1	KRB BSA 4.0% w/v [9]	No	No	✖	✖	✓	✖	1
Category 3a	KRB BS 20.0 mM PL 4.0 mM	Yes	Yes	✖	✖	✖	✖	4
	PBS BS 19.8 mM PL 7.9 mM	Yes	No	✖	✖	✓	✖	3
	KRB BS 20.0 mM PL 4.0 mM BSA 4.0% w/v	No	No	✖	✖	✖	✖	4
	PBS BS 19.8 mM PL 7.9 mM BSA 4.0% w/v	No	No	✖	✖	✖	✓	3
Category 3b	KRB SLS 1.5 mM	Yes	No	✓	✖	✖	✖	2
	PBS SLS 1.4 mM	Yes	No	✓	✖	✓	✖	1
	KRB SLS 30.0 mM BSA 4.0% w/v	Yes	No	✖	✖	✖	✖	2
	PBS SLS 60.0 mM BSA 4.0% w/v	Yes	No	✖	✖	✖	✖	1
Category 3c	PBS SLS 30.0 mM BSA 2.0% w/v	ND	ND	ND	ND	ND	ND	1

	PBS SLS 30.0 mM BSA 4.0% w/v	ND	ND	ND	ND	ND	ND	1
	PBS SLS 60.0 mM BSA 2.0% w/v	ND	ND	ND	ND	ND	ND	1

CRS: AmB clinically relevant solubility, CRD: AmB clinically relevant degradation rate constant, Osm: osmolality, Vis: viscosity, BC HCl: buffer capacity determined with HCl,

3.3.4. Dissolution studies of AmB with the flow through cell apparatus in clinically relevant media

Dissolution studies were performed in clinically relevant media from category 3a and 3b, and in each of the media explored in category 3c (Figure 3.8).

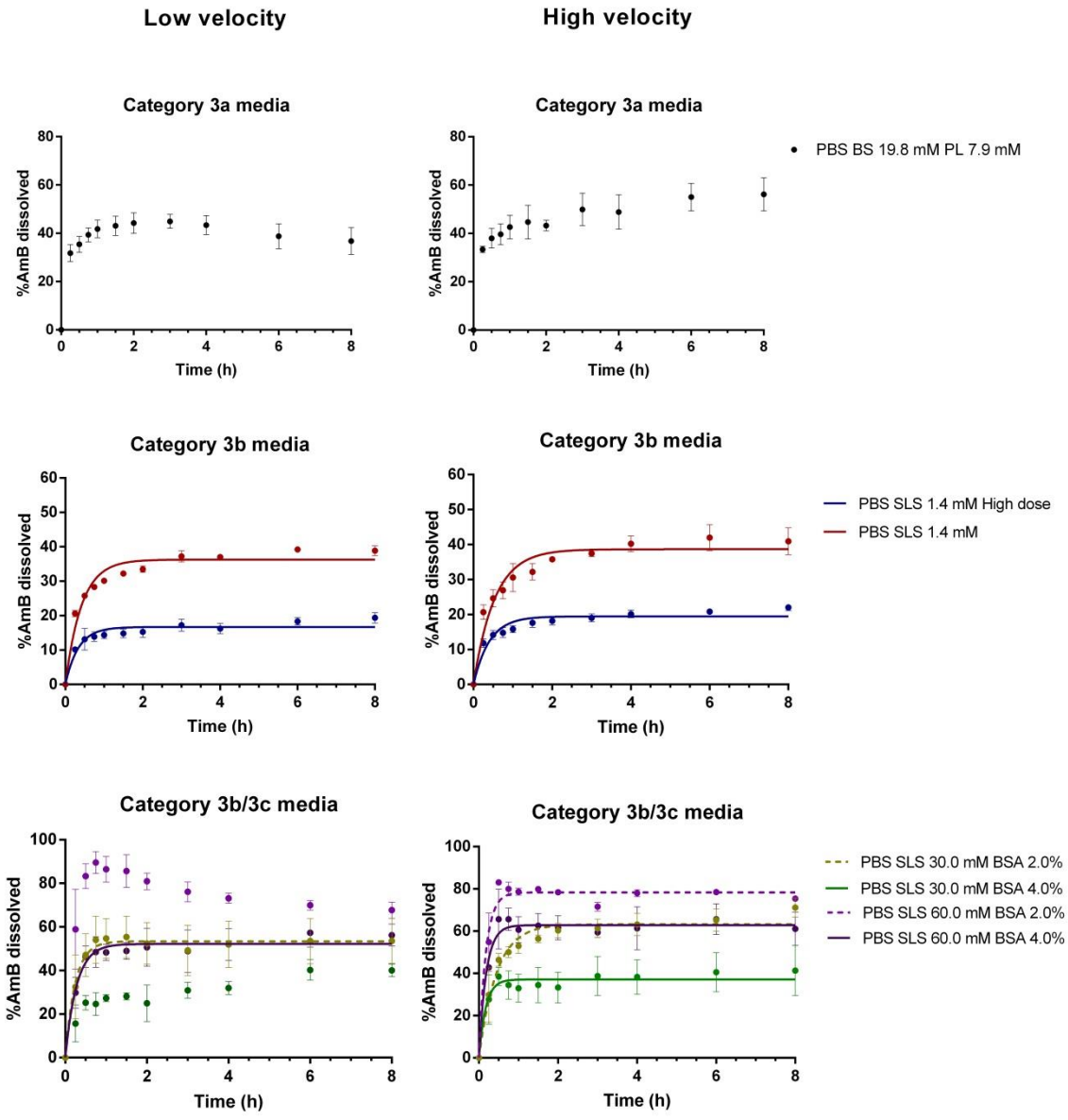

Figure 3.8. %AmB dissolved as a function of time in the category 3a and 3b clinically relevant media and in category 3c media with the flow through cell apparatus at 37°C (mean ± SD; n= 3). High dose = 5 mg of AmB. BSA concentration is in %w/v units. Points represent observed data and the lines the first order (Eq 3.3) equation fittings.

Clinically AmB solubility values were obtained in PBS and in KRB, but the media with PBS were selected for dissolution studies due to their easiness of preparation

(compared to KRB). First order equation parameters of AmB for corrected for degradation dissolution profiles fitted to Eq 3.3, are listed in Table 3.4

Dissolution profiles in PBS BS 19.8 mM PL 7.9 mM could not be modeled using Eq 3.3 in either low or high velocity conditions. In the low velocity environment, the % AmB dissolved reached a maximum value of 44.93 ± 2.89% at 3.0 h and then started to decrease until the end of the experiment (8 h). This could indicate that mixed micelles of BS – PL need a stronger agitation (as in the bottle/stirrer setup of solubility and degradation studies) to be able to have a steady effect on AmB solubility and not only for one part of the test. There was not reduction of the AmB percent dissolved when the test was conducted at high velocity, however in this situation there was no discernible plateau and rather a very gradual increase in % dissolved over time, prohibiting fitting of Eq 3.3 to the data. In summary, AmB is dissolved better under the high velocity conditions in the clinical relevant category 3a medium (Figure 3.8).

There was a statistically significant negative effect of velocity in dissolution rate constant for the 0.5 mg dose and a positive effect on maximum % dissolved on the 5 mg dose, however these differences were of low practical significance and possibly reflect process variability.

The % AmB dissolved in the experiment with the high dose of AmB reached a plateau value of around 30%, due to the solubility of AmB in this medium (~30 µg/mL), (Figure 3.8). In category 3b media with BSA, with respect to velocity, the low and high velocity conditions had little effect on AmB dissolution in comparison to medium composition.

Table 3.4. Parameters obtained after fitting (Eq 3.3) of %AmB dissolution profiles in category 3b clinically relevant media and 3c media with the flow through cell apparatus (Mean ± SD, n = 3).

Type of medium	Medium	Flow/velocity	k_{diss} (h^{-1})	X_{max} (%)	R^2	AIC
Category 3b	PBS SLS 1.4 mM Low dose	Low	2.39 ± 0.13	36.28 ± 0.59	0.94 ± 0.00	50.03 ± 0.29
	PBS SLS 1.4 mM High dose	Low	2.98 ± 0.74	16.75 ± 1.16	0.91 ± 0.01	38.77 ± 2.28
	PBS SLS 60.0 mM BSA 4.0% w/v	Low	3.65 ± 1.59	52.79 ± 5.52	0.91 ± 0.05	63.05 ± 3.77
	PBS SLS 1.4 mM Low dose	High	1.88 ± 0.26	38.66 ± 2.08	0.93 ± 0.02	53.94 ± 4.06
	PBS SLS 1.4 mM High dose	High	2.50 ± 0.40	19.47 ± 0.81	0.92 ± 0.01	40.40 ± 1.32
	PBS SLS 60.0 mM BSA 4.0% w/v	High	5.60 ± 1.30	62.86 ± 5.22	0.91 ± 0.10	63.03 ± 12.28

Category 3c	PBS SLS 30.0 mM BSA 2.0% w/v	Low	4.21 ± 0.96	53.38 ± 9.94	0.96 ± 0.05	50.47 ± 9.28
	PBS SLS 30.0 mM BSA 2.0% w/v	High	2.33 ± 0.35	63.07 ± 3.48	0.94 ± 0.01	63.20 ± 1.21
	PBS SLS 30.0 mM BSA 4.0% w/v	High	7.66 ± 5.39	37.22 ± 8.20	0.89 ± 0.04	57.06 ± 3.45
	PBS SLS 60.0 mM BSA 2.0% w/v	High	6.43 ± 2.87	78.38 ± 0.50	0.96 ± 0.01	63.08 ± 3.31

R^2: correlation coefficient, AIC: Akaike Information Criterion.

In the velocity regimes in the flow through apparatus, both of which are low overall in comparison to the bottle/stirrer set up (low velocity: 0.07, high velocity: 0.52, bottle/stirrer:10.2 cm/s), a faster dissolution and a higher % AmB dissolved is observed in the category 3b medium with BSA compared to the one observed in the medium without BSA. This could be attributed to increased wetting/dispersion from either the BSA or the SLS. PBS SLS 1.4 mM is suggested as a simplified medium that could be used in compendial dissolution testing of AmB parenteral formulation, as clinically relevant AmB solubility values were obtained in this medium.

In category 3c media, the %AmB dissolved in PBS SLS 60.0 mM BSA 2.0% w/v started to decrease before the 1.5 h sample in the low velocity conditions. The results suggest that the agitation required to keep SLS, BSA and AmB in solution at these concentrations was higher as the decrease was not observed when the high velocity conditions were used. The highest %AmB dissolved was observed in PBS SLS 60.0 mM BSA 2.0% w/v and the lowest in PBS SLS 30 mM BSA 4.0% w/v, supporting the hypothesis that BSA binds the surfactants and prevents their interaction with AmB. The AmB dissolution profiles in PBS SLS 30.0 mM BSA 2.0% w/v and PBS SLS 60 mM BSA 4.0% w/v were similar, probably due to the same ratio of SLS/BSA in these two media. Velocity had a negative effect only on the dissolution rate of AmB in PBS SLS 30.0 mM BSA 2.0% w/v whereas this was not observed in the AmB dissolution in the other category 3c media. It could be hypothesized that for this specific medium, this difference could be due to that with the low velocity setup (large cell and a flow rate of 16/mL), the powder is in contact with a larger volume of medium and for a longer period of time than with the high velocity which could help to dissolve the powder faster. The results suggest that the most suitable clinically releavant medium to simulate hypoalbuminaemic conditions is PBS SLS 30 mM BSA 4.0% w/v; confirmation with solubility studies in plasma from hypoalbunaemic patients would be needed. This is only based on the hypothesis that in plasma from hypoalbuminaemic patients, AmB solubility values will be lower than in healthy subjects as a decreasing concentration of albumin decreases AmB solubility. As the dissolution profiles were calculated based on concentrations corrected accounting for AmB degradation, the degradation rate constant was not a factor to be considered in the analysis, as it was already taken into account in the profiles. AmB had clinically relevant solubility values in the media used for the dissolution studies (~ 30 µg/mL)

and with the amount of AmB and the volume of medium used in the studies, in case of the 100% dissolution of AmB the maximum concentration that could be obtained was 10 µg/mL which is the third part of the solubility value, thus, the solubility could not be a factor affecting the dissolution. Only in category 3c media, where the solubility values were different, the differences of AmB percent dissolved could be accounted to the solubility.

3.4. Conclusions

AmB is an antifungal drug that is highly bound to plasma proteins, including albumin and lipoproteins. It is administered to patients intravenously as lipid-based formulations. Therefore, a test medium to assess the release profile of the drug from its lipid-based parenteral formulations that can provide clinically relevant results is desirable.

In this study we have developed biorelevant media based on plasma composition (which was not useful) and clinically relevant dissolution media based on the solubility of AmB in plasma. This was achieved by using saline buffers, surfactants (biorelevant and synthetic) and BSA. It was shown that addition of BSA in the medium generally induces a faster degradation of AmB. Another role of BSA in the media is the capability to interfere with the solubilizing activity of almost all of the components that were added to the media. Instead of resulting in an improved AmB solubility by combining surfactants with BSA, the opposite effect was observed. This has to be taken into consideration for development of *in vitro* test media where the protein binding is an important feature. From the dissolution studies, it can be concluded that PBS SLS 1.4 mM could be a good option for future release tests of AmB formulations, as the degradation in this medium is minimal. This medium was the easiest to prepare suggesting its potential suitability for routine use in compendial testing. For the simulated hypoalbuminaemic media, PBS SLS 30 mM BSA 4.0% w/v is suggested as a potential candidate medium for further (patient centric) medium development, although future experiments with hypoalbuminaemic plasma are needed to confirm the effect of hypoalbuminaemia on solubility. Development of clinically relevant media is a first step for developing clinically relevant dissolution/ release tests with a view to obtaining *in vitro* data predictive of the *in vivo* behaviour of the formulation and the drug.

Acknowledgments

Part of this work has been previously presented at the AAPS annual meeting in San Diego November 2017 (poster presentation). The authors would like to thank the Mexican Council of Science and Technology (CONACyT) for the PhD scholarship of Mr R Diaz de Leon-Ortega, Mr Fernando Acosta (Department of Chemical Engineering, University of Bath) for his help with the operation of the rheometer and to Dr Giordano Pula (Medical School Exeter, University of Exeter) for his help with the extraction of blood from healthy volunteers.

3.5. References

[1]. Ansel's pharmaceutical dosage forms and drug delivery systems. 10th edition. ed. Ansel HC, Allen LV, Lippincott W, Wilkins, Wolters Kluwer H, editors: Philadelphia : Wolters Kluwer/Lippincott Williams & Wilkins Health; 2014.

[2]. Seidlitz A, Nagel S, Semmling B, Grabow N, Sternberg K, Weitschies W. Biorelevant Dissolution Testing of Drug-Eluting Stents: Experiences with a Modified Flow-Through Cell Setup. Dissolution Technologies. 2011;18(1):26-34.

[3]. Shen J, Burgess DJ. In vitro dissolution testing strategies for nanoparticulate drug delivery systems: recent developments and challenges. Drug delivery and translational research. 2013;3(5):409-15.

[4]. D'Souza SS, DeLuca PP. Methods to assess in vitro drug release from injectable polymeric particulate systems. Pharm Res. 2006;23(3):460-74.

[5]. Shen J, Burgess DJ. Accelerated in-vitro release testing methods for extended-release parenteral dosage forms. J Pharm Pharmacol. 2012;64(7):986-96.

[6]. Wang Q, Fotaki N, Mao Y. Biorelevant dissolution: methodology and application in drug development. Dissolution Technologies. 2009;16(3):6-12.

[7]. Norris K, et al. Moving towards Clinically Relevant Dissolution Specifications 2016. Available from: http://www.aaps.org/NewsMagazine/print.aspx?id=29891.

[8]. Abend A, Heimbach T, Cohen M, Kesisoglou F, Pepin X, Suarez-Sharp S. Dissolution and Translational Modeling Strategies Enabling Patient-Centric Drug Product Development: the M-CERSI Workshop Summary Report. The AAPS Journal. 2018;20(3):60.

[9]. Diaz de Leon-Ortega R, D'Arcy DM, Bolhuis A, Fotaki N. Investigation and simulation of dissolution with concurrent degradation under healthy and hypoalbuminaemic simulated parenteral conditions- case example Amphotericin B. Eur J Pharm Biopharm. 2018.

[10]. Brajtburg J, Elberg S, Bolard J, Kobayashi GS, Levy RA, Ostlund RE, Jr., et al. Interaction of plasma proteins and lipoproteins with amphotericin B. The Journal of infectious diseases. 1984;149(6):986-97.

[11]. Ridente Y, Aubard J, Bolard J. Absence in amphotericin B-spiked human plasma of the free monomeric drug, as detected by SERS. FEBS letters. 1999;446(2-3):283-6.

[12]. Joanna B, Isabelle D, Claire O, Ilona G. Amphotericin B toxicity as related to the formation of oxidatively modified low-density lipoproteins. Biospectroscopy. 1998;4(2):135-44.

[13]. Torrado JJ, Espada R, Ballesteros MP, Torrado-Santiago S. Amphotericin B formulations and drug targeting. Journal of pharmaceutical sciences. 2008;97(7):2405-25.

[14]. Hospitals RC. Obstetric cholestasis – clinical guideline for diagnosis and management. http://wwwrchtnhsuk/DocumentsLibrary/RoyalCornwallHospitalsTrust/Clinical/MidwiferyAndObstetrics/CholestasisClinicalGuidelinesForTheManagementOfObstetricpdf. 2014.

[15]. Ambros-Rudolph CM, Glatz M, Trauner M, Kerl H, Müllegger RR. The importance of serum bile acid level analysis and treatment with ursodeoxycholic acid in intrahepatic cholestasis of pregnancy: A case series from central europe. Archives of Dermatology. 2007;143(6):757-62.

[16]. Egan N, Bartels A, Khashan AS, Broadhurst DI, Joyce C, O'Mullane J, et al. Reference standard for serum bile acids in pregnancy. BJOG : an international journal of obstetrics and gynaecology. 2012;119(4):493-8.

[17]. Salvioli G, Lugli R, Pradelli JM, Gigliotti G. Bile acid binding in plasma: the importance of lipoproteins. FEBS letters. 1985;187(2):272-6.

[18]. Schaefer LE, Adlersberg D, Steinberg AG. Serum phospholipids: genetic and environmental influences. Circulation. 1958;18(3):341-7.

[19]. Abdelmagid SA, Clarke SE, Nielsen DE, Badawi A, El-Sohemy A, Mutch DM, et al. Comprehensive profiling of plasma fatty acid concentrations in young healthy Canadian adults. PloS one. 2015;10(2):e0116195.

[20]. Moschetta A, vanBerge-Henegouwen GP, Portincasa P, Palasciano G, van Erpecum KJ. Cholesterol crystallization in model biles: effects of bile salt and phospholipid species composition. Journal of Lipid Research. 2001;42(8):1273-81.

[21]. Fotaki N. Flow-through cell apparatus (USP apparatus 4): Operation and features. Dissolution Technologies. 2011;18(4):46-9.

[22]. Dasgupta A, Wahed A. Chapter 5 - Water, Homeostasis, Electrolytes, and Acid–Base Balance. In: Dasgupta A, Wahed A, editors. Clinical Chemistry, Immunology and Laboratory Quality Control. San Diego: Elsevier; 2014. p. 67-84.

[23]. Rand PW, Lacombe E, Hunt HE, Austin WH. Viscosity of normal human blood under normothermic and hypothermic conditions. Journal of Applied Physiology. 1964;19(1):117-22.

[24]. Shepherd JT. The human cardiovascular system : facts and concepts. Vanhoutte PM, editor. New York: New York : Raven Press; 1979.

[25]. Ellison G, Straumfjord JV, Jr., Hummel JP. Buffer capacities of human blood and plasma. Clin Chem. 1958;4(6):452-61.

[26]. Sigma-Aldrich. L-a-Phosphatidylcholine 2019 [07/01/2019]. Available from: https://www.sigmaaldrich.com/content/dam/sigma-aldrich/docs/Sigma/Product_Information_Sheet/1/p7443pis.pdf.

[27]. Information NCfB. Cholesterol, CID=5997: PubChem Compound Database; 2019 [07/01/2019]. Available from: https://pubchem.ncbi.nlm.nih.gov/compound/5997.

[28]. Pico GA, Houssier C. Bile salts-bovine serum albumin binding: spectroscopic and thermodynamic studies. Biochimica et Biophysica Acta (BBA) - Protein Structure and Molecular Enzymology. 1989;999(2):128-34.

[29]. Green HO, Moritz J, Lack L. Binding of sodium taurocholate by bovine serum albumin. Biochimica et Biophysica Acta (BBA) - Lipids and Lipid Metabolism. 1971;231(3):550-2.

[30]. Farruggia B, Picó GA. The binding of 3,6-disubstituted bile salts to human serum albumin induces conformational change on the molecule of this protein.

Biochimica et Biophysica Acta (BBA) - Protein Structure and Molecular Enzymology. 1999;1429(2):299-306.

[31]. Zhao Y, Marcel YL. Serum Albumin Is a Significant Intermediate in Cholesterol Transfer between Cells and Lipoproteins. Biochemistry. 1996;35(22):7174-80.

[32]. Sankaranarayanan S, de la Llera-Moya M, Drazul-Schrader D, Phillips MC, Kellner-Weibel G, Rothblat GH. Serum albumin acts as a shuttle to enhance cholesterol efflux from cells. Journal of Lipid Research. 2013;54(3):671-6.

[33]. Jonas A. Interaction of phosphatidylcholine with bovine serum albumin. Specificity and properties of the complexes. Biochimica et biophysica acta. 1976;427(1):325-36.

[34]. Attwood D, Florence AT. Surfactant systems: their chemistry, pharmacy and biology: Chapman and Hall; 1983.

[35]. Thongngam M, McClements DJ. Influence of pH, Ionic Strength, and Temperature on Self-Association and Interactions of Sodium Dodecyl Sulfate in the Absence and Presence of Chitosan. Langmuir. 2005;21(1):79-86.

[36]. Sigma-Aldrich. Amphotericin B. https://wwwsigmaaldrichcom/content/dam/sigma-aldrich/docs/Sigma/Datasheet/6/a9528datpdf. 2015.

[37]. De S, Girigoswami A, Das S. Fluorescence probing of albumin–surfactant interaction. Journal of Colloid and Interface Science. 2005;285(2):562-73.

[38]. Gull N, Chodankar S, Aswal VK, Sen P, Khan RH, Kabir ud D. Spectroscopic studies on the interaction of cationic surfactants with bovine serum albumin. Colloids and Surfaces B: Biointerfaces. 2009;69(1):122-8.

[39]. Valstar A, Almgren M, Brown W, Vasilescu M. The Interaction of Bovine Serum Albumin with Surfactants Studied by Light Scattering. Langmuir. 2000;16(3):922-7.

Chapter 4: *In vitro in vivo* relations for the parenteral liposomal formulation of Amphotericin B. Part 1: A biorelevant and clinically relevant approach

Abstract

There is limited information of how to perform *in vitro* release tests for intravenously administered parenteral formulations and how to relate the *in vitro* release with an *in vivo* pharmacokinetic parameter after the administration of the formulation. In this study, the effect of hydrodynamics (sample and separate and continuous flow) and medium components (synthetic surfactants, albumin and buffers) on the release of Amphotericin B from the liposomal Ambisome® formulation were investigated. Pharmacokinetic modeling of plasma concentration profiles from healthy subjects administered with Ambisome® was used to estimate the *in vivo* release rate constant of drug from the formulation in order to compare them with the *in vitro* release profiles. With the estimated *in vivo* release rate constant and with the *in vitro* release rate constant, release concentrations profiles were calculated and percent release profiles calculated. Two approaches were followed: comparison of release rate constants and comparison of the area under the curve of the percent release. Albumin was found to be most critical factor for the release of the drug by having a negative effect on the amount of Amphotericin B released. The release profiles obtained with the sample and separate setup in Krebs Ringer buffer - albumin 4.0% w/v and the release profile in Krebs Ringer buffer - albumin 2.0% w/v medium with the continuous flow setup at low velocity were similar to the *in vivo* release profiles in healthy subjects. Determining the factors affecting drug release from parenteral formulations and relating the release profiles to a pharmacokinetic parameter *in vivo* could lead to the development of *in vitro in vivo* correlations and relations.

Keywords:

Amphotericin B; liposomes; parenteral; formulation; *in vitro*; release; pharmacokinetics;

4.1. Introduction

The timescale of therapeutic effect of parenterals can be controlled, to a certain extent, by the type of the formulation (e.g. microparticles, nanoparticles, suspensions, liposomes). Liposomes, the focus of this study, are vesicles formed by one or more phospholipid bilayers with an internal aqueous phase and a size ranging from 25 nm to 2500 nm that could encapsulate or integrate drugs in their structure [1]. There is a lack of regulatory guidance with specific release tests conditions for *in vitro* release tests for liposomes. Shah et. al. [2] provide some recommendations for the release testing: the use of the flow through cell dialysis adapter in the flow through cell apparatus. The FDA guideline for liposomal products only states that a validated release test should be performed with a suitable release medium (plasma, simulated physiological or a non-physiological medium) and with suitable agitation [3]. *In vitro* release from liposomes has been studied using several methods including dialysis and sample and separate methods [4-7]. In sample and separate methods, a critical step is the separation of the released drug from the liposomes. Ultracentrifugation can be used, but the long times required to pellet small liposomes makes this technique unsuitable to capture a snapshot of drug release for construction of a release profile [8-13]. Solid phase extraction (SPE) provides a quicker separation and the drug still entrapped in the liposomes can also be quantified; making it possible to calculate the release based on how much drug remains in the formulation (particularly suitable if the released drug has degradation or solubility issues) [14, 15].

For the development of an *in vitro* release test for liposomes the first step is to consider selection of relevant conditions: a suitable release medium based on the physicochemical properties of the drug, suitable hydrodynamics and an adequate dialysis membrane with an appropriate molecular weight cut-off (MWCO) if needed. *In vitro* hydrodynamics would relate to the agitation applied in the form of predominantly rotational flow, provided by e.g. a magnetic stirrer, or by a predominantly linear flow e.g. the flow through cell apparatus [2].

Amphotericin B (AmB) is a polyene anti-fungal antibiotic, which is highly protein bound *in vivo* [16]. Ambisome® is a commercially available liposomal parenteral formulation of AmB. Ambisome® liposomes have a diameter less than 100 nm and consist of a unilamellar bilayer with AmB intercalated within the membrane, where

the drug is an integral part of the liposomal structure [17]. Ambisome® is administered by intravenous infusion to patients with suspected or proven systemic fungal infections [18]. Such patients can be critically ill and frequently exhibit hypoalbuminaemia.

The release of polydiacetylene, a colorimetric compound, from liposomes has been reported, with the same charge and made of similar components as Ambisome® (negative charged liposomes of dimyristoylphosphatidycholine and polymerized 10, 12-pentacosadiynoic), using CTAB (cationic surfactant), SLS (anionic surfactant) and Triton 100X (non-ionic surfactant) [19]. CTAB produced the fastest release followed by Triton 100X. The release with SLS was minimal but the addition of NaCl increased the amount released; as for charged surfactants, an increase in the ionic strength decreased the critical micellar concentration (CMC), while non-ionic surfactants were not affected [20]. Therefore, the buffer used in the release test is another factor to investigate. Mechanistically, it has been reported that surfactant monomers partition into the surface of the liposomes, then surfactant-saturated vesicles and lipid-saturated micelles start to coexist followed by the lipids forming mixed micelles with the surfactants eventually leading to liposomal disruption [21-23].

Whereas *in vitro* release tests are frequently conducted for quality control purposes, *in vitro* release test conditions which reflect the *in vivo* prefromance are desirable. For parenteral formulations administered intravenously such as liposomes, pharmacokinetic (PK) models of formulated and released drug circulating concurrently could be exploited to estimate the *in vivo* release profile, in order to guide *in vitro* release test development.

In previous studies, biorelevant media representing the plasma albumin concentration (Category 1 media [24] Chapter 3]) and media able to provide clinically relevant AmB solubility values using synthetic surfactants (Category 3b media [Chapter 3]) have been developed. These media were developed based on the AmB active pharmaceutical ingredient (API) and tests are needed to investigate how these media will affect the release from the liposomal formulation. Ambisome® liposomes are negatively charged [17] and this will define how surfactants, depending on their charge, will interact with them.

The aims of this study were a) to investigate how media composition including synthetic surfactants, buffers and protein content (bovine serum albumin (BSA) concentration); and hydrodynamic conditions affect the release of AmB from Ambisome® liposomes and b) using PK modelling of published data of AmB plasma concentration from healthy subjects to estimate *in vivo* release rates and area under the curve of the percent released profile, in order to identify clinically relevant *in vitro* test conditions for a parenteral liposomal formulation using Ambisome® as model formulation.

4.2. Materials and Methods

4.2.1. Materials

AmB analytical standard (87.8%), methanol (MeOH) high performance liquid chromatography (HPLC) grade, formic acid mass spectrometry grade, NaOH, $MgCl_2$, $CaCl_2$, hexadecyltrimethylammonium bromide (CTAB), $NaHCO_3$ were obtained from Sigma Aldrich (Germany); AmB API powder (85%) from Cayman Chemical (USA); BSA protease free powder fraction V, dimethyl sulfoxide (DMSO), dextrose, sodium dodecyl sulphate (SLS), Na_2HPO_4, NaH_2PO_4, KH_2PO_4, NaCl and KCl from Fisher Scientific (USA); Tween 80 from Amresco (USA); GF/D (pore size 2.7 μm, 25 mm diameter) and GF/F (pore size 0.7 μm, 25 mm diameter) filters from Whatman (UK); regenerated cellulose (RC) filters 0.45 μm 13 mm diameter from Cronus (UK); cellulose ester dialysis tubing of 300 kDa MWCO from Spectrum Labs® (USA) and Sep – Pak® Vac 3cc (500 mg) tC18 SPE column from Waters (Massachusetts, USA).

4.2.2. Sample treatment of AmB from release media

The SPE method to separate liposomal AmB from released AmB was a modification of the method reported by Egger et al [15]. Briefly, the SPE column was conditioned with 1.0 mL of MeOH followed by 1.0 mL of water. 1.0 mL of sample was passed through the column and the eluate was collected in a clean vial (liposomal AmB), the column was washed with 2.0 mL of water and collected in the same tube (remaining liposomal AmB in the column). 1.0 mL of methanol was passed through the column to elute the AmB retained in the column (released AmB). In the case of samples with proteins, samples were treated as described previously [24]. Briefly, proteins were precipitated by adding 2 volumes of methanol to 1 volume of the sample followed by mixing in a vortex for 30 seconds and then centrifuged for 10 minutes at 12000 rpm

and 5°C in an Eppendorf centrifuge. Supernatant was filtered through a 0.45 μm RC filter before injection to the HPLC.

4.2.3. Chromatographic conditions for the analysis of AmB from release media

The chromatographic method to quantify AmB was described previously [24]. Briefly, AmB was quantified by HPLC with a C18 Waters Sunfire column (Ireland) 150 x 46 mm 5μm at 25°C. The mobile phase was formate buffer (50 mM; pH = 3.2): MeOH (25:75, v/v); the flow rate was 1 mL/min and AmB was detected at λ = 406 nm. The UV spectrum was recorded from 300 to 450 nm. Quantification of AmB in samples was made based on calibration curves. Freshly prepared standard solutions (0.5 – 15 μg/mL) in the corresponding medium were prepared by appropriate dilution of a 500 μg/mL stock solution of AmB analytical standard in 1:1 MeOH: DMSO v/v. The limit of detection and the limit of quantification were 0.12 and 0.37 μg/mL, respectively.

4.2.4. *In vitro* release studies of AmB from Ambisome® formulation

The factors investigated for the development of the *in vitro* release studies were: i. the composition of the release media: type of buffer, BSA concentration and synthetic surfactants concentration, and ii. the hydrodynamic conditions in terms of the apparatus used i.e. sample and separate (bottle/stirrer) or continuous flow (flow through cell apparatus).

4.2.4.1. Sample and separate method (bottle/stirrer setup)

Ambisome® powder (0.5 mg AmB) was placed into a 100 mL glass bottle (56 mm diameter/ 105 mm height; Duran, Germany) with 30 mL of release medium and stirred with a magnetic stirrer (in a Variomag multipoint stirring plate) at 37°C. Release studies were performed based on a two level factorial design of experiments (DoE) (section 4.2.9). The composition of release media and agitation conditions used in the DoE are shown in Table 4.1, the combination of all the factors resulted in 8 experimental setups.

Table 4.1. Levels and factors investigated with the sample and separate setup for the release studies of AmB from Ambisome®.

Factors in KRB (no synthetic surfactants added)			
Level	BSA %w/v	Buffer	Agitation (rpm)
-1	2.0	PBS	130 (Low Agitation)
+1	4.0	KRB	380 (High Agitation)
Factors in media with synthetic surfactant (SLS)			
Level	BSA %w/v	Buffer	Agitation (rpm)
- 1	0.0	PBS	130 (Low Agitation)
+ 1	4.0	KRB	380 (High Agitation)

The agitation rates in the bottle/stirrer setup were selected based on the linear velocity of the stirrer edge, which at 130 rpm (10.2 cm/s) is comparable to the veins and at 380 rpm (29.5 cm/s) to the aorta (Table 4.2).

Table 4.2. *In vivo* (bloodstream) and *in vitro* (flow through cell apparatus with the large cell: 22.6 mm diameter) flow rates and velocities [25-27].

In vivo ***(bloodstream)***			***In vitro*** **(flow through cell apparatus)**	
Blood vessel	Flow rate (mL/min)	Velocity (cm/s)	Flow rate (mL/min)	Velocity (cm/s)
Arteries	3.0 - 26.0	4.9 - 19.0	3.0 - 26.0	0.01 - 0.11
Veins	1.2 - 4.8	1.50 - 7.80	1.2 - 4.8	0.00 - 0.02
Coronary artery	35.0	-	35.0	0.15
Capillaries	-	0.03	7.0	0.03
Aorta	-	30.0- 40.0	9655.0	40.00
Vena cave	-	15.00	3620.0	15.00

The concentration of SLS was as described previously [Chapter 3] to produce clinically relevant AmB solubility values (PBS SLS 1.4 mM, KRB SLS 1.5 mM, PBS SLS 60.0 mM BSA 4.0% w/v and KRB SLS 30.0 mM BSA 4.0% w/v). In addition to the experimental conditions described in Table 4.1, release studies were also performed in KRB with CTAB and Tween 80 without BSA at low agitation. The concentration selected was the CMC + 5% CMC of the surfactant in KRB (CTAB CMC = 0.2 mM [Chapter 3], Tween 80 = 10.0 µM [28]) being 0.2 mM for CTAB and 10.5 µM for Tween 80 the concentrations tested. Sampling times were 1, 2, 4, 6, 8, and 12 h and after sample treatment (SPE and protein precipitation; section 4.2.3), samples were injected to the HPLC and the % AmB release over time was calculated. All experiments were performed in triplicate.

4.2.4.2. Continuous flow (flow through cell apparatus)

AmB release studies were carried out in a flow-through cell dissolution apparatus (Sotax CE7 smart connected to a Sotax piston pump CP7, Sotax, Aesch, Switzerland)

operated in the closed mode [29]. A 5mm ruby glass bead was positioned at the bottom of the cell (large cell: 22.6 mm diameter). The dialysis membrane was placed onto the flow through cell apparatus dialysis adapter and Ambisome® powder (0.5 mg AmB) was placed into the membrane with 1.0 mL of the release medium. Glass fibre filters (GF/D, GF/F) were positioned at the top of the cell.

Release studies were performed considering a) biorelevant conditions and b) conditions using synthetic surfactants. The biorelevant release studies were based on a two level factorial DoE, where the velocity [low velocity: 8 mL/min, high velocity: 35 mL/min; at 8 mL/min, has linear velocity comparable to capillary linear velocities and at 35 mL/min, a flow rate comparable to the coronary artery (Table 4.2)] and BSA concentration in KRB (2.0 and 4.0% w/v, representing hypoalbuminaemic and healthy subjects, respectively) were the factors investigated. 36 mL of release medium were used in order to simulate the equivalent volume available on administration of 1 mg/kg of AmB as Amphotericin B® to a 70 kg subject (assuming 5 L of blood volume).

For studies performed in media with synthetic surfactants PBS SLS 1.4 mM was the release medium and the effect of velocity was investigated [medium velocity: 16 mL/min, high velocity: 35 mL/min] and 50 mL of medium were used in order to achieve sink conditions (3x saturation solubility) [Chapter 3].

Samples were taken for up to 12 h and, after sample treatment (if necessary), were injected to the HPLC and the %AmB release over time was calculated. All experiments were performed in triplicate at 37°C.

4.2.5. Release data treatment

Data treatment was previously described [24]. Briefly, for the studies with the sample and separate method, %AmB released over time was calculated based on the percent of AmB still entrapped in the liposomes at the time of sampling ($\%AmB_{liposomal}$) (Equation 4.1) to construct the calculated $\%AmB_{released}$ profile.

$$\%AmB_{released} = \%AmB_{initial} - \%AmB_{liposomal} \quad \text{(Equation 4.1)}$$

where $\%AmB_{initial}$ is the mass of AmB placed into the reservoir initially (100%) and $\%AmB_{released}$ is the calculated AmB percent released at time t. There was no correction for degradation for these profiles as the AmB still in the liposome cannot be subject of degradation.

For the studies with the continuous flow method, %AmB released over time was corrected for degradation using the degradation rate constant [Chapter 3] with Equation 4.2 to construct the calculated $\%AmB_{released}$ profile.

$$\%AmB_{released} = \%AmB_{released_{(obs)}} + k_{deg} * AUC_{0-t} \quad \text{(Equation 4.2)}$$

where $\%AmB_{released}$ is the corrected AmB percent released accounting for degradation, $\%AmB_{released_{(obs)}}$ is the AmB percent released at time *t*, AUC_{0-t} is the Area Under the Curve of the observed concentration – time curve from time 0 to time t and k_{deg} is the degradation rate constant obtained from the degradation experiments [Chapter 3].

First order curve fitting (Eq 4.3) was performed on the $\%AmB_{released}$ profiles in order to obtain the release rate constant (k_{rel}) (GraphPad Prism 7, GraphPad Software, Inc, USA).

$$\%AmB_{released} = \%AmB_{released}max * (1 - e^{-k_{rel}t}) \text{ Eq 4.3.}$$

where t is time and $\%AmB_{released}max$ is the maximum AmB amount released. The coefficient of determination (R^2) and Akaike information criterion (AIC) were calculated.

AUC_{0-12h} was calculated for all the $\%AmB_{released}$ profiles.

4.2.6. Atomic Force Microscopy (AFM)

To further investigate the effect of proteins and surfactants on the liposomes, AFM studies were performed. Ambisome® liposomes were incubated in the following media: KRB, KRB BSA 4.0% w/v, KRB SLS 1.5 mM BSA 4.0% w/v (for 30 minutes) and in KRB CTAB 0.2 mM, KRB Tween 10.0 µM and KRB SLS 1.5 mM (for 5 minutes; a shorter period of incubation was set in order to reflect the fast release of AmB from the liposomes observed in the absence of BSA). After the incubation, samples were centrifuged for 30 minutes at 13,300 rpm in an Eppendorf centrifuge, the supernatant was discarded and the pellet was dried under vacuum. The pellets were diluted with 1 mL of HPLC water, and then 10 µL of the liposomal solution was placed on a freshly cleaved mica surface (1.5 cm × 1.5 cm; G250-2 Mica sheets 1″ × 1″ × 0.006″; Agar Scientific Ltd., Essex, UK). The sample was then air-dried for ~30 min

and imaged immediately by scanning the mica surface in air under ambient conditions using a Bruker MultiMode 8 Scanning Probe Microscope (Digital Instruments, Santa Barbara, CA, USA) operated on Peak Force QNM mode. The AFM measurements were obtained using ScanAsyst-air probes; the spring constant was calibrated by thermal tune (Nominal 0.4 N m^{-1}) and the deflection sensitivity calibrated using a silica wafer. AFM scans were acquired at a resolution of 512 × 512 pixels at scan rate of 1 Hz, and produced topographic images of the samples in which the brightness of features increases as a function of height. The surface roughness (R_a) of each substrate was determined by using Nanoscope Analysis' algorithm to analyse several scans of the surface from different locations (n = 20). AFM images were collected from random spot surface sampling (at least four areas).

4.2.7. PK modeling for the estimation of the *in vivo* AmB release rate constant from plasma concentration profiles

4.2.7.1. Data for PK modeling of Ambisome® following administration to healthy subjects

Published data of plasma concentration profiles from healthy subjects administered with Fungizone® (AmB deoxycholate formulation, molar fractions: sodium deoxycholate and AmB, 0.7 and 0.3 respectively [30,31]) and Ambisome®, where the liposomal and released AmB were quantified, were digitalized with Webplot digitalizer 3.8 software (Table 4.3).

Table 4.3. *In vivo* studies of administration of AmB formulations (Fungizone® and Ambisome®) to healthy subjects.

Population	Healthy subjects	
Formulation	Fungizone®	Ambisome®
# of subjects	5	5
Dose	0.6 mg/kg	2.0 mg/kg
Infusion time	2.0 h	2.0 h
Reference	[32]	[33]

4.2.7.2. Workflow for PK modeling and estimation of *in vivo* release profile

The workflow for the PK modeling to estimate the *in vivo* release rate constant of AmB from Ambisome® (k_{rel-iv}) and for model optimization are shown in Figures 4.1 and 4.2, respectively.

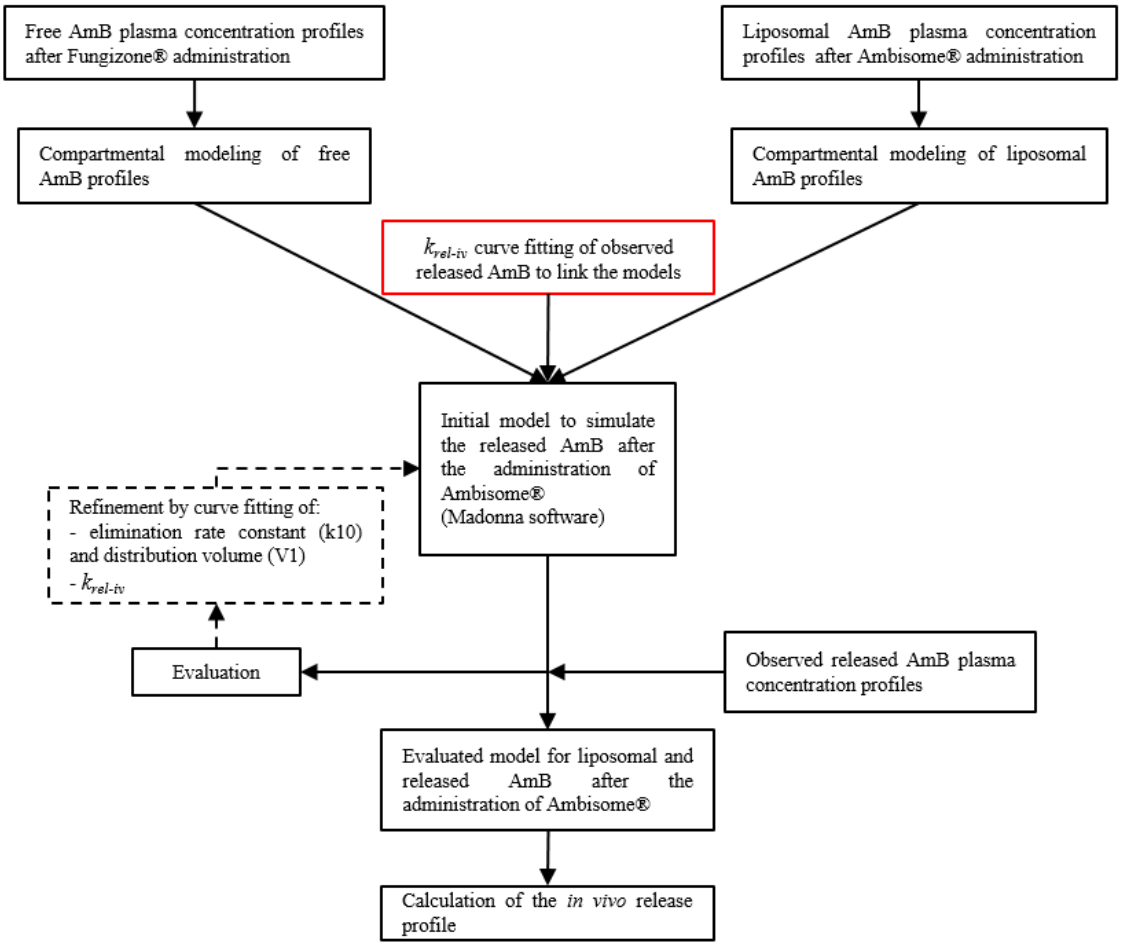

Figure 4.1. Workflow for the PK modeling of free AmB (Fungizone® administration) and liposomal AmB (Ambisome® administration) in order to estimate k_{rel-iv} (*in vivo* release rate constant).

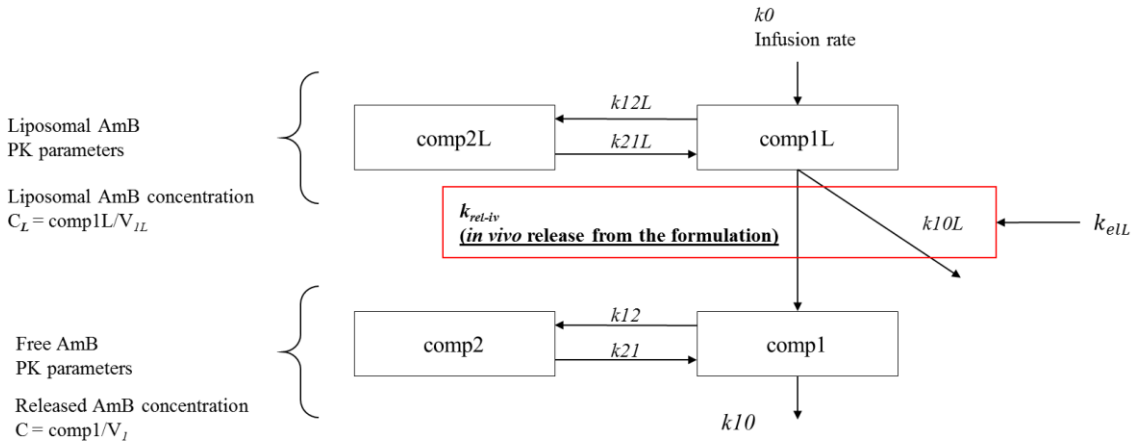

Figure 4.2. Compartmental PK modeling of liposomal AmB and free AmB for the estimation of k_{rel-iv}.

Compartmental modeling was performed with the excel add-in PKSolver [34] and the estimation of k_{rel-iv}, the optimization of the models and the simulations were performed with Berkeley Madonna® 8.3.23 software. The R^2 was obtained from observed plasma concentration profiles vs predicted plasma concentration profiles of both liposomal and released AmB . The *in vivo* elimination rate constant from liposomal AmB models (k_{elL}) comprised the sum of the rate constants of liposomal AmB elimination (k_{10L}) and *in vivo* AmB release (k_{rel-iv}), i.e. $k_{elL} = k_{10L} + k_{rel-iv}$.

4.2.8. Evaluation of the *in vitro* tests using the PK model

The evaluation of the capacity of the AmB *in vitro* release tests to predict the *in vivo* release was explored in two parts:

Part A. *In vitro* release rate constants (k_{rel}) (from the profiles that fitted a first-order release profile) were compared to k_{rel-iv}.

Part B. *In vivo* release profiles were simulated using k_{rel-iv}, using the same dose and available volume as was used in the *in vitro* release tests to facilitate comparison with *in vitro* data. Three simulated % AmB released profiles of mean +/- 1 standard deviation were generated using k_{rel-iv}, followed by calculation of $AUC_{0\text{-}12h}$.

4.2.9. Statistical analysis

Pareto charts, based on the DoE analysis, were constructed for the identification of significant factors affecting the $AUC_{0\text{-}12h}$ obtained from the *in vitro* release tests. A factor was significant when the standardized effect (bars) was larger than the line for

statistical significance level (α = 0.05) (vertical line). An independent means t – tests was performed to compare 2 independent means: for the continuous flow studies with PBS SLS 1.4 mM at low and high velocity; in the AFM studies, data were compared against the control sample [KRB control (centrifugation/vacuum)]; and for AUC_{0-12h} values from simulated *in vivo* and observed *in vitro* AmB release profiles. A $p<0.05$ was considered significant. Additionally, the 90% confidence interval (90% CI) for the ratio of the averages of the measures for the observed *in vitro* and predicted *in vivo* $\ln AUC_{0-12h}$ were calculated. Data analysis, creation and analysis of the design of experiments were performed with the statistical software Statgraphics Centurion XVII (USA) and the 90% CI were calculated with IBM SPSS Statistics 25 (USA).

4.3. Results and discussion

4.3.1. *In vitro* release studies of AmB from Ambisome® using sample and separate and continuous flow setups

4.3.1.1. Sample and separate method

In vitro release profiles of AmB from Ambisome® using the sample and separate method are shown in Figure 4.3 and their corresponding AUC_{0-12h} values are presented in Table 4.4.

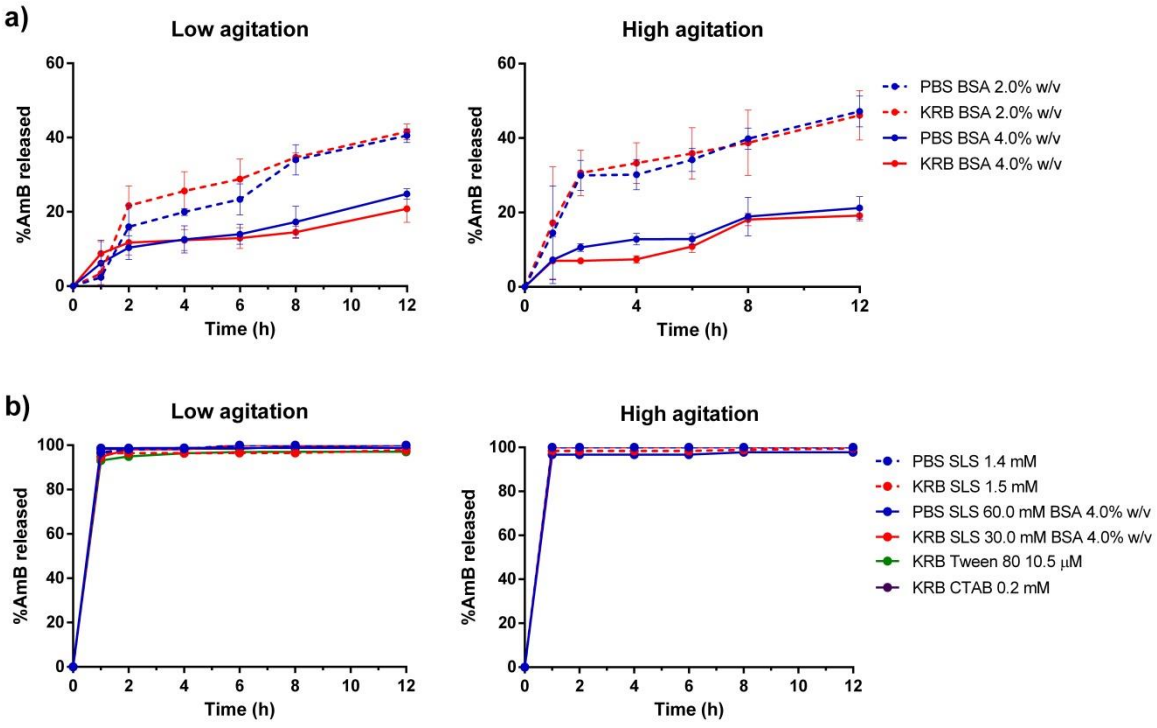

Figure 4.3. %AmB released as a function of time using the sample and separate method at 37°C to investigate the effects of buffer, agitation, composition including a) BSA concentration and b) type of synthetic surfactant and BSA 4.0% w/v presence) on AmB release (Mean ± SD; n = 3).

Table 4.4. %AmB AUC_{0-12h} calculated for all the *in vitro* release profiles: sample and separate and continuous flow investigating the effect of buffers, BSA concentration, surfactants and agitation [for sample and separate; LA: low agitation, HA: high agitation. For continuous flow; LV: low velocity, HV: high velocity] (Mean ± SD; n = 3).

Bottle/stirrer setup				
Buffer	**BSA (%w/v)**	**Agitation/Velocity**	**Surfactant**	$\boldsymbol{AUC_{0-12h}}$**(%AmB** $*$ **h)**
PBS	2.0	LA	-	296.04 ± 24.89
KRB	2.0	LA	-	327.34 ± 23.63
PBS	4.0	LA	-	176.35 ± 36.09
KRB	4.0	LA	-	162.14 ± 29.63
PBS	2.0	HA	-	401.98 ± 28.82
KRB	2.0	HA	-	409.86 ± 69.55
PBS	4.0	HA	-	173.78 ± 24.78
KRB	4.0	HA	-	146.79 ± 8.11
PBS	0.0	LA	SLS	1140.67 ± 0.78
KRB	0.0	LA	SLS	1112.47 ± 1.37
PBS	4.0	LA	SLS	1136.05 ± 5.95
KRB	4.0	LA	SLS	1138.21 ± 2.3
KRB	0.0	LA	Tween 80	1107.72 ± 5.25
KRB	0.0	LA	CTAB	1137.93 ± 3.23

PBS	0.0	HA	SLS	1150
KRB	0.0	HA	SLS	1117.67 ± 8.98
PBS	4.0	HA	SLS	1135.18 ± 6.79
KRB	4.0	HA	SLS	1150
Flow through cell apparatus				
KRB	2.0	LV	-	174.38 ± 15.63
KRB	4.0	LV	-	376.23 ± 13.76
KRB	2.0	HV	-	745.35 ± 97.47
KRB	4.0	HV	-	408.91 ± 80.85
PBS	0.0	MV	SLS	442.33 ± 129.39
PBS	0.0	HV	SLS	694.36 ± 124.82

In media with synthetic surfactants, the release is almost complete at the first sampling point (1 h) regardless of the buffer or the surfactant tested. Consequently, the statistical analysis of release rates could not be performed for the release profiles in synthetic surfactants using the sample and separate method. As it is observed *in vivo* that liposomal AmB is in circulation for more than 1 h [33], ~100% release from the liposomes at 1 h would not be considered a clinically relevant profile. The statistical analysis of $AUC_{0-12\mathrm{h}}$ of the release profiles obtained with the sample and separate method (Figure 4.4a) shows that the buffer used to prepare the medium does not have any effect on the release, while BSA concentration and agitation had a negative and positive effect on AmB release, respectively.

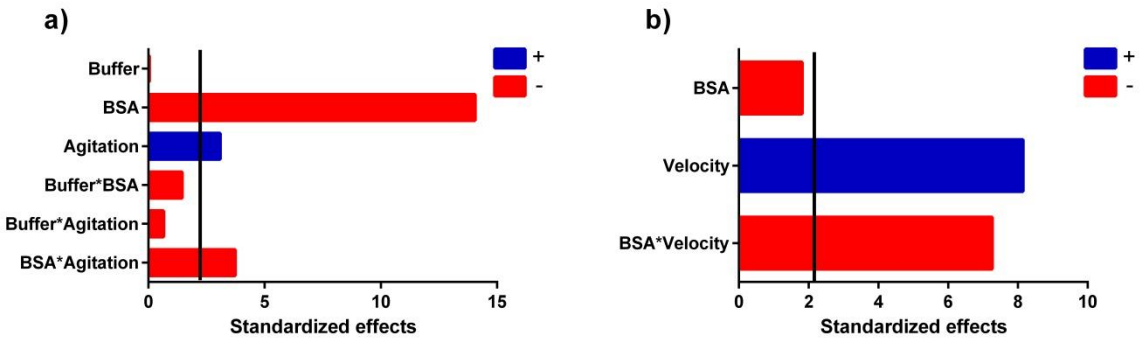

Figure 4.4. Pareto charts for the estimated effects of the main factors and 2 level interactions of the analysis of AUC_{0-12h} from a) sample and separate and b) continuous flow methods. A factor was significant when the estimated effect (horizontal bars) was larger than the standardized effect (vertical line).

The interaction between BSA concentration and agitation was significant, revealing that even though agitation does not affect the release of AmB in media containing BSA 4.0% w/v, at the higher agitation in media with a lower concentration of BSA (2.0% w/v) affect the release as observed by the higher AUC_{0-12h}.The positive effect of agitation on the release of AmB from the liposomal formulation could be attributed to the increased suspension or dispersal of the liposomes and thus exposure to the medium, and/ or the increased mechanical stress exerted on the liposomes (i.e. collision with the bottle's wall or the magnetic stirrer). It is interesting that in higher agitation conditions the release of AmB from the liposomes in media with a lower BSA concentration (2.0% w/v), was higher than in the media with a higher BSA concentration (4.0% w/v). BSA seems to provide some kind of protective effect to the liposome, as the release of AmB from Ambisome® did not change significantly between both agitation conditions when BSA 4.0% w/v was present in the media. It has been reported that an increasing concentration of BSA (from 0.05 to 0.50% w/v in PBS) increases the permeability of liposomes as BSA is adsorbed on their surface. This adsorption (possibly due to hydrophobic interaction) is higher in negatively charged liposomes than in neutral or positively charged liposomes [35-37]. It could be suggested that this interaction increases the permeability of liposomes but as AmB is part of the structure of the liposome itself and not part of the liposome core that could be leaked when the permeability has been increased. Further studies for the characterization of this interaction of BSA with the Ambisome® liposomes would

provide a mechanistic understanding of the release process of AmB from the liposomal formulation.

The release profiles of AmB from liposomes in PBS and KRB BSA 2.0% w/v at low agitation and PBS and KRB BSA 4.0% at high agitation showed first order release and the parameters from the first order fitting are listed in Table 4.5.

Table 4.5. Parameters obtained after fitting (first order equation model) of %AmB released profiles from Ambisome® in the sample and separate setup and in continuous flow setup (Mean ± SD, n = 3).

Buffer	**BSA (%w/v)**	**Agitation/ Velocity**	k_{rel} **(h^{-1})**	$\%AmB_{released}max$	**R^2**	**AIC**
Sample and separate						
PBS	2.0	LA	0.117 ± 0.040	56.07 ± 10.04	0.93 ± 0.04	35.01 ± 2.81
KRB	2.0	LA	0.215 ± 0.083	44.96 ± 4.88	0.94 ± 0.06	31.99 ± 9.93
PBS	4.0	HA	0.322 ± 0.245	21.90 ± 4.37	0.85 ± 0.11	30.01 ± 7.03
KRB	4.0	HA	0.127 ± 0.022	25.09 ± 3.50	0.86 ± 0.04	29.36 ± 3.11
Continuous flow						
KRB	4.0	HV	0.467 ± 0.162	43.10 ± 10.56	0.86 ± 0.03	66.54 ± 7.51
PBS SLS 1.4 mM	0.0	MV	0.725 ± 0.102	41.87 ± 12.27	0.93 ± 0.10	49.69 ± 8.84
PBS SLS 1.4 mM	0.0	HV	1.547 ± 0.523	60.66 ± 9.09	0.97	54.91 ± 3.18

4.3.1.2. Continuous flow method

In vitro release profiles of AmB from Ambisome® obtained using the continuous flow setup are shown in Figure 4.5 and their corresponding AUC_{0-12h} values are presented in Table 4.4.

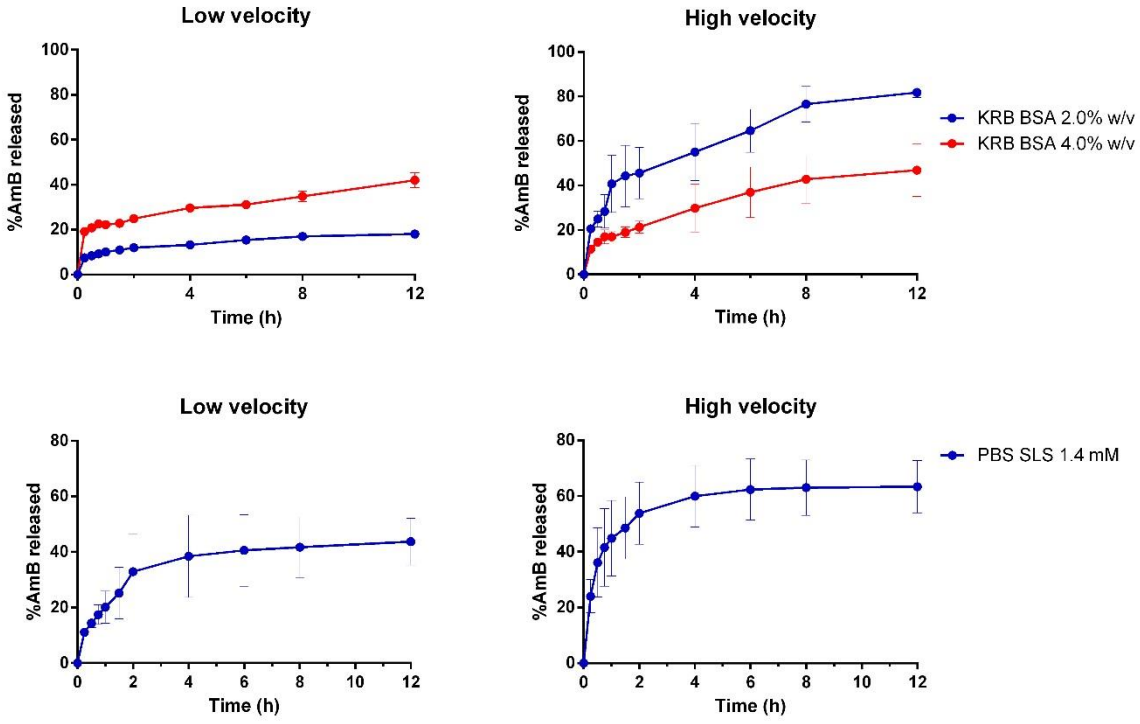

Figure 4.5. %AmB released as a function of time with the continuous flow setup at 37°C in a) KRB to investigate the effects of BSA concentration and velocity, and b) in PBS SLS 1.4 mM to investigate the effect of velocity on AmB release (Mean ± SD; n = 3).

The release of AmB from the liposomes in media incorporating synthetic surfactant (SLS) was slower than the one observed with the sample and separate setup. The slower release observed with this method could be attributed to the use of the dialysis membrane with this set up.

The statistical analysis showed that the flow rate had a positive effect on the AmB release from the liposomes. The BSA*Flow rate interaction had a similar positive effect on the AmB release (as observed for the sample and separate setup studies), whereas the BSA concentration on its own was not a significant factor for the release (Figure 4.4b). The flow rates (in PBS SLS 1.4 mM) shows that AUC_{0-12h} is not

statistically similar when a high velocity is used compared to the low velocity. The release profiles of AmB from liposomes KRB BSA 4.0% w/v medium at high velocity and in PBS SLS 1.4 mM at both medium and high velocities showed first order release and the parameters from the first order fitting are listed in Table 4.5.

4.3.2. AFM studies

Figure 4.6 shows the images obtained from the AFM and Table 4.6 contains the parameters of the liposome characteristics measured with the AFM.

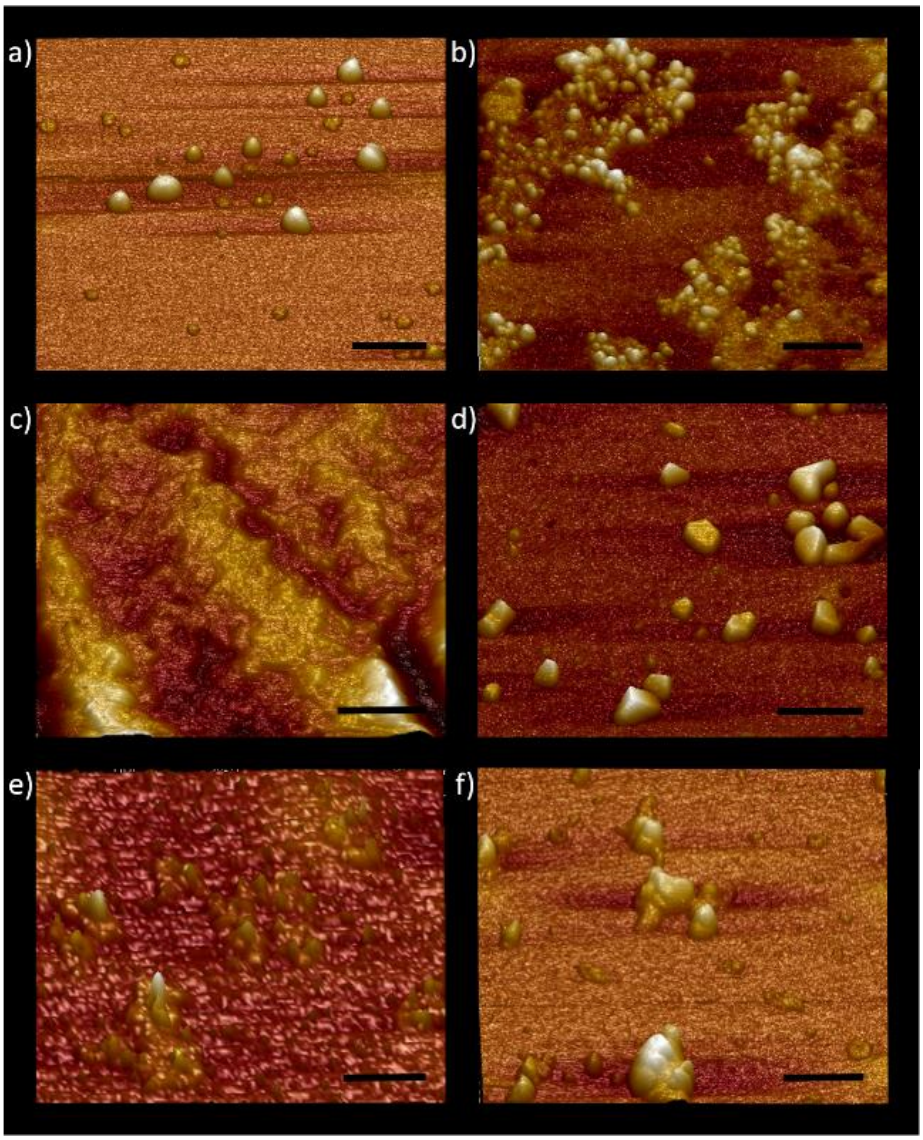

Figure 4.6. AFM images to evaluate the effect of media components on Ambisome® liposomes. a) KRB, b) KRB BSA 4.0% w/v, c) KRB SLS 1.5 mM, d) KRB SLS 1.5 mM BSA 4.0% w/v, e) KRB CTAB 0.2 mM and f) KRB Tween 80 10.0 µM. The scale bar represents 200 nm.

Table 4.6. Parameters of liposomes obtained from AFM from the samples prepared with the media components investigated in the *in vitro* release studies

Sample	**Diameter (nm)**	**Surface Roughness (nm)**
KRB control (centrifugation/vacuum)	69.4 ± 18.9	12.9 ± 1.6
KRB BSA 4.0% w/v	29.0 ± 2.6	4.1 ± 0.2
KRB SLS 1.5 mM	No Particles	
KRB SLS 1.5 mM BSA 4.0% w/v	100.0 ± 27.4	10.0 ± 3.1
KRB CTAB 0.2 mM	No Particles	
KRB Tween 10.0 μM	81.4 ± 7.7	11.6 ± 2.4

Liposomes could not be seen on the samples from media with SLS and CTAB (Figure 4.6c and 4.6e), probably due to quick disruption of the liposomes in the presence of these surfactants in the media, as revealed also from the complete AmB release at the first sampling point in these media with the sample and separate setup (Figure 4.3). Liposomes were found in the sample with Tween 80 (Figure 4.6f) as expected by the slightly slower release in this medium. The liposomes in the medium with Tween 80 appear to be larger in size than the control sample, which could reflect occurrence of the reported mechanism of surfactant-liposome interaction, with surfactant-saturated vesicles and lipid-saturated micelles, which increase the size of the liposomes before the liposomal disruption [21-23]. The presence of BSA in the media with SLS results in an alteration of the interaction of the surfactant (SLS) with the liposomal structure, as liposomes were present in this sample, revealing the interference of the surfactant by BSA (Figure 4.6d) [38-40]. The liposomes in the sample with BSA and SLS were larger in size than those observed in the corresponding sample without SLS, possibly due to changes in BSA structure on interaction with SLS because of alterations in liposome permeability on interaction with BSA or due to aggregation. Aggregation can be observed in the sample with BSA only (Figure 4.6b) as in the sample with Tween 80, probably due to the same process described above. The diameter and surface roughness of the liposomes were statistically significant different to the control

sample [KRB control (centrifugation/vacuum)] for the samples in KRB BSA 4.0% w/v, KRB CTAB 0.2 mM and KRB SLS 1.5 mM, showing that the charged surfactants and proteins have an effect on the size and shape of the liposomes. These parameters (diameter and surface roughness) were not statistically significantly different compared to the controlled sample for the samples in KRB SLS 1.5 mM BSA 4.0 % w/v and KRB Tween 80, revealing that the interaction between SLS and BSA changes the way that these molecules interact with the liposomes and that the non-ionic surfactant is slightly less aggressive to the liposomes than the charged ones.

4.3.3. PK modeling of *in vivo* release profiles in healthy subjects

Observed and predicted *in vivo* liposomal and released AmB plasma profiles are shown in Figure 4.7. Table 4.7 shows the PK parameters obtained from compartmental modeling before and after model optimization, and the estimated value of k_{rel-iv}.

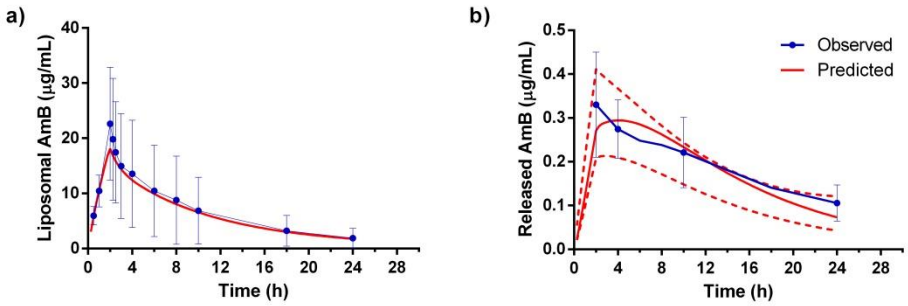

Figure 4.7. Observed and predicted liposomal and released AmB plasma profiles simulated with the optimized models. Healthy subjects data (Bekersky et al, n = 5, [31]), a) Liposomal AmB, b) released AmB. Blue points and line: observed data; red solid lines: mean of the prediction, red dotted lines: standard deviation of the prediction.

Table 4.7. PK parameters from the compartmental modeling and model optimization from liposomal and released AmB after administration to healthy subjects.

		PK parameters	
Population		Healthy subjects	
AmB form		Free	Liposomal
V1 (L)	*initial*	4.830	4.820
	optimized	4.830	4.820
k_{10} **(h^{-1})**	*initial*	0.539	0.155
	optimized	1.052 ± 0.301	0.129 ± 0.002
k_{12} **(h^{-1})**		4.955	0.285
k_{21} **(h^{-1})**		0.737	0.538
R^2	*initial*	0.19	0.99
	optimized	0.92 ± 0.06	0.99
k_{rel-iv} **(h^{-1})**		-	0.025 ± 0.002

The liposomal AmB profile for healthy subjects was explained by the model developed (R^2 = 0.99). The model for liposomal AmB did not change after the optimization as the only relevant parameter is the k_{elL} which includes k_{rel-iv} and k_{10L}. The k_{rel-iv} value was set to be lower than k_{elL} and the difference of the value with k_{elL} was k_{10L}. After the optimization, the elimination rate constant of released drug was higher than the initial value due to the presence of sodium deoxycholate in Fungizone®; this could suggest that released AmB is being removed from plasma more quickly than the AmB administered as Fungizone®. As k_{10} was an optimized parameter the decrease in the amount of drug in plasma could also be due to distribution to tissues, accounting for the value of k_{12} instead of k_{10}. However, with limited data this cannot be considered as a conclusion.

The difference in the half – life of elimination for AmB from Fungizone® (0.17 ± 0.14 h; calculated after poly-exponential fiting) [33] and from Ambisome® (0.66 h; calculated from the PK modeling, reflects the difference of the administered formulation.

4.3.4. Evaluation of clinical relevance of the *in vitro* release tests

4.3.4.1. Part A. Comparison of *in vitro* and *in vivo* release rate constants

The *in vitro* k_{rel} (obtained from the first order fitting of the *in vitro* release profiles) and the k_{rel-iv} of healthy subjects (obtained from the PK modeling of liposomal and released plasma concentration profiles [33]) are presented in Table 4.8.

Table 4.8. Statistical comparison of *in vitro* release rate constants (from the sample and separate and continuous flow setups) and *in vivo* release rate constants (estimated with the PK model for healthy subjects, k_{rel-iv} = 0.025 ± 0.002 h^{-1}). * = statistically similar [for sample and separate; LA: low agitation, HA: high agitation. For continuous flow; LV: low velocity, HV: high velocity] (Mean ± SD; n = 3).

Buffer	**BSA (%w/v)**	**Agitation/ velocity**	***In vitro*** k_{rel} **(h^{-1})**	***t-test* comparison (p value)**
PBS	4.0	HA	0.322 ± 0.245	0.17*
KRB	4.0	HA	0.127 ± 0.022	0.01
KRB	4.0	HV	0.467 ± 0.162	0.04
PBS SLS 1.4 mM	0.0	LV	0.725 ± 0.102	0.00
PBS SLS 1.4 mM	0.0	HV	1.547 ± 0.523	0.00

The *in vitro* k_{rel} are higher than the *in vivo* release rate. However, this analysis assumes a first-order release rate *in vivo* and is hindered by the lack of first order release *in vitro* in several of the test conditions.The *in vitro* k_{rel} estimated from the study in PBS BSA 4.0% w/v at high agitation was statistically similar to the k_{rel-iv} of healthy subjects this result needs to be interpreted with caution though as the coefficient of variation for the *in vitro* k_{rel} is 75% and the constants could be considered similar due to this high variability.

4.3.4.1. Part B. Comparison of *in vivo* and *in vitro* AUC_{0-12h}

The AUC_{0-12h} of the *in vitro* release profiles and the *in vivo* simulated profile (obtained from the developed PK model) are presented in Table 4.9.

Table 4.9. Statistical analysis for the comparison of *in vitro* AUC_{0-12h} (from the sample and separate and continuous flow setups) and *in vivo* simulated AUC_{0-12h}(AUC_{0-12h} = 165.18 ± 11.49 %AmB*h) [LA: low agitation, HA: high agitation, LV: low velocity, MV: medium velocity, HV: high velocity] (Mean ± SD; n = 3).

Buffer	**BSA (%w/v)**	**Agitation/ velocity**	***t-test* comparison (p value)**	**90% CI (healthy subjects)**
PBS	4.0	LA	0.70	80.20 - 138.51
KRB	4.0	LA	0.81	77.03 - 122.87
PBS	4.0	HA	0.65	85.87 - 127.55
KRB	4.0	HA	0.09	79.65 - 99.27
KRB	4.0	LV	< 0.05	206.96 - 251.27
KRB	4.0	HV	< 0.05	186.82 - 320.08
PBS SLS 1.4 mM	0.0	MV	< 0.05	176.82 - 382.93
PBS SLS 1.4 mM	0.0	HV	< 0.05	323.96 - 534.58

Simulated %AmB AUC_{0-12h} was 165.18 ± 11.49 (%AmB*h) for healthy subjects. The t-tests results show that for healthy subjects, the *in vitro* AUC_{0-12h} calculated from the %AmB released profiles obtained in media with BSA 4.0% w/v with the sample and separate setup were statistically similar to the *in vivo* AUC_{0-12h}. Despite the fact that the t-test comparisons show that some results were statistically similar, if the 90% CI are compared against the usual bioequivalence interval (80% - 125%) [41], all the 90% CI from sample and separate setup with BSA 4.0% w/v, either the lower or upper bound was between 80 - 125% which leave the test as inconclusive but with room for improvement (ideally increasing the number of subjects tested).

4.4. Conclusions

There is a lack of guidance for *in vitro* release of parenteral formulations. In this work, factors including medium components and hydrodynamics were tested to understand how they affect drug release from a liposomal formulation for intravenous administration (Ambisome®). For hydrodynamics, in both setups tested (sample and separate and continuous flow), an increase in the agitation/velocity resulted in significant increase of AmB release. The characterization of drug release from liposomes after the direct contact of synthetic surfactants with the liposomes (sample and separate method) is not possible due to fast disruption of the liposomes. The use of the dialysis membrane in the continuous flow setup could overcome this issue and allows the use of simple media with synthetic surfactants for the characterization of release from these formulations. The presence of proteins (BSA) is a critical factor on release of drugs with high protein binding (as AmB) with an increasing protein concentration leading to a decrease of drug release. A novel approach for the estimation of the *in vivo* release rate constant from liposomes was developed through PK modeling. An *in vitro- in vivo* relation was developed, with AUC_{0-12h} of *in vitro* release profiles in media with BSA 4.0% w/v with the sample and separate setup being statistically similar to the *in vivo* calculated AUC_{0-12h}. Establishing an *in vitro- in vivo* relation by using clinically relevant release testing and PK modeling is of high importance in order to make more efficient the development and the quality assessment of these types of formulations.

4.5. References

[1]. Akbarzadeh A, Rezaei-Sadabady R, Davaran S, Joo SW, Zarghami N, Hanifehpour Y, et al. Liposome: classification, preparation, and applications. Nanoscale Research Letters. 2013;8(1):102-.

[2]. Shah VP, DeMuth J, Hunt DG. Performance test for parenteral dosage forms. Dissolution Technol. 2015;22(4):16-21.

[3]. FDA. Liposome Drug Products: Chemistry, Manufacturing, and Controls; Human Pharmacokinetics and Bioavailability; and Labeling Documentation. https://wwwfdagov/downloads/drugs/guidances/ucm070570pdf. 2005.

[4]. Panwar P, Pandey B, Lakhera PC, Singh KP. Preparation, characterization, and in vitro release study of albendazole-encapsulated nanosize liposomes. International Journal of Nanomedicine. 2010;5:101-8.

[5]. Briuglia ML, Rotella C, McFarlane A, Lamprou DA. Influence of cholesterol on liposome stability and on in vitro drug release. Drug Deliv Transl Res. 2015;5(3):231-42.

[6]. Duangjit S, Opanasopit P, Rojanarata T, Ngawhirunpat T, editors. Effect of Surfactants on Characteristic and In Vitro Release of Meloxicam Loaded in Deformable Liposomes. Advanced Materials Research; 2012: Trans Tech Publ.

[7]. D'Souza S. A Review of In Vitro Drug Release Test Methods for Nano-Sized Dosage Forms. Advances in Pharmaceutics. 2014;2014.

[8]. Deniz A, Sade A, Severcan F, Keskin D, Tezcaner A, Banerjee S. Celecoxib-loaded liposomes: effect of cholesterol on encapsulation and in vitro release characteristics. Biosci Rep. 2010;30(5):365-73.

[9]. Mayer LD, St-Onge G. Determination of free and liposome-associated doxorubicin and vincristine levels in plasma under equilibrium conditions employing ultrafiltration techniques. Anal Biochem. 1995;232(2):149-57.

[10]. Shahidi F, Ho CT. Phytochemicals and Phytopharmaceuticals: AOCS Press; 2000.

[11]. Tortorella D, London E. Method for efficient pelleting of small unilamellar model membrane vesicles. Anal Biochem. 1994;217(2):176-80.

[12]. Duzgunes N. Liposomes, Part E: Elsevier Science; 2005.

[13]. Torchilin V, Weissig V. Liposomes: A Practical Approach: OUP Oxford; 2003.

[14]. Shibata H, Izutsu K-i, Yomota C, Okuda H, Goda Y. Investigation of factors affecting in vitro doxorubicin release from PEGylated liposomal doxorubicin for the development of in vitro release testing conditions. Drug Development and Industrial Pharmacy. 2015;41(8):1376-86.

[15]. Egger P, Bellmann R, Wiedermann CJ. Determination of amphotericin B, liposomal amphotericin B, and amphotericin B colloidal dispersion in plasma by high-performance liquid chromatography. J Chromatogr B: Anal Technol Biomed Life Sci. 2001;760(2):307-13.

[16]. Torrado JJ, Espada R, Ballesteros MP, Torrado-Santiago S. Amphotericin B formulations and drug targeting. Journal of pharmaceutical sciences. 2008;97(7):2405-25.

[17]. Gilead. Ambisome®.

http://wwwgileadcom/~/media/files/pdfs/medicines/other/ambisome/ambisome_pipdf?la=en. 2015.

[18]. Adedoyin A, Bernardo JF, Swenson CE, Bolsack LE, Horwith G, DeWit S, et al. Pharmacokinetic profile of ABELCET (amphotericin B lipid complex injection): combined experience from phase I and phase II studies. Antimicrobial Agents and Chemotherapy. 1997;41(10):2201-8.

[19]. Su Y-L, Li J-R, Jiang L. A study on the interactions of surfactants with phospholipid/polydiacetylene vesicles in aqueous solutions. Colloids and Surfaces A: Physicochemical and Engineering Aspects. 2005;257-258(Supplement C):25-30.

[20]. Palladino P, Ragone R. Ionic Strength Effects on the Critical Micellar Concentration of Ionic and Nonionic Surfactants: The Binding Model. Langmuir. 2011;27(23):14065-70.

[21]. Deo N, Somasundaran P. Effects of Sodium Dodecyl Sulfate on Mixed Liposome Solubilization. Langmuir. 2003;19(18):7271-5.

[22]. Hermida LG, Sabes-Xamani M, Barnadas-Rodriguez R. Characteristics and behaviour of liposomes when incubated with natural bile salt extract: implications for their use as oral drug delivery systems. Soft Matter. 2014;10(35):6677-85.

[23]. Richards MH, Gardner CR. Effects of bile salts on the structural integrity of liposomes. Biochimica et Biophysica Acta (BBA) - General Subjects. 1978;543(4):508-22.

[24]. Diaz de Leon-Ortega R, D'Arcy DM, Bolhuis A, Fotaki N. Investigation and simulation of dissolution with concurrent degradation under healthy and hypoalbuminaemic simulated parenteral conditions- case example Amphotericin B. Eur J Pharm Biopharm. 2018.

[25]. Caro CG. The Mechanics of the Circulation: Oxford University Press; 1978.

[26]. Tortora GJ. Principles of anatomy and physiology. 11th ed. ed. Derrickson B, Tortora GJ, editors. Hoboken, N.J.: Hoboken, N.J. : Wiley; 2006.

[27]. Klarhofer M, Csapo B, Balassy C, Szeles JC, Moser E. High-resolution blood flow velocity measurements in the human finger. Magn Reson Med. 2001;45(4):716-9.

[28]. Dawson RMC. Data for Biochemical Research: Clarendon Press; 1989.

[29]. Fotaki N. Flow-through cell apparatus (USP apparatus 4): Operation and features. Dissolution Technologies. 2011;18(4):46-9.

[30]. Brajtburg J, Bolard J. Carrier effects on biological activity of amphotericin B. Clinical microbiology reviews. 1996;9(4):512-31.

[31]. Kagan L, Gershkovich P, Wasan KM, Mager DE. Dual Physiologically Based Pharmacokinetic Model of Liposomal and Nonliposomal Amphotericin B Disposition. Pharmaceutical Research. 2014;31(1):35-45.

[32]. Bekersky I, Fielding RM, Dressler DE, Lee JW, Buell DN, Walsh TJ. Pharmacokinetics, Excretion, and Mass Balance of Liposomal Amphotericin B (AmBisome) and Amphotericin B Deoxycholate in Humans. Antimicrobial agents and chemotherapy. 2002;46(3):828-33.

[33]. Bekersky I, Fielding RM, Dressler DE, Lee JW, Buell DN, Walsh TJ. Plasma protein binding of amphotericin B and pharmacokinetics of bound versus unbound amphotericin B after administration of intravenous liposomal amphotericin B (AmBisome) and amphotericin B deoxycholate. Antimicrob Agents Chemother. 2002;46(3):834-40.

[34]. Zhang Y, Huo M, Zhou J, Xie S. PKSolver: An add-in program for pharmacokinetic and pharmacodynamic data analysis in Microsoft Excel. Comput Methods Programs Biomed. 2010;99(3):306-14.

[35]. Yokouchi Y, Tsunoda T, Imura T, Yamauchi H, Yokoyama S, Sakai H, et al. Effect of adsorption of bovine serum albumin on liposomal membrane characteristics. Colloids and Surfaces B: Biointerfaces. 2001;20(2):95-103.

[36]. Hernández-Caselles T, Villalaín J, Gómez-Fernández JC. Influence of liposome charge and composition on their interaction with human blood serum proteins. Molecular and Cellular Biochemistry. 1993;120(2):119-26.

[37]. Law SL, Lo WY, Pai SH, Teh GW, Kou FY. The adsorption of bovine serum albumin by liposomes. International Journal of Pharmaceutics. 1986;32(2):237-41.

[38]. De S, Girigoswami A, Das S. Fluorescence probing of albumin–surfactant interaction. Journal of Colloid and Interface Science. 2005;285(2):562-73.

[39]. Gull N, Chodankar S, Aswal VK, Sen P, Khan RH, Kabir ud D. Spectroscopic studies on the interaction of cationic surfactants with bovine serum albumin. Colloids and Surfaces B: Biointerfaces. 2009;69(1):122-8.

[40]. Valstar A, Almgren M, Brown W, Vasilescu M. The Interaction of Bovine Serum Albumin with Surfactants Studied by Light Scattering. Langmuir. 2000;16(3):922-7.

[41]. FDA. Statistical Approaches to Establishing Bioequivalence: U.S. Department of Health and Human Services Food and Drug Administration, Center for Drug Evaluation and Research (CDER); 2001 [cited 2018 27/09/2018].

Available from: https://www.fda.gov/downloads/drugs/guidances/ucm070244.pdf.

Chapter 5: *In vitro in vivo* correlation for the parenteral liposomal formulation of Amphotericin B: Part 2: A clinically relevant approach with PBPK modeling

Abstract

In vitro release testing is a useful tool for the quality control of controlled release parenteral formulations, but *in vitro* release test which conditions that reflect or are able to predict the *in vivo* performance are advantageous. Therefore, it is important to investigate the factors that could affect drug release from formulations and relate them to the *in vivo* performance. In this study the effect media composition including the albumin presence, type of buffer and hydrodynamics (sample and separate and continuous flow setup) on drug release were evaluated on a liposomal Amphotericin B formulation (Ambisome®). A pharmacokinetic physiologically based (PBPK) model was developed using plasma concentration profiles from healthy subjects, in order to investigate the impact of each variable from the *in vitro* release tests on the prediction of the *in vivo* performance. It was found that albumin presence was the most important factor for the release of Amphotericin B from Ambisome®; both hydrodynamics setups (coupled with the PBPK model) gave the same degree of prediction of simulate the *in vivo* plasma concentration profiles. The PBPK model was extrapolated to a hypoalbuminaemic population and the Amphotericin B plasma concentration and its activity against fungal cells was simulated. The development of *in vitro* release tests for controlled release parenteral formulations able to predict their *in vivo* behaviour could be beneficial for the formulation development of and to assure the good *in vivo* performance of these formulations.

Keywords:

Amphotericin B; liposomes; PBPK; modeling; *in vitro*; release; PBPKPD; clinically; relevant

5.1. Introduction

A clinically relevant *in vitro* release test is defined as the implication of a link between the *in vitro* release and the *in vivo* performance [1]. In order to establish a clinically relevant test, it is important to understand how the test conditions (media composition and hydrodynamics) affect the *in vitro* release from the formulation. In some cases, the information obtained from *the in vitro* release tests, is not enough to explain the *in vivo* behaviour of the formulation and the released drug and a mechanistic understanding of the *in vivo* performance is required [2]. This can be achieved by the use of physiologically based pharmacokinetic modeling (PBPK). The general concept of PBPK modeling is to mathematically describe relevant physiological, physicochemical, and biochemical processes that determine the pharmacokinetic behaviour of a compound [3-5]. PBPK modeling and simulation are currently a trending tendency and commercial software are available (for example, Gastro- Plus®, simCYP® or PK-Sim® [6]). PBPK modeling is now accepted by regulatory agencies [7]. The FDA have published the "Physiologically Based Pharmacokinetic Analyses — Format and Content (Guidance for Industry) [8]" and the EMA the "Guideline on the qualification and reporting of physiologically based pharmacokinetic (PBPK) modelling and simulation [9]". A PBPK model can be developed considering 4 stages: i) setting the model equations to represent the system, ii) input data to the model; iii) perform the simulation, and iv) model validation (observed vs simulated data, parameter sensitivity analysis) [2]. A sensitivity analysis allows the identification of the parameters that have the greatest influence on the simulation [10, 11]. A biopredictive release method consists of *in vitro* release testing conditions that coupled with a mathematical modeling, are capable of predicting *in vivo* pharmacokinetic profiles [1]. The PBPK modeling could be extrapolated to simulate diseased populations, e.g., hypoalbuminaemic patients (plasma albumin < 25 g/L [12]), in order to investigate the pharmacodynamics (PD) of the drug [13]. PBPK/PD models integrate the movement of the drug in the body with its pharmacological activity [13]. In antimicrobial therapy, the pharmacological effect is the activity against infectious agent [14-16]. If a PBPK/PD model is used to evaluate the antimicrobial activity, the microbial killing is considered to be dependent on the PK profile of antimicrobial concentration in plasma [10, 17]. Amphotericin B (AmB) is a poorly soluble highly protein bound drug which is the drug of choice for the treatment of severe systemic

fungal disease (e.g. *Candida sp., Aspergillus sp*. [18, 19]) and is commerically available as parenteral lipid formulations (including the liposomal formulation Ambisome®) for intravenous administration. The development of PBPK models for Amphotericin B in mice and rats after the administration of Fungizone® (colloidal AmB) and Ambisome® have been reported [20, 21], which showed good predictive performance after being extrapolated to humans. For PBPK modeling of Ambisome®, the uptake of particles by macrophage cells in organs like the liver and spleen, were taken into account by using a saturable model. When this model was developed, the authors reported that there was no *in vitro* AmB release data available and they fitted to the model with a release rate constant of 0.0035 h^{-1} (in all the tissues) with an initial rapid release of the 8% of the dose in humans [20, 21]. AmB is administered as an antifungal agent to patients who can be presenting the hypoalbuminaemia condition.

The aims of this study were i) to investigate how the presence of albumin in clinically relevant media containing physiological surfactants (bile salts – phospholipids, Category 3a media [Chapter 3]), combined with a biorelevant hydrodynamics model [Chapter 4], impact on the release of AmB from Ambisome®; ii) to develop a PBPK model to predicted plasma drug concentrations in healthy subjects and iii) coupled with the use of the PBPK model, guide the development of a biopredictive release test for the liposomal AmB formulation Ambisome® and iv) the extrapolation of the PBPK model to a hypoalbuminaemic population to build a PBPK/pharmacodynamics model to simulate the pharmacological effect of AmB on fungal cells.

5.2. Materials and Methods

5.2.1. Materials

AmB analytical standard (87.8%), methanol (MeOH) high performance liquid chromatography (HPLC) grade, formic acid mass spectrometry grade, Sabouraud dextrose (SBD) broth, NaOH, $MgCl_2$, $CaCl_2$, $NaHCO_3$ were obtained from Sigma Aldrich (Germany); AmB API powder (85%) from Cayman Chemical (USA); bovine serum albumin protease free powder fraction V (BSA), dimethyl sulfoxide (DMSO), dextrose, sodium dodecyl sulphate (SLS), Na_2HPO_4, NaH_2PO_4, KH_2PO_4, NaCl and KCl from Fisher Scientific (USA); phosphatidylcholine (PL) from egg from Lipoid GmbH (Ludwigshafen, Germany); sodium taurocholate (BS) from Prodotti Chimici e Alimentaria (Italy); Sabouraud dextrose (SBD) agar was obtained from Oxoid (UK),

25 mL sterile universal culture tubes were obtained from Sterilin Thermo Scientific (UK); 10 μL plastic loops from Microspec (UK); GF/D (pore size 2.7 μm, 25 mm diameter) and GF/F (pore size 0.7 μm, 25 mm diameter) filters from Whatman (UK); regenerated cellulose (RC) filters 0.45 μm 13 mm diameter from Cronus (UK); cellulose ester dialysis tubing of 300 kDa MWCO from Spectrum Labs (USA), C18 Sep – Pak® Vac 3cc (500 mg) solid phase extraction (SPE) column from Waters (USA) and Ambisome® liposomal AmB formulation from Gilead (Gilead, UK).

5.2.2. Sample treatment of AmB in release media

The sample treatment of AmB was described previously [Chapter 4]. Briefly, the SPE method to separate "liposomal AmB" (AmB still entrapped in the liposome) from "released AmB" (AmB released from the liposome) was modified from Egger et al [22]. The SPE column was conditioned with methanol, followed by water. 1.0 mL of sample was passed through the column and the eluate is collected in a clean vial (liposomal AmB), the column was washed with 2.0 mL of water and collected in the same tube. 1.0 mL of methanol was flushed through the column to elute the AmB retained in the column (released AmB). In the case of samples with proteins, proteins were precipitated by adding 2 volumes of methanol to 1 volume of the sample followed by mixing in a vortex mixer, then centrifuged for 10 minutes at 12000 rpm and 5°C. The supernatant was filtered through a 0.45 μm RC filter before injection to the HPLC.

5.2.3. Chromatographic conditions for the analysis of AmB from release media

The chromatographic method to quantify AmB was described previously [23]. Briefly, AmB was quantified by HPLC analysis using a Hewlett Packard Series 1100 equipped with an auto sampler, temperature regulated column compartment, quaternary pump and diode array detector (DAD detector) (Agilent Technologies). The column was a C18 Waters Sunfire Column (Ireland) 150 x 46 mm 5 μm. The temperature of the column compartment was set at 25°C. The mobile phase consisted of formate buffer 50 mM pH = 3.2: MeOH (27.5:72.5, v/v); the flow rate was 1 mL/min and analysis was performed with the DAD detector at λ = 406 nm. The UV spectrum was recorded from 300 to 450 nm. Quantification of AmB in samples was made based on calibration curves. Freshly prepared standard solutions (0.5 – 15 μg/mL) in the corresponding medium were prepared by appropriate dilution of a 500 μg/mL stock solution of AmB

analytical standard in 1:1 MeOH: DMSO v/v. The limit of detection and the limit of quantification were 0.12 and 0.37 μg/mL, respectively.

5.2.4. *In vitro* release studies of AmB from Ambisome®

The factors investigated for the development of the *in vitro* release studies were: i. the composition of the clinically relevant media with biorelevant surfactants (AmB solubility value in the media as the one observed in plasma from healthy subjects [Chapter 3]): type of buffer, BSA concentration and synthetic surfactants concentration, and ii. the hydrodynamic conditions in terms of the apparatus used i.e. sample and separate (bottle/stirrer) or continuous flow (flow through cell apparatus).

Media composition was PBS BS 19.8 mM PL 7.9 mM and KRB BS 20.0 mM PL 4.0 mM. Media preparation was previously described [Chapter 3]. Briefly, BS were weighed and dissolved in buffer and then PL from a stock solution of 100 mg/mL in dichloromethane were added. Organic solvents were evaporated with a rotary evaporator set at 40°C and attached to a vacuum pump. The pressure was decreased from 650 mbar by steps of 70 mbar every two minutes to 100 mbar, where the pressure was maintained for 10 minutes. If BSA was part of the medium, it was added after the evaporation of the organic solvents.

5.2.4.1. Sample and separate method (bottle/stirrer setup)

The sample and separate method was described previously [Chapter 4]. Briefly, Ambisome® powder (0.5 mg AmB) was placed into a 100 mL glass bottle with 30 mL of release medium and stirrer with a magnetic stirrer at 37°C. Release studies were performed based on a two level factorial design of experiments (DoE) (section 5.2.9). The composition of release media and agitation conditions are shown in Table 5.1, the combination of all the factors resulted in 8 experimental setups.

Table 5.1. Levels and factors investigated with the sample and separate setup for the release studies of AmB from Ambisome® in clinically relevant media (category 3a media [Chapter 3])

Level	BSA %w/v	Buffer	Agitation (rpm)
- 1	2.0	PBS	130 (Low Agitation)
+ 1	4.0	KRB	380 (High Agitation)

The agitation rates in the bottle/stirrer setup were selected based on the linear velocity of the stirrer edge, which at 130 rpm (10.2 cm/s, low agitation) is comparable to the veins and at 380 rpm (29.5 cm/s, high agitation) to the aorta [Chapter 4]. Sampling times were 1, 2, 4, 6, 8, and 12 h and after sample treatment (SPE and protein precipitation; section 5.2.3), samples were injected to the HPLC and AmB concentration in the samples was calculated. All experiments were performed in triplicate.

5.2.4.2. Continuous flow (flow through cell apparatus)

The flow-through apparatus studies were described previously [Chapter 4]. Briefly, AmB release studies were carried out in a flow-through dissolution apparatus (Sotax CE7 smart connected to a Sotax piston pump CP7, Sotax, Aesch Switzerland) operated in the closed mode [24]. A 5mm ruby glass bead was positioned at the bottom of the cell (large cell: 22.6 mm diameter). The dialysis membrane was placed into the flow through cell apparatus dialysis adapter and Ambisome® powder (0.5 mg AmB) was placed into the membrane with 1 mL of the release medium. Glass fibre filters (GF/D, GF/F) were positioned at the top of the cell. The release studies were based on a two level factorial DoE, where the velocity [low velocity: 8 mL/min, high velocity: 35 mL/min; at 8 mL/min, has linear velocity comparable to capillary linear velocities and at 35 mL/min, a flow rate comparable to the coronary artery [Chapter 4] and BSA presence (4.0% w/v) or not were the factors investigated. 36 mL of release medium were used in order to simulate the equivalent volume available on administration of 1 mg/kg of AmB as Amphotericin B® to a 70 kg subject (assuming 5 L of blood volume).

5.2.5. Release data treatment

The release data treatment was described previously [Chapter 4].

Briefly, for the studies with the sample and separate method, %AmB released over time was calculated based on the percent of AmB still entrapped in the liposomes at the time of sampling ($\%AmB_{liposomal}$) (Equation 5.1) to construct the calculated $\%AmB_{released}$ profile.$\%AmB_{released} = \%AmB_{initial} - \%AmB_{liposomal}$

(Equation 5.1)

where $\%AmB_{initial}$ is the mass of AmB placed into the reservoir initially (100%) and $\%AmB_{released}$ is the calculated AmB percent released. There was no correction for degradation for these profiles as the AmB still in the liposome cannot be subject of degradation.

For the studies with the continuous flow setup the $\%AmB_{released_{(obs)}}$ over time was corrected for degradation using Equation 5.2 to construct the calculated $\%AmB_{released}$ profile.

$$\%AmB_{released} = \%AmB_{released_{(obs)}} + k_{deg} * AUC_{0-t} \quad \text{(Equation 5.2)}$$

where $\%AmB_{released}$ is the corrected AmB percent released accounting for degradation, $\%AmB_{released_{(obs)}}$ is the AmB percent released at time *t*, AUC_{0-t} is the Area Under the Curve of the observed concentration – time curve from time 0 to time t and k_{deg} is the degradation rate constant obtained from the degradation experiments [Chapter 3].

AmB release rate constant (k_{rel}) from Ambisome® was obtained from first order fitting of calculated $\%AmB_{released}$ individual profiles (Equation 5.3) and mean and standard deviation values were calculated (GraphPad Prism 7, GraphPad Software, Inc, USA).

$\%AmB_{released} = \%AmB_{released}max * (1 - e^{-k_{rel}t})$ (Equation 5.3),

where $\%AmB_{released}max$ is the maximum AmB percent released and t is time.

5.2.6. Atomic Force Microscopy (AFM) studies

To further investigate the effect of the clinically relevant media components (BS, PL and BSA) on the liposomes, AFM studies were performed. The AFM studies' methodology has been described previously [Chapter 4]. Ambisome® liposomes were incubated in KRB BS 20.0mM PL 4.0 mM BSA 4.0% w/v (for 30 minutes) and in KRB BS 20.0mM PL 4.0 mM (for 5 minutes; a shorter period of incubation was set in order to reflect the fast release of AmB from the liposomes observed in the absence of BSA). After the incubation time, samples were centrifuged for 30 minutes at 13300 rpm in an Eppendorf centrifuge, the supernatant was discarded and the pellet was dried under vacuum. The pellets were diluted with 1 mL of HPLC water, and then 10 μL of the lipid solution was placed on a freshly cleaved mica surface (1.5 cm × 1.5 cm; G250-2 Mica sheets 1″ × 1″ × 0.006″; Agar Scientific Ltd., Essex, UK). The sample was then air-dried for ~30 min and imaged immediately by scanning the mica surface in air under ambient conditions using a Bruker MultiMode 8 Scanning Probe Microscope (Digital Instruments, Santa Barbara, CA, USA) operated on Peak Force QNM mode. The AFM measurements were obtained using ScanAsyst-air probes; the spring constant was calibrated by thermal tune (Nominal 0.4 N m^{-1}) and the deflection sensitivity calibrated using a silica wafer. AFM scans were acquired at a resolution of 512 × 512 pixels at scan rate of 1 Hz, and produced topographic images of the samples in which the brightness of features increases as a function of height. The surface roughness (R_a) of each substrate was determined by using Nanoscope Analysis' algorithm to analyse several scans of the surface from different locations (n = 20). AFM images were collected from random spot surface sampling (at least four areas).

5.2.7. PBPK modeling for Ambisome® administration to healthy subjects

5.2.7.1 Data for PBPK modeling.

Published data of plasma concentration profiles from a population of 5 healthy subjects (4 males, 1 female; ages from 33 to 65 years; height from 1.61 to 1.68 m; and weight from 68 to 86 kg) infused for 2 h with 2.0 mg/kg of Ambisome® where the "liposomal AmB" and "released AmB" were quantified [25, 26], were digitalized with Webplot digitalizer 3.8 software.

"Liposomal AmB" and "released AmB" distribution, clearance, protein binding; and physicochemical properties are shown in Table 5.2.

Table 5.2. PK-Sim model set up: physicochemical properties, distribution and clearance parameters of "released AmB" and "liposomal AmB" (Ambisome®) after administration to healthy subjects.

"Released AmB"	
Molecular weight (g/mol)	924 [27, 28]
log P	0.80 [27], 0.94 [29], 1.84[29], 2.14 [29]
clog P	- 2.33 [27], - 0.66 [27], 1.16 [30]
pka	acidic 5.5 [28], basic 10.0 [28]
Solubility at pH = 7	0.09 µg/mL [31], 1.38 µg/mL [32], 6.00 µg/mL [33]
fraction unbound (albumin)	0.05 [26]
Distribution volume	2340 ± 202 mL/kg [25]
Cl $_{renal}$	0.07 ± 0.01 mL/min/kg [25]. GFR fraction = 0.875
Cl $_{biliary}$	0.09 ± 0.02 mL/min/kg [25]. k_{bil} = 0.002 h^{-1}
Binding partners	alfa 1 acid glycoprotein (AAG1), EST expression [25], k_{diss} = 1.07 – 2.44 x 10^{-6} M^{-1} (approximation from unbound fraction) [25]
	beta lipoprotein (APOB), EST expression, k_{diss} = 4 x 10^{-6} M^{-1} [34]

"Liposomal AmB"	
Distribution volume	1628 ± 876 mL/kg [25]
Cl *renal*	0.01 ± 0.00 mL/min/kg [25], GFR fraction = 0.125
Cl *biliary*	0.01 ± 0.00 mL/min/kg [25], k_{bil} = 0.0003 h^{-1}
Assumptions for the model, considering the "liposomal AmB" as a molecule	
Molecular weight (g/mol)	924
Radius (solute)	80 nm [35]
log P	Parameter to identify, starting value 0.8
pka	Neutral
Solubility at pH = 7	290 mg/mL [calculated from the total amount of powder in a formulation vial (14.5 g), dissolved in 50 mL of water]
fraction unbound albumin	0.05

Immune removal	Metabolizing enzymes -> Intrinsic clearance First order -> Relative expression -> Intracellular -> Endosomal Plasma 100% Liver periportal 100% Liver pericentral 100% Spleen 100%

The PK parameters (distribution, clearance and protein binding) for "released AmB", were the ones reported after the administration of the colloidal AmB formulation Fungizone® as reported by Kagan et al [21] (Table 5.2). Protein binding is characterized by k_{diss} (equilibrium dissociation constant). The nominal glomerular filtration rate (GFR) for AmB is 0.08 mL/min/kg as calculated with equation 5.4, based on a fraction unbound to albumin of 0.05. This value was used to calculate the GFR fraction for the "liposomal AmB" and "released AmB".

$$Nomimal\ GFR\ =\ fraction\ unbound\ (albumin) * (120\ mL/min) * (1/73\ kg)$$

Eq 5.4.

Elimination rate constant of biliary elimination was calculated using Eq 5.5.

$$k_{bil} = (Cl_{biliary}/distributuion\ volume)(60\ min/1\ h)$$ Eq 5.5.

For the development of the model, "liposomal AmB" was assumed to behave as a molecule as the concentration of AmB is what is quantified in the *in vivo* studies and not the concentration or amount of liposomes.

An "immune" enzyme was added for the "liposomal AmB" to account for the removal of circulation of the "liposomal AmB" by the macrophages of the immune system. The enzyme was set to be located in the plasma, liver and spleen. The fraction unbound value for the "liposomal AmB" was hypothesized to be smaller than 0.95 based on the reported interaction between albumin and liposomes [36-38]. All the other parameters were left as software's default values.

5.2.7.2. Workflow for PBPK modeling for Ambisome® administration to healthy subjects

The workflow for the PBPK modeling to describe the pharmacokinetics of "liposomal AmB" and "released AmB" in a healthy individual after the administration of the Ambisome® is presented in Figure 5.1.

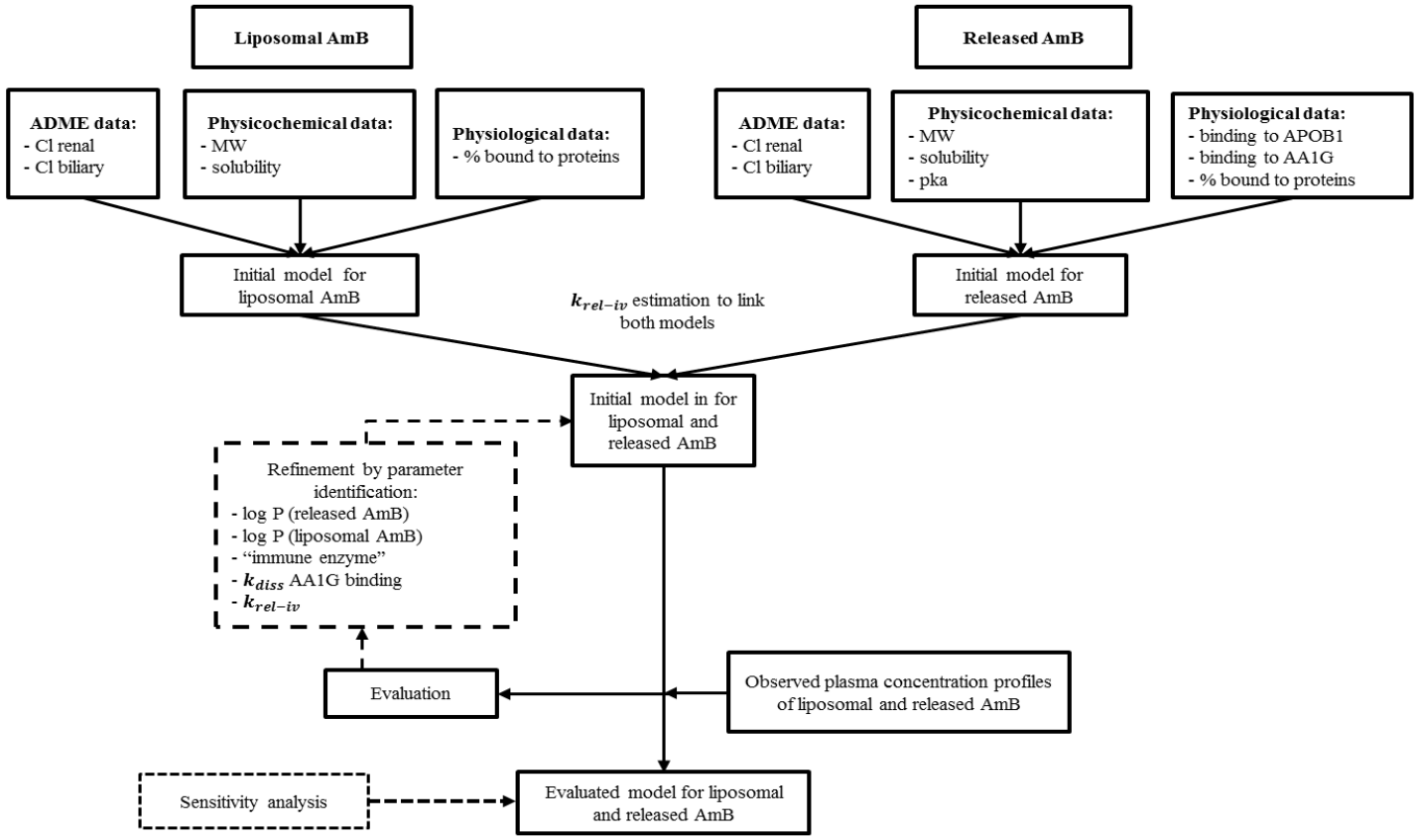

Figure 5.1. Workflow for the PBPK modeling of "liposomal AmB" and "released AmB" after the administration of Ambisome® to healthy subjects.

PBPK modeling was performed with PKSim® 7.2.1 (Bayer, Germany) and MoBi® 7.2 (Bayer, Germany). The five parameters listed in Figure 5.1 were optimized simultaneously with the MoBi® built in function "Parameter identification" using an algorithm based on Monte Carlo methods and the default software setup (the Parameter identification tool varies selected input parameters in a given range to identify the best values to obtain output simulated curves similar to the observed curves). The *in vivo* release of AmB from liposome was set to occur only in plasma (k_{rel-iv}.only in plasma of venous blood).

Comparing the developed PBPK model in this study with the one reported by Kagan et al [21], there were some differences: i) this model was developed in order to link the *in vitro* release data to the observed plasma concentration data while Kagan and coworkers developed their model to have a better understanding of AmB PK in order to improve the dosing; ii) the release of AmB took place in all of the compartments [21] while in this study, the release was only in plasma.

Sensitivity analysis was performed on all the parameters of the model (PK data and physicochemical properties of "liposomal AmB" and "released AmB") except for the molecular weight and the pka values of "released AmB". The parameters and the range in which the sensitivity analysis was evaluated are presented in Table 5.3.

Table 5.3. Parameters and the range in which the parameters were investigated in the sensitivity analysis of the validated PBPK model of Ambisome® administration.

Parameter	**Abbreviation**	**Interval tested**
log P ("liposomal AmB")	logP (lip)	0 – 2 (log units)
log P ("released AmB")	logP (rel)	2.24 – 4.24 (log units)
Aqueous solubility ("liposomal AmB")	Sol (lip)	90 – 490 (μg/mL)
Aqueous solubility ("released AmB")	Sol (rel)	0.01 – 6.00 (μg/mL)
Radius solute ("liposomal AmB")	Rad (lip)	40 – 120 (nm)
Specific biliary clearance ("liposomal AmB")	Bil (lip)	0.0001 – 0.0005 (h^{-1})
Specific biliary clearance ("released AmB")	Bil (rel)	0.001 – 0.003 (h^{-1})
GFR ("liposomal AmB")	GFR (lip)	0 – 1 (fraction)
GFR ("released AmB")	GFR (rel)	0 – 1 (fraction)
"Immune enzyme" specific clearance	Imm	1.57 – 3.57 (h^{-1})
APOB1 k_{diss}	APOB1	2 – 6 (μmol/L)
AAG1 k_{diss}	AAG1	0.21 – 0.63 (μmol/L)
k_{rel-iv}	krel	0.114 - 3.539 (h^{-1})
Unbound fraction ("liposomal AmB")	fU (lip)	0.05 – 0.95 (fraction)
Unbound fraction ("released AmB")	fU (rel)	0.05 – 0.95 (fraction)

The range were selected as follows: logP of "liposomal AmB" and "released AmB": ± 1 log unit of the optimized value, immune enzyme of "liposomal AmB": ± 1 h^{-1} of the optimized value, aqueous solubility of "released AmB": the range was selected to cover the solubility values reported in the literature [31, 33], aqueous solubility of "liposomal AmB": ± 200 µg/mL in order to cover a wide range as the value was based on an assumption (Table 5.2); for radius solute ("liposomal AmB"), biliary clearance ("liposomal AmB" and "released AmB"), k_{diss} of APOB and AAG1 the interval was ± 50% of the literature value (Table 5.2 and 5.3). GFR fraction ("liposomal AmB" and "released AmB") was investigated from 0 to 1; and the unbound to protein fraction ("liposomal AmB" and "released AmB") from 0.05 to 0.95. k_{rel-iv} was investigated in the interval of the k_{rel} found in the *in vitro* tests (Table 5.3). AUC_{0-24h} of both liposomal and released AmB was used as response to evaluate the effect of the parameters investigated. Sensitivity analysis was performed with the MoBi Toolbox for R esqLABS version 7.2.1 (esq LABS, Germany). All the intervals tested, were normalized to 0 – 1 for clarity of presentation.

After the sensitivity analysis, the model was applied to the population described in section 5.2.7.1. The variability (standard deviation) for the parameters input into the model was as described in Table 5.2. As the values of k_{rel-iv} and specific clearance for the immune removal "enzyme" were obtained by parameter identification and there are no reported values for their variability, 20% of the identified value was used as standard deviation.

5.2.7.3. Evaluation of the *in vitro* tests using PBPK modeling

The *in vitro* k_{rel} (Mean ± SD) obtained from the *in vitro* release profiles of AmB from Ambisome® were input to the validated PBPK model in order to predict the observed *in vivo* AmB ("liposomal AmB" and "released AmB") plasma concentration profiles. The AUC_{0-24h} was calculated from the predicted "liposomal AmB" and "released AmB" plasma concentration profiles

5.2.8. PBPK-PD model for the pharmacological activity of AmB against *Candida albicans*

The effect of AmB on *Candida albicans* (*C. albicans*) was investigated in order to develop a PBPK-PD model: i. for a patient population receiving Ambisome® with a reduced albumin plasma concentration (hypalbuminaemia: albumin < 25 mg/mL), and

ii. for a healthy population receiving Ambisome® with normal concentration of albumin.

5.2.8.1. Quantification of *C. albicans*

The culture and quantification of *C. albicans* was described previously [23]. A single colony culture was started in a tube with 5 mL of SBD broth and incubated overnight at 37°C in a shaking incubator; the optical density was measured at 600 nm (OD_{600}). The colony forming units (CFU) were determined by preparing serial dilutions and the suspensions were plated on SBD agar plates, incubated overnight at 37°C; the number of colonies were counted and related to the OD_{600} of the culture.

5.2.8.2. Time killing experiments

Time killing experiments were performed with 10^5 CFU/mL of *C. albicans* using different AmB final concentrations (0.00, 0.75, 1.50 and 3.00 µg/mL) in the presence of BSA 2.0% and 4.0% w/v in KRB. The percent of CFUs remaining at each time point were used for curve fitting to the exponential decay equation to obtain the killing rate constant for each concentration tested (Eq 5.6).

$$\%CFU = \%CFU_{max} * e^{-k_{kill}t}$$ Eq 5.6.

where $\%CFU$ are the percent of CFU at time t, $\%CFU_{max}$ is the maximum percent of CFU, k_{kill} is the time killing rate constant and t is time.

A linear relation was found between k_{kill} and AmB concentration and it was used in the PBPK-PD model.

5.2.8.3 PBPK-PD modeling

The workflow for the development of the PBPK-PD model is shown in Figure 5.2.

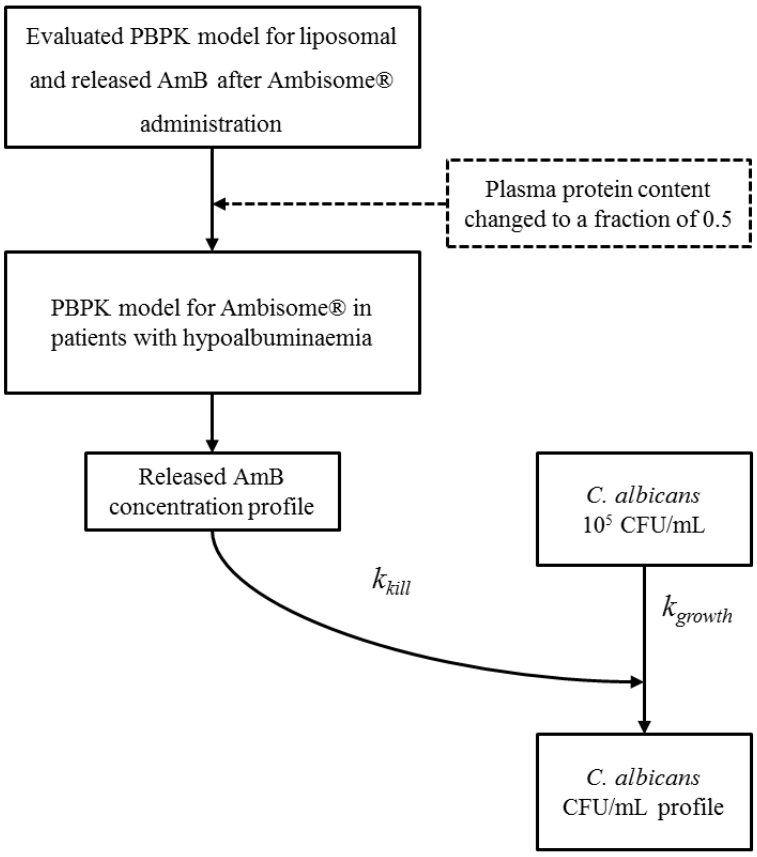

Figure 5.2. Workflow for the PBPK-PD modeling of the liposomal and released AmB after the administration of Ambisome® l to a hypoalbuminaemic population in order to simulate the pharmacological activity of the released AmB on *C. albicans*.

To simulate the patient population (hypoalbuminaemic), the protein content was halved in the validated PBPK model for the healthy subject and the rest of the parameters remained unchanged. The "released AmB" concentration was used to calculate the k_{kill} for the 24 h time course to simulate the "released AmB" activity against *C. albicans* which was set to be at a concentration of 10^5 CFU/mL at time zero. The *C. albicans* rate growth constant (k_{growth}) was obtained from the control time killing experiment (0.00 µg/mL AmB).

5.2.9. Statistical analysis

The statistical analysis was described previously [Chapter 4]. Pareto charts, based on the DoE analysis, were performed for the identification of significant effects from the *in vitro* release tests. A factor was significant when the standardized effect (bars) was larger than the line for statistical significance level ($\alpha = 0.05$) (vertical line). An independent means t – test was performed to compare 2 independent means: in the

AFM studies, size and surface roughness were compared against the control sample. A $p<0.05$ was considered statistically significant. Due to the lack of individual observed data of plasma concentration profiles, the PK parameters obtained with the *in vitro* k_{rel} were compared against the PK parameters obtained from the simulation of the PBPK validated model.

Additionally, the 90% confidence interval (90% CI) for the ratio of the averages of the measures for the observed *in vitro* and predicted *in vivo* $\ln AUC_{0-24h}$ were calculated. As recommended by the FDA guidance, both "liposomal AmB" and "released AmB" were evaluated [39]. Data analysis, creation and analysis of DoE were performed with the statistical software Statgraphics Centurion XVII (USA) and the 90% CI were calculated with IBM SPSS Statistics 25 (USA).

5.3. Results and discussion

5.3.1. *In vitro* release testing of Ambisome® in category 3a media

In vitro release profiles of AmB from Ambisome® in both hydrodynamic setups are shown in Figure 5.3 and parameters obtained after fitting to the first order equation model are presented in Table 5.4.

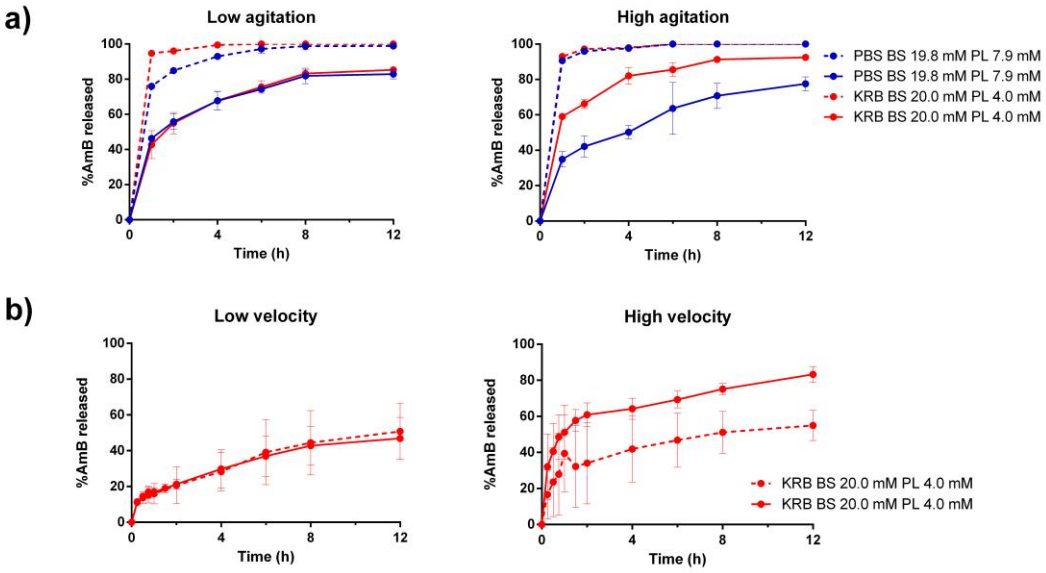

Figure 5.3. %AmB released with the a) sample and separate and the b) continuous flow setup at 37 °C to investigate the effect of the type of buffer, the BSA 4.0% w/v presence and the hydrodynamics in clinically relevant media with BS – PL. (Mean ± SD, n=3; solid lines: media with BSA 4.0% w/v; dotted lines: media without BSA 4.0% w/v).

Table 5.4. Parameters obtained after fitting (Equation 5.3) of %AmB released profiles from Ambisome® with the sample and separate setup and the continuous flow setup [LA: low agitation, HA: high agitation, LV: low velocity, HV: high velocity] (Mean ± SD, n = 3).

Buffer	**BSA (%w/v)**	**Surfactant concentrations**	**Agitation/velocity**	k_{rel} **(h^{-1})**	$\%AmB_{released}max$
Sample and separate					
PBS	0.0	BS 19.8 mM PL 7.9 mM	LA	1.425 ± 0.101	96.258 ± 0.101
PBS	4.0	BS 19.8 mM PL 7.9 mM	LA	0.701 ± 0.060	78.573 ± 2.548
KRB	0.0	BS 20.0 mM PL 4.0 mM	LA	3.034 ± 0.106	99.201 ± 0.321
KRB	4.0	BS 20.0 mM PL 4.0 mM	LA	0.621 ± 0.192	81.662 ± 2.931
PBS	0.0	BS 19.8 mM PL 7.9 mM	HA	2.437 ± 0.129	98.953 ± 0.158
PBS	4.0	BS 19.8 mM PL 7.9 mM	HA	0.410 ± 0.052	73.031 ± 6.013
KRB	0.0	BS 20.0 mM PL 4.0 mM	HA	2.747 ± 0.046	99.146 ± 0.072
KRB	4.0	BS 20.0 mM PL 4.0 mM	HA	0.896 ± 0.041	88.141 ± 2.480
Continuous flow					
KRB	0.0	BS 20.0 mM PL 4.0 mM	LV	0.305 ± 0.071	49.181 ± 17.119

KRB	4.0	BS 20.0 mM PL 4.0 mM	LV	0.467 ± 0.162	43.101 ± 10.563
KRB	0.0	BS 20.0 mM PL 4.0 mM	HV	1.364 ± 1.890	60.416 ± 4.593
KRB	4.0	BS 20.0 mM PL 4.0 mM	HV	-	-

For the sample and separate setup, the statistical analysis (Figure 5.4a) showed that the buffer was a significant factor on $\%AmB_{released}max$ with a higher release in KRB, the presence of BSA 4.0% w/v had a significant negative effect and the interaction between buffer and BSA was significant as the amount released in KRB with BSA is slightly higher than in PBS with BSA while in media without BSA there is no difference. The release rate constant was affected in the same way as $\%AmB_{released}max$ but the interaction between buffer and BSA showed that the release rate is faster in KRB than in PBS without BSA and there is not a statistical significant difference in KRB and PBS with BSA. For the continuous flow setup (Figure 5.4b), the flow rate was the only significant factor on AmB release from the liposomes, with a positive effect on the AUC_{0-12h}.

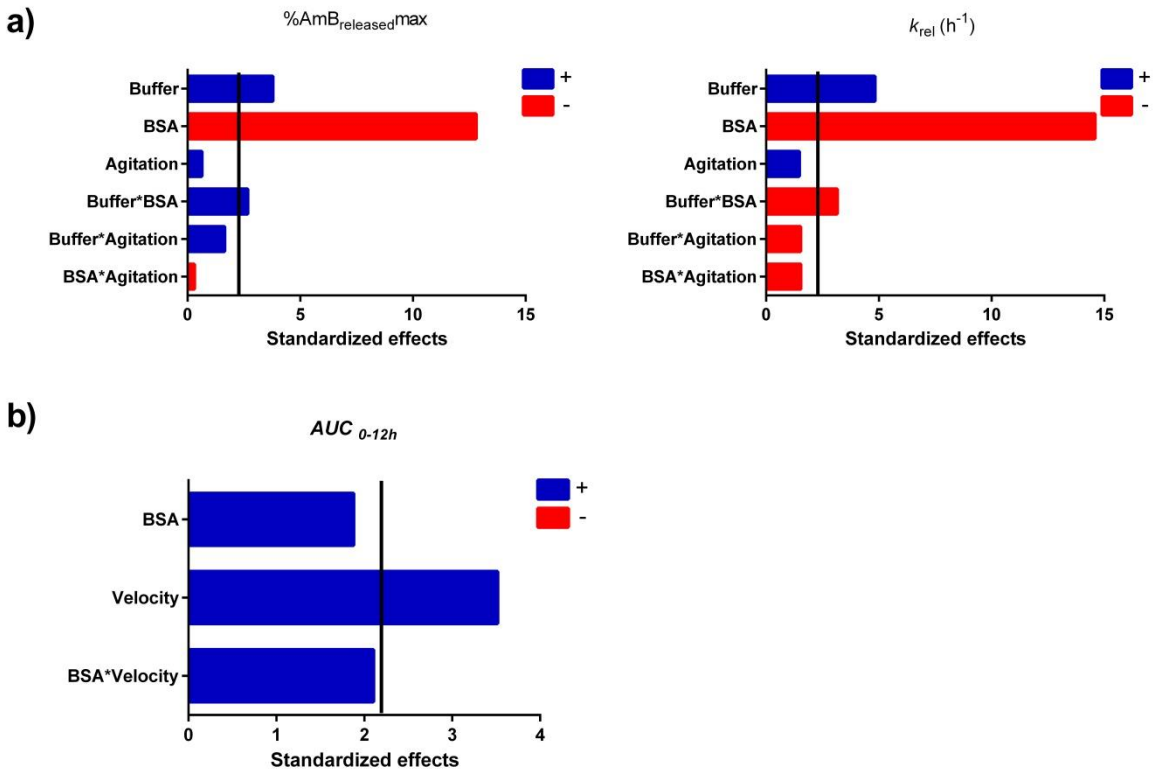

Figure 5.4. Pareto charts for the estimated effects of the main factors and 2 level interactions of the analysis of a) $\%AmB_{released}max$ and k_{rel} from the sample and separate setup and b) the AUC_{0-12h} from the continuous flow method. A factor was significant when the estimated effect (horizontal bars) was larger than the standardized effect (vertical line).

5.3.2. AFM studies

Figure 5.5 shows the images obtained from the AFM and Table 5.5 contains the parameters of the liposome characteristics measured with the AFM.

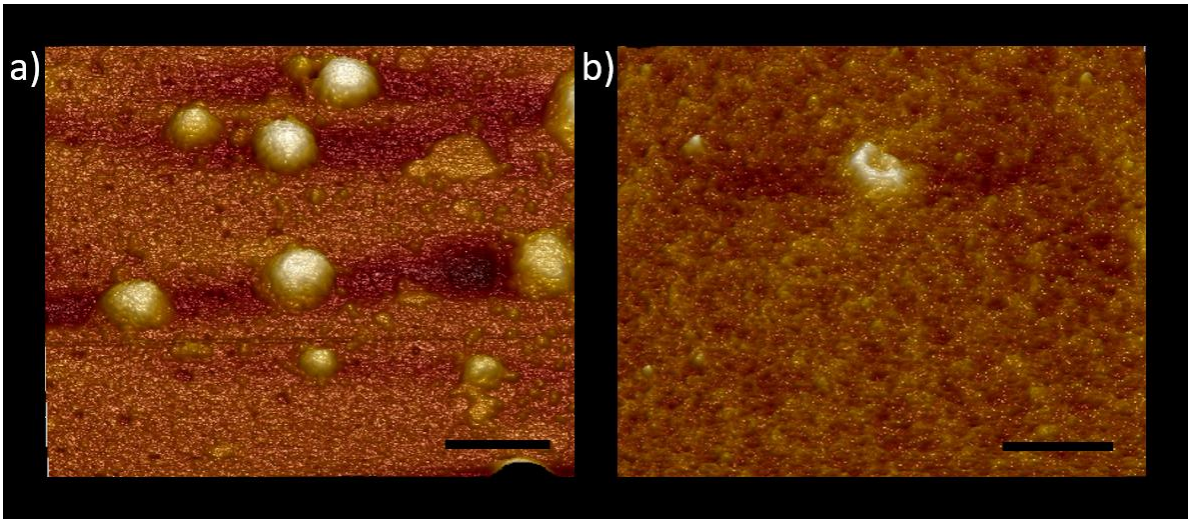

Figure 5.5. AFM images to evaluate the effect of media components on Ambisome® liposomes. a) KRB BS 20.0 mM PL 4.0 mM, b) KRB BS 20.0 mM PL 4.0 mM BSA 4.0% w/v. The scale bar represents 200 nm.

Diameter and surface roughness of the liposomal structures in samples from KRB BS 20.0 mM PL 4.0 mM are significantly higher than the control sample; liposomes could be merging with each other or the inclusion of BS PL could alter the structure of the liposome resulting in a higher size before the disruption. Liposomes were not visible in the sample of from KRB BS 20.0 mM PL 4.0 mM BSA 4.0% w/v, probably due to the incubation period of this sample.

Table 5.5. Properties of liposomes obtained from atomic force microscopy from the samples prepared in media with BS PL in the presence and absence of BSA. Mean ± SD. n = 20 Random Particles.

Sample	Diameter (nm)	Surface Roughness (nm)
KRB control (centrifugation/vacuum)	69.4 ± 18.9	12.9 ± 1.6
KRB BS 20.0 mM PL 4.0 mM	130.0 ± 13.0	10.1 ± 2.7
KRB BS 20.0 mM PL 4.0 mM BSA 4.0% w/v	No Particles	

5.3.3. PBPK modeling of Ambisome® administered to healthy subjects

The simulated plasma concentration profiles obtained with the validated PBPK model for the administration of Ambisome® to healthy subjects are shown in Figure 5.6.

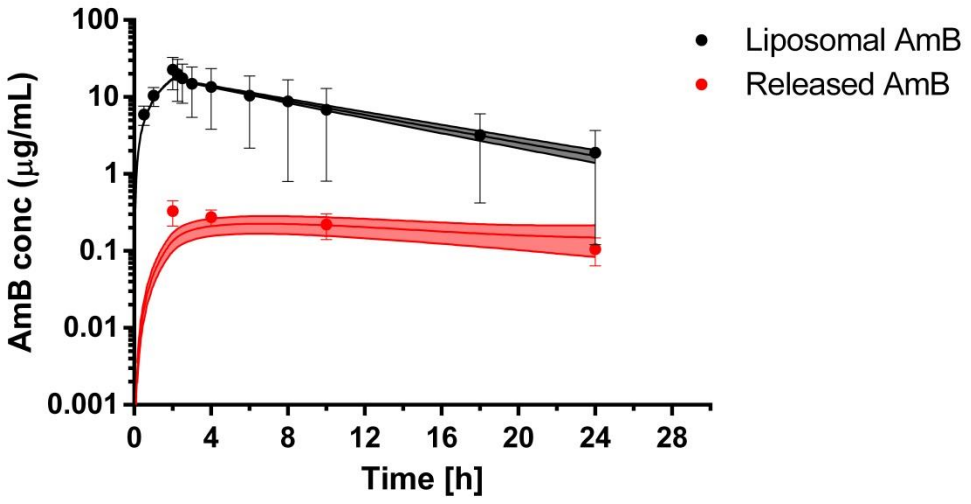

Figure 5.6. Observed and simulated (PBPK model) plasma concentration profiles of "liposomal AmB" and "released AmB" after the administration of Ambisome® to healthy subjects [25, 26].

Using the parameter identification method, the values for the parameters investigated were: k_{rel-iv} = 0.60 h^{-1}, logP (released AmB) = 3.24, logP (liposomal AmB) = 1.0, Specific clearance for the immune removal "enzyme" = 2.57 h^{-1} and AAG1 k_{diss} = 0.42 µmol/L. The logP and clogP values reported in the literature, are between -2.33

to 2.14 (Table 5.2) providing a wide interval for the actual value. The value obtained from parameter identification fitting was 3.24 which could be supported due to the dispersion of the values previously reported (Table 5.2).

The PBPK model described closely the average observed data for "liposomal AmB" and "released AmB" (%.AUC_{0-24h} predicted/AUC_{0-24h} observed = 94% and 101%, respectively). Comparing the developed PBPK model in this study with the one reported by Kagan et al [21], the main difference was the k_{rel-iv} from this model was faster: 0.60 h^{-1} > 0.0035 h^{-1} [21] and there was no initial rapid release of the 8% of the dose. It could be due to that the release of AmB took place in all of the compartments [21] while in this study; the release was only in plasma.

The sensitivity analysis is shown in Figure 5.7.

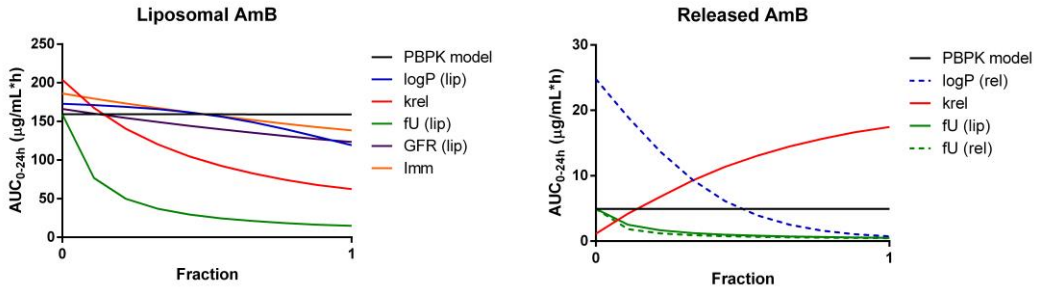

Figure 5.7. Sensitivity analysis of PBPK model parameters on the "liposomal AmB" and "released AmB" AUC_{0-24h} obtained from simulated plasma concentrations in healthy subjects. The black line is the AUC_{0-24h} obtained from the validated PBPK model for healthy subjects.

Parameters such as aqueous solubility ("liposomal AmB" and "released AmB"), solute radius ("liposomal AmB"), specific biliary clearance ("liposomal AmB" and "released AmB"), k_{diss} for AAG1 and APOB ("released AmB"), and the GFR for "released AmB" did not have a significant impact on the AUC_{0-24h} of "liposomal AmB" and "released AmB". For the "liposomal AmB", the fraction unbound to proteins had the greatest impact on the model. It can be observed how the "liposomal AmB" in plasma decreases as the fraction unbound increases, leading to a decreased on "released AmB", as there will be less "liposomal AmB" available in plasma to release drug.

k_{rel-iv} had a high impact on both "liposomal AmB" and "released AmB" (Figure 5.7), with a higher release rate constant leading to an increase of the "released AmB" and a decrease of the "liposomal AmB". For "released AmB", logP is the factor with the highest effect on AUC_{0-24h}.

5.3.4. Evaluation of the *in vitro* release profiles using the PBPK model

The predictability of the *in vitro* release tests is presented in Figure 5.8 for both "liposomal AmB" and "released AmB".

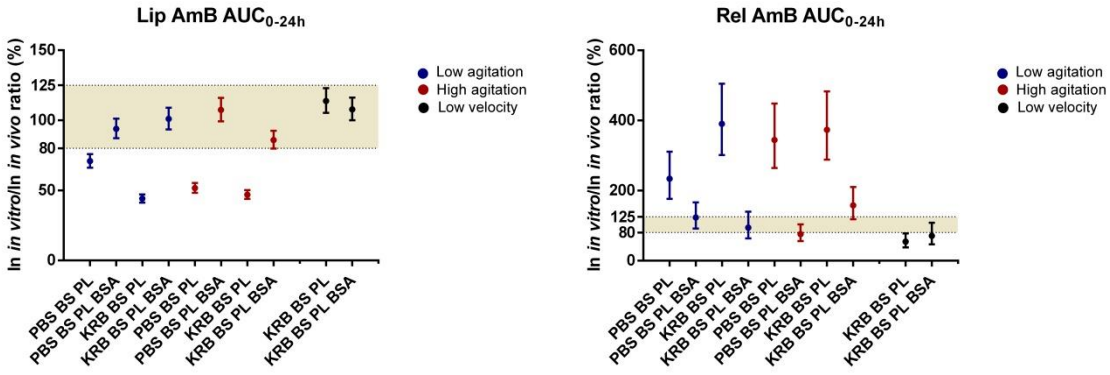

Figure 5.8. AUC_{0-24h} calculated from simulated plasma concentration profiles with with the k_{rel} from the *in vitro* release profiles against the AUC_{0-24h} obtained from the validated PBPK model for "liposomal AmB" and "released AmB". n = 5 subjects for each population.

For the "liposomal AmB", the AUC_{0-24h} obtained with the *in vitro* release profiles where BSA was present in the media were similar to the AUC_{0-24h} obtained from the validated PBPK model, regardless of the type of the buffer or the hydrodynamic conditions. The AUC_{0-24h} values were only similar for a medium without BSA in the low velocity setup (Figure 5.8). For the "released AmB", the AUC_{0-24h} obtained with the *in vitro* release profiles in media with BSA were close to attaining similarity to the *in vivo* profiles, as all the tests (except KRB BS PL BSA low agitation) revealed one extreme of the 90% CI between 80 – 125%. It can be noticed that the tests performed with the continuous flow setup under-predicted the plasma concentration of the "released AmB". An increasing flow rate leads to a higher drug release (Figure 5.4) thus further exploration of flow rate effect could be conducted to identify the flow rate resulting in release profiles suitable for simulation of *in vivo* release. The model

developed is suitable for the evaluation of the *in vitro* release tests and could support the development of a biopredictive *in vitro* release test. It has to be noted that for the prediction of the plasma concentration of "liposomal AmB" and "released AmB", the presence of BSA was a critical factor, thus, information on the exact mechanism of the protein binding to the liposomes could further improve the model developed.

5.3.5. PBPK – PD modeling for the patient (hypoalbuminaemic) population.

Parameters obtained after fitting to the exponential decay equation model for the time killing experiments are presented in Table 5.6.

Table 5.6. Parameters obtained after fitting (Equation 5.6) of CFU time profiles from time killing experiments in KRB BSA 2 and 4% w/v using different concentrations of AmB (0.75, 1.5 and 3.0 μg/mL) (Mean ± SD, n = 2).

BSA (%w/v)	**AmB (μg/mL)**	$\%CFU_{max}$	k_{kill} **(h^{-1})**	**R^2**	**AIC**
2.0	0.75	105.1 ± 5.23	0.33 ± 0.03	0.86 ± 0.02	52.88 ± 0.3
	1.50	110.65 ± 4.17	0.54 ± 0.03	0.93 ± 0.05	47.16 ± 6.17
	3.00	110.6 ± 5.37	0.77 ± 0.11	0.92 ± 0.05	48.00 ± 6.43
4.0	0.75	101.75 ± 4.6	0.11 ± 0.01	0.89 ± 0.01	47.25 ± 2.38
	1.50	123.8 ± 10.04	0.17 ± 0.03	0.84 ± 0.07	54.71 ± 5.18
	3.00	107.65 ± 6.15	0.37 ± 0.01	0.90 ± 0.00	50.27 ± 1.06

The simulated plasma concentration profiles for "liposomal AmB" and "released AmB" in the extrapolated hypoalbuminaemic population and the healthy subjects' population are presented in Figure 5.9a. It can be observed that both "liposomal AmB" and "released AmB" are in a lower concentration as a consequence of the decrease of the amount of proteins present. It could be hypothesized that the unbound "liposomal AmB" and "released AmB" are distributing to tissues leading to a lower concentration of AmB in plasma.

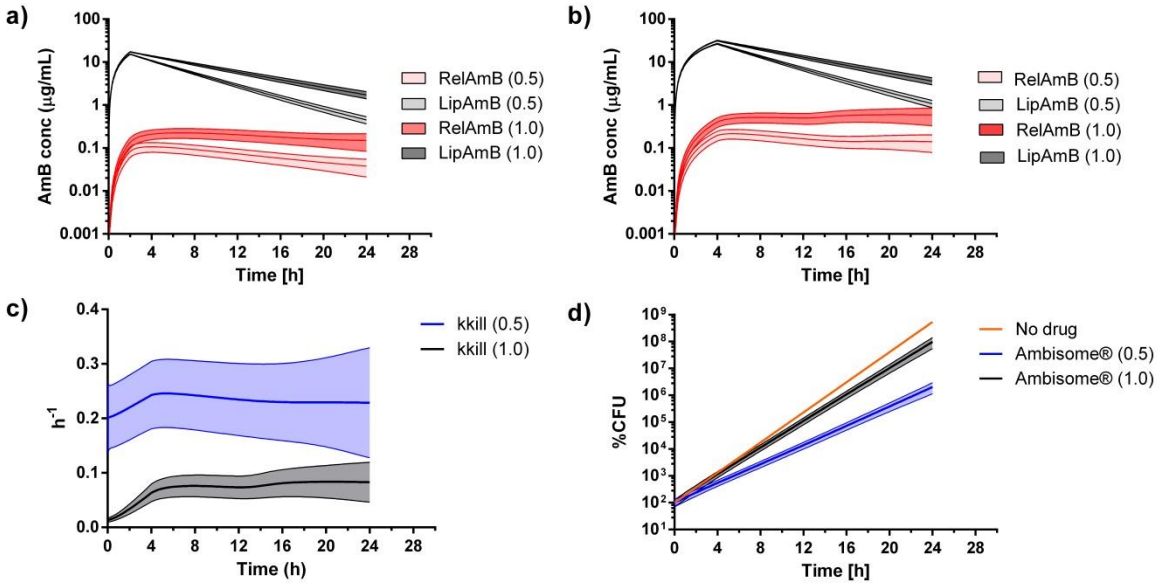

Figure 5.9. PBPK-PD model for a hypoalbuminaemic population (plasma protein fraction 0.5; healthy subjects: plasma protein fraction 1.0) and its pharmacodynamic effect on fungal cells. a) Simulated plasma concentration profiles of "liposomal AmB" and "released AmB" from the validated PBPK model for healthy subjects and the hypoalbuminaemic population, b) simulation of a dose administered to patients receiving Ambisome®, c) simulated k_{kill} (corresponding to the simulated plasma concentration profile of Figure 5.9b), and d) effect of the administration of Ambisome® on the growth of *Candida albicans*.

Figure 5.9b shows the simulated plasma concentration profiles for a typical administration of Ambisome® to a patient with a systemic fungal infection (300 mg, infusion 4 h) in the simulated hypoalbumianemic patient and in a subject with normal albumin levels. A linear relationship between the AmB concentration and the time killing rate coefficient was found for experiments with BSA 2.0 and 4.0% w/v, (Eq 5.7 and eq. 5.8, respectively) and used in the PBPK-PD model to simulate the killing of *C. albicans* (Figure 5.9c).

$$time\ killing\ rate\ coefficient\ (h^{-1}) = 0.1923(mL * h^{-1})\ /\ \mu g + 0.2102\ h^{-1}$$ Eq 5.7.

$$time\ killing\ rate\ coefficient\ (h^{-1}) = 0.1167\ (mL * h^{-1})\ /\ \mu g + 0.014\ h^{-1}$$ Eq 5.8.

It can be observed how the growth of the fungal cells is reduced by the administration of Ambisome® (Figure 5.9d) with a higher effect in the simulated hypoalbuminaemic

patient than in the subject with normal albumin levels. From the time killing studies and previous data [23], a higher fungicidal effect is reached with a lower AmB concentration in the presence of BSA 2.0% w/v as there is more unbound drug able to exert its pharmacological effect. It has to be noted that only the effect of released AmB is evaluated in this PBPK-PD model. The humoral and cellular immune responses and the effect that the liposomal AmB could have on *C. albicans* are not considered. A number of 10^5 CFU/mL were used to simulate the effect of AmB *in vivo* as this was the concentration of the fungal cell suspensions used in the time killing experiments. It has been reported that a concentration of 100 – 1000 CFU/mL are found in cultures of blood from patients with systemic fungal infection [40, 41]. The PBPK-PD analysis could be further improved by using the adequate number of CFU quantified in plasma from infected patients to evaluate the response of the humoral immune response and not only the effect of the protein content. In plasma from healthy subjects the fungal cells did not grow (data not shown), thus, the results of the PBPK-PD model for the healthy subject must be only considered as an exercise for comparative purposes. For this model, only the changes in the albumin levels were considered, leaving aside the physiological characteristics of septic or critically ill patients. In order to improve the model, the change in the activity of the immune enzyme should be adjusted to the patients' population as the immune system might be compromised, and the k_{rel-iv}, which the *in vitro* tests showed to be dependent on the albumin concentration, should be adjusted too. This approach reveals the potential of the use of *in vitro* release data and suitable microbiology data in combination with a PBPK-PD model in order to guide parenteral formulation development based on pharmacodynamics and therapeutic outcomes.

5.4. Conclusions

The literature available for *in vitro* release testing of controlled release parenteral formulations is limited. The evaluation of the factors that can affect the release from these formulations and the development of *in vitro* release tests that are able to predict the *in vivo* performance are of high importance. In this work, the development of a clinically relevant *in vitro* release test for the liposomal formulation of AmB (Ambisome®) was investigated. A PBPK model was developed for the administration of Ambisome® to healthy subjects, which was used to evaluate the critical factors for the AmB release from the liposomes and the *in vivo* predictability of the *in vitro* release

tests. The presence of BSA in the media was the most critical factor on the AmB release, and the *in vitro* release profiles from tests with BSA in the medium were biopredictive. Successful predictions of the “liposomal AmB” and the “released AmB” plasma concentration profile were obtained with both hydrodynamic setups tested (sample and separate method and continuous flow method). A PBPK-PD model of the activity of AmB on fungal cells was developed based on the predicted "released AmB" plasma concentration profile in a hypoalbuminaemic population in order to illustrate the potential of linking *in vitro* release testing, PBPK modeling and microbiology data.

Acknowledgments

Part of this work has been previously presented at the AAPS annual meeting in Washington, DC November 2019 (poster presentation). The authors would like to thank the Mexican Council of Science and Technology (CONACyT) for the PhD scholarship of Mr R Diaz de Leon-Ortega.

5.5. References

[1]. Abend A, Heimbach T, Cohen M, Kesisoglou F, Pepin X, Suarez-Sharp S. Dissolution and Translational Modeling Strategies Enabling Patient-Centric Drug Product Development: the M-CERSI Workshop Summary Report. The AAPS Journal. 2018;20(3):60.

[2]. Espié P, Tytgat D, Sargentini-Maier M-L, Poggesi I, Watelet J-B. Physiologically based pharmacokinetics (PBPK). Drug Metabolism Reviews. 2009;41(3):391-407.

[3]. Khalil F, Laer S. Physiologically based pharmacokinetic modeling: methodology, applications, and limitations with a focus on its role in pediatric drug development. J Biomed Biotechnol. 2011;2011:907461.

[4]. Jones HM, Gardner IB, Watson KJ. Modelling and PBPK Simulation in Drug Discovery. The AAPS Journal. 2009;11(1):155-66.

[5]. Batchelor HK, Fotaki N, Klein S. Paediatric oral biopharmaceutics: key considerations and current challenges. Adv Drug Deliv Rev. 2014;73:102-26.

[6]. Kesisoglou F, Chung J, van Asperen J, Heimbach T. Physiologically Based Absorption Modeling to Impact Biopharmaceutics and Formulation Strategies in Drug Development-Industry Case Studies. J Pharm Sci. 2016;105(9):2723-34.

[7]. Zhuang X, Lu C. PBPK modeling and simulation in drug research and development. Acta Pharmaceutica Sinica B. 2016;6(5):430-40.

[8]. FDA. Physiologically Based Pharmacokinetic Analyses — Format and Content 2018 [cited 2018 15/11/2018]. Available from: https://www.fda.gov/downloads/Drugs/GuidanceComplianceRegulatoryInformation/Guidances/UCM531207.pdf.

[9]. EMA. Guideline on the qualification and reporting of physiologically based pharmacokinetic (PBPK) modelling and simulation: EMA; 2016 [cited 2018 15/11/2018]. Available from: https://www.ema.europa.eu/documents/scientific-guideline/guideline-qualification-reporting-physiologically-based-pharmacokinetic-pbpk-modelling-simulation_en.pdf.

[10]. Zhang XY, Trame MN, Lesko LJ, Schmidt S. Sobol Sensitivity Analysis: A Tool to Guide the Development and Evaluation of Systems Pharmacology Models. CPT Pharmacometrics Syst Pharmacol. 2015;4(2):69-79.

[11]. McNally K, Cotton R, Loizou GD. A Workflow for Global Sensitivity Analysis of PBPK Models. Front Pharmacol. 2011;2:31.

[12]. Ulldemolins M, Roberts JA, Rello J, Paterson DL, Lipman J. The effects of hypoalbuminaemia on optimizing antibacterial dosing in critically ill patients. Clinical Pharmacokinetics. 2011;50(2):99-110.

[13]. Kuepfer L, Niederalt C, Wendl T, Schlender JF, Willmann S, Lippert J, et al. Applied Concepts in PBPK Modeling: How to Build a PBPK/PD Model. CPT: pharmacometrics & systems pharmacology. 2016;5(10):516-31.

[14]. Chen K, Teo S, Seng KY. Sensitivity analysis on a physiologically-based pharmacokinetic and pharmacodynamic model for diisopropylfluorophosphate-induced toxicity in mice and rats. Toxicol Mech Methods. 2009;19(8):486-97.

[15]. Asin-Prieto E, Rodriguez-Gascon A, Isla A. Applications of the pharmacokinetic/pharmacodynamic (PK/PD) analysis of antimicrobial agents. J Infect Chemother. 2015;21(5):319-29.

[16]. Nielsen EI, Cars O, Friberg LE. Pharmacokinetic/pharmacodynamic (PK/PD) indices of antibiotics predicted by a semimechanistic PKPD model: a step toward model-based dose optimization. Antimicrob Agents Chemother. 2011;55(10):4619-30.

[17]. Sadiq MW, Nielsen EI, Khachman D, Conil JM, Georges B, Houin G, et al. A whole-body physiologically based pharmacokinetic (WB-PBPK) model of ciprofloxacin: a step towards predicting bacterial killing at sites of infection. J Pharmacokinet Pharmacodyn. 2017;44(2):69-79.

[18]. Mora-Duarte J, Betts R, Rotstein C, Colombo AL, Thompson-Moya L, Smietana J, et al. Comparison of caspofungin and amphotericin B for invasive candidiasis. N Engl J Med. 2002;347(25):2020-9.

[19]. Johnson EM, Ojwang JO, Szekely A, Wallace TL, Warnock DW. Comparison of In Vitro Antifungal Activities of Free and Liposome-Encapsulated Nystatin with

Those of Four Amphotericin B Formulations. Antimicrob Agents Chemother. 1998;42(6):1412-6.

[20]. Kagan L, Gershkovich P, Wasan KM, Mager DE. Physiologically Based Pharmacokinetic Model of Amphotericin B Disposition in Rats Following Administration of Deoxycholate Formulation (Fungizone®): Pooled Analysis of Published Data. The AAPS Journal. 2011;13(2):255.

[21]. Kagan L, Gershkovich P, Wasan KM, Mager DE. Dual Physiologically Based Pharmacokinetic Model of Liposomal and Nonliposomal Amphotericin B Disposition. Pharmaceutical Research. 2014;31(1):35-45.

[22]. Egger P, Bellmann R, Wiedermann CJ. Determination of amphotericin B, liposomal amphotericin B, and amphotericin B colloidal dispersion in plasma by high-performance liquid chromatography. J Chromatogr B: Anal Technol Biomed Life Sci. 2001;760(2):307-13.

[23]. Diaz de Leon-Ortega R, D'Arcy DM, Bolhuis A, Fotaki N. Investigation and simulation of dissolution with concurrent degradation under healthy and hypoalbuminaemic simulated parenteral conditions- case example Amphotericin B. Eur J Pharm Biopharm. 2018.

[24]. Fotaki N. Flow-through cell apparatus (USP apparatus 4): Operation and features. Dissolution Technol. 2011;18(4):46-9.

[25]. Bekersky I, Fielding RM, Dressler DE, Lee JW, Buell DN, Walsh TJ. Pharmacokinetics, Excretion, and Mass Balance of Liposomal Amphotericin B (AmBisome) and Amphotericin B Deoxycholate in Humans. Antimicrobial Agents and Chemotherapy. 2002;46(3):828-33.

[26]. Bekersky I, Fielding RM, Dressler DE, Lee JW, Buell DN, Walsh TJ. Plasma protein binding of amphotericin B and pharmacokinetics of bound versus unbound amphotericin B after administration of intravenous liposomal amphotericin B (AmBisome) and amphotericin B deoxycholate. Antimicrob Agents Chemother. 2002;46(3):834-40.

[27]. DrugBank. Amphotericin B. 2005.

[28]. Sigma-Aldrich. Amphotericin B. https://wwwsigmaaldrichcom/content/dam/sigma-aldrich/docs/Sigma/Datasheet/6/a9528datpdf. 2015.

[29]. Bharate SS, Kumar V, Vishwakarma RA. Determining Partition Coefficient (Log P), Distribution Coefficient (Log D) and Ionization Constant (pKa) in Early Drug Discovery. Comb Chem High Throughput Screen. 2016;19(6):461-9.

[30]. ChemSpider. Amphotericin B. 2015.

[31]. Lamy-Freund MT, Ferreira VF, Schreier S. Polydispersity of aggregates formed by the polyene antibiotic amphotericin B and deoxycholate. A spin label study. Biochim Biophys Acta, Biomembr. 1989;981(2):207-12.

[32]. Mazerski J, Grzybowska J, Borowski E. Influence of net charge on the aggregation and solubility behaviour of amphotericin B and its derivatives in aqueous media. European biophysics journal. 1990;18(3):159-64.

[33]. Barwicz J, Christian S, Gruda I. Effects of the aggregation state of amphotericin B on its toxicity to mice. Antimicrob Agents Chemother. 1992;36(10):2310-5.

[34]. Ridente Y, Aubard J, Bolard J. Absence in amphotericin B-spiked human plasma of the free monomeric drug, as detected by SERS. FEBS Lett. 1999;446(2-3):283-6.

[35]. Gilead. Ambisome®. http://wwwgileadcom/~/media/files/pdfs/medicines/other/ambisome/ambisome_pipdf?la=en. 2015.

[36]. Yokouchi Y, Tsunoda T, Imura T, Yamauchi H, Yokoyama S, Sakai H, et al. Effect of adsorption of bovine serum albumin on liposomal membrane characteristics. Colloids and Surfaces B: Biointerfaces. 2001;20(2):95-103.

[37]. Hernández-Caselles T, Villalaín J, Gómez-Fernández JC. Influence of liposome charge and composition on their interaction with human blood serum proteins. Molecular and Cellular Biochemistry. 1993;120(2):119-26.

[38]. Law SL, Lo WY, Pai SH, Teh GW, Kou FY. The adsorption of bovine serum albumin by liposomes. International Journal of Pharmaceutics. 1986;32(2):237-41.

[39]. FDA. Draft Guidance on Amphotericin B 2016 [cited 2018 22/11/2018]. Available from: https://www.fda.gov/downloads/Drugs/GuidanceComplianceRegulatoryInformation/Guidances/UCM384094.pdf.

[40]. Misme-Aucouturier B, Albassier M, Alvarez-Rueda N, Le Pape P. Specific Human and Candida Cellular Interactions Lead to Controlled or Persistent Infection Outcomes during Granuloma-Like Formation. Infection and Immunity. 2017;85(1):e00807-16.

[41]. Pfeiffer CD, Samsa GP, Schell WA, Reller LB, Perfect JR, Alexander BD. Quantitation of Candida CFU in Initial Positive Blood Cultures. Journal of Clinical Microbiology. 2011;49(8):2879-83.

Conclusions and future directions

Conclusions

In vitro release tests are mainly designed to characterize the release of the drug from a formulation and hopefully, predict the *in vivo* behaviour. Currently, for *in vitro* release tests for parenterals, there are no guidelines from the regulatory agencies (FDA or EMA) where well defined characteristics and specifications are provided. The investigation of the variables that might influence drug release (both release medium and hydrodynamics) from these formulations would be the first step in order to develop compendial and biopredictive *in vitro* release tests.

Towards the development of clinically relevant *in vitro* release testing for controlled released parenteral formulations, three steps were followed: i) development of suitable release media, ii) *in vitro* release testing of a controlled released parenteral formulation administered intravenously, and iii) PK and PBPK modeling in order to relate the *in vitro* data with observed *in vivo* data.

Media with different albumin (BSA) concentration were developed using KRB (Chapter 2). It was found that BSA was a critical factor for the solubility, degradation rate constant, dissolution and pharmacological activity of a poorly soluble, highly protein bound drug (AmB as model drug) in a concentration dependent manner. The importance of incorporating BSA as a medium component for the *in vitro* release testing of these types of drugs in a suitable concentration for the population that is attempting to simulate (healthy subjects, hypoalbuminaemic subjects) was revealed.

After measuring the AmB solubility in plasma (clinically relevant solubility value), more complex media were developed. Media with BSA (Chapter 2) and media with biorelevant plasma components in biorelevant concentrations were not clinically relevant. Clinically relevant media were developed with biorelevant and synthetic surfactants. When BSA was added to the media, a decrease on the surfactants' activity was observed.

With the developed media (Chapter 2 and 3), the *in vitro* release of AmB from a liposomal formulation (Ambisome®) was investigated in two setups: sample and

separate and continuous flow. It was found that BSA was the most significant factor for the release of AmB from Ambisome® liposomes. The presence of BSA was found to slow and decrease the *in vitro* release (Chapter 4 and 5).

A PK and a PBPK model were developed to characterise the PK of the liposomal and released AmB in healthy subjects in order to relate them to the *in vitro* release profiles (Chapter 4 and 5). The *in vitro* release profiles were linked with the modeling in order to predict the *in vivo* release. An *in vitro- in vivo* relation was developed, with the *in vitro* release profiles in category 1 media with BSA 4.0% w/v with the sample and separate setup. The *in vitro* release profiles from tests with category 3a media with BSA were biopredictive. Successful predictions of the liposomal AmB and the released AmB plasma concentration profile were obtained with both hydrodynamic setups.

Summarizing, in this project are presented the steps suggested in order to develop an *in vitro* clinically relevant release test for an intravenous parenteral formulations, which with appropriate adaptations, could be extrapolated to other type of parenteral formulations.

Future directions

In this project a clinically relevant *in vitro* test for a controlled release parenteral formulation (intravenously administered) was developed but there were some limitations. As this was the first step for the investigation and development of clinically relevant media and release testing for these formulations, only the conditions of healthy subjects in fasted state with relevant changes of albumin concentration were simulated.

In future studies, the effect of the prandial state on the release from these formulations could be explored. The physiological changes that occur after the meal ingestion include changes in the composition of plasma (increased concentration of phospholipids, bile salts) and increase of the flow rate (increase in the heart beat rate leads to increase of the blood flow to the gastrointestinal tract). Based on the findings of the current project, alteration of the performance of the formulation in the fed state would be expected.

The human PK data for this formulation, and in general for the AmB formulations, is scarce. Plasma concentration of AmB after administration of an AmB formulation is often quantified as total AmB and not as formulation-bound AmB and released AmB; this affects the development of an accurate PK or PBPK model. There are studies where both species are quantified in patients but the data sets are from only just one patient and it could not be used for a robust analysis. The *in vitro* release profiles in the sample and separate setup were successful in predicting the *in vivo* release. The drawback of this setup is that it is not performed in a compendial apparatus and it might not be suitable for routinely or quality control analysis. Future experiments could be designed in order to translate the hydrodynamics from the bottle/stirrer setup to a compendial apparatus (paddle, mini paddle apparatus).

As BSA plays an important role in the release of drug and interferes with release media components, more studies to confirm these interactions are needed. Studies confirming the interaction between AmB, surfactants and liposomes with BSA could reveal how the interaction takes place and update the *in vitro* tests. Also, microscopy time-dependent studies to show the changes in the liposomes occurring during the release would be beneficial to understand the mechanism of AmB release from the liposomes.

The PD model developed was only a demonstration of how the PBPK model could be used to predict the PD effect of the released drug. In order to get meaningful *in vitro* data for its incorporation to the model, the tests should be performed simulating closely the conditions patients receiving AmB therapy.

The causes of hypoalbunaemia should be considered for the development of the PBPK model. For example, in case of infection, damage to the endothelium could lead to leakage of the liposomes to the lymphatic system. In patients with fungal infection, oncology patients or patients with a transplant, the response of the immune system needs to be taken into account in the model.

The MIC, MFC and time killing determinations in plasma from patients receiving AmB would be more suitable than only using a simulated plasma medium as there are more plasma components that could slow or reduce the proliferation of fungal cells.

Working into more depth in these topics, the *in vitro* release test would increase their prediction capability, the outcome would be improved and their applications expanded.